

Fall 12-19-2012

# Modeling and Characterization of Power Distribution Networks with Installed Distributed Generation and Connected PHEVs

Santhosh Basineni

Follow this and additional works at: [https://scholarworks.uttyler.edu/ee\\_grad](https://scholarworks.uttyler.edu/ee_grad)



Part of the [Electrical and Computer Engineering Commons](#)

---

## Recommended Citation

Basineni, Santhosh, "Modeling and Characterization of Power Distribution Networks with Installed Distributed Generation and Connected PHEVs" (2012). *Electrical Engineering Theses*. Paper 8.  
<http://hdl.handle.net/10950/103>

This Thesis is brought to you for free and open access by the Electrical Engineering at Scholar Works at UT Tyler. It has been accepted for inclusion in Electrical Engineering Theses by an authorized administrator of Scholar Works at UT Tyler. For more information, please contact [tbianchi@uttyler.edu](mailto:tbianchi@uttyler.edu).

**MODELING AND CHARACTERIZATION OF POWER DISTRIBUTION NETWORKS  
WITH INSTALLED DISTRIBUTED GENERATION AND CONNECTED PHEVs**

by

**SANTHOSH BASINENI**

A thesis submitted in partial fulfillment  
of the requirements for the degree of  
Master of Science in Electrical Engineering  
Department of Electrical Engineering

Hassan El-Kishky, Ph.D., P.E., Committee Chair

College of Engineering and Computer Science

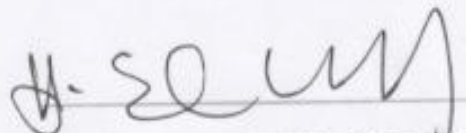
The University of Texas at Tyler

December 2012

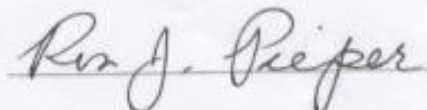
The University of Texas at Tyler  
Tyler, Texas

This is to certify that the Master's Thesis of  
SANTHOSH BASINENI  
has been approved for the thesis requirements on  
November 9<sup>th</sup>, 2012

Approvals:



Thesis Chair: Hassan El-Kishky, Ph.D., P.E.



Member: Ron J. Pieper, Ph.D., P.E.



Member: Hector A. Ochoa, Ph.D.



Chair and Graduate Coordinator: Mukul V. Shirvaikar, Ph.D.



James K. Nelson, Jr., Ph.D., P.E.

Dean, College of Engineering and Computer Science

## **Acknowledgements**

I am heartily thankful to my thesis chair Dr. Hassan El-Kishky for his continuous support, patience and encouragement throughout the thesis work. His interest, vast knowledge, supervision and helpful suggestions made my thesis work easy and valuable. This thesis would not been possible without his guidance.

I appreciate my thesis committee members Dr. Ron J. Pieper and Dr. Hector Ochoa for their valuable time to reviews and helpful suggestions. I appreciate my department chair and program advisor Dr. Mukul V.Shirvaikar for his valuable guidance throughout my Master's program. I would like to show my gratitude to all my professors for their teaching.

I am thankful to my parents for their love, motivation and encouragement. I owe my friends for their continuous support throughout my research work.

## Table of Contents

Chapter One: Introduction.....	1
1.1 Energy Demand and Supply .....	1
1.2 Organization of Thesis.....	3
Chapter Two: Background .....	4
2.1 Distributed Generation .....	4
2.2 Early Development of Distributed Generation .....	4
2.3 Plug-in Hybrid Electric Vehicle Technology .....	6
Chapter Three: Grid Connected Distributed Generations.....	8
3.1 Introduction .....	8
3.2 Grid Connected Wind Turbine Induction Generators (WTIGs) .....	8
3.3 Modeling and Simulation of Test Power System Network.....	9
3.3.1 Wind Turbine Induction Generator .....	9
3.3.2 Matlab®Simulink Model of the Test Power System Network .....	11
3.4 Simulation Results .....	14
3.4.1 Constant Wind Speed.....	14
3.4.2 Linear Wind Speed .....	15
3.5 Modeling and Simulation of Photovoltaic Generation .....	16
3.5.1 Photovoltaic Cells .....	16
3.5.2 Characteristics of PV Cell.....	17
3.5.3 Efficiency of PV Cell.....	20
3.5.4 Maximum Power Point Tracking (MPPT).....	20
3.5.5 Types of PV Inverters .....	20
3.6 Matlab®Simulink Modeling of PV Technology .....	22
3.6.1 PV Array .....	22
3.6.2 Simulation Results .....	26
3.7 Simulation of PV Array with Multi Stage Inverter.....	30
3.7.1 Matlab®Simulink Modeling of Multi Stage PV Technology .....	30
3.7.2 Simulation Results .....	32
3.8 12-Power System Network.....	35

3.8.1 Matlab@Simulink Model of the 12-bus IEEE Test Power System Network .....	37
3.8.2 Simulation Results .....	38
Chapter Four: Electrical Vehicle Battery Charger for Smart Grids.....	46
4.1 Introduction .....	46
4.2 Battery Models .....	47
4.3 Bi-directional Battery Charger .....	49
4.4 Control Strategy.....	51
4.5 Matlab@Simulink Modeling of Bi-directional Converter.....	52
4.6 Simulation Results .....	54
Chapter Five: Grid Connected Distributed Generation with PHEV loads .....	61
5.1 Introduction .....	61
5.2 Power Quality of Power System.....	62
5.2.1 Steady-state Voltage Problems .....	62
5.2.2 Transients in Power System.....	63
5.2.3 Harmonic Distortion .....	63
5.3 Grid Connected Wind Turbine Induction Generator with PHEV load .....	63
5.4 Grid Connected PV Inverter with PHEV load .....	74
5.5 Matlab@Simulink Model of Grid Connected PHEV .....	75
5.6 Simulation Results .....	76
5.7 12-bus Power System Network with PHEV load .....	80
5.8 Matlab@Simulink Modeling.....	80
5.9 Simulation Results .....	82
5.10 Grid Connected PHEV load with Distributed Wind and PV Generation .....	90
5.11 Simulation Results .....	91
Chapter Six: Conclusions and Future Work .....	101
6.1 Conclusions .....	101
6.2 Future Work.....	102
References .....	103

## **List of Tables**

Table 3.1 Distribution line details.....	35
Table 3.2 Load details.....	35
Table 5.1 Case study.....	75

## List of Figures

Figure 3.1 One line diagram of the distribution system with WTIG .....	9
Figure 3.2 Block diagram of wind turbine induction generator .....	10
Figure 3.3 Matlab®Simulink model of wind turbine induction generator .....	11
Figure 3.4 Matlab®Simulink model of the test power system network .....	12
Figure 3.5 Matlab®Simulink model of the distribution network connected to WTIG.....	13
Figure 3.6 (a) Active power, (b) Reactive powers, (c) Wind speed, and (d) Pitch angel of the WTIG at constant speed .....	14
Figure 3.7 (a) Active power, (b) Reactive powers, (c) Wind speed, and (d) Pitch angel of the WTIG at linear change of wind speed .....	16
Figure 3.8 Equivalent circuit of a PV cell .....	17
Figure 3.9 Types of PV inverters .....	21
Figure 3.10 Mathematical model of photovoltaic cell.....	22
Figure 3.11 Circuit diagram of the boost converter.....	22
Figure 3.12 Gate control circuit of IGBT converter.....	23
Figure 3.13 3- $\Phi$ three level bridge inverter .....	24
Figure 3.14 Gate control circuit of inverter .....	25
Figure 3.15 Simulink diagram of the grid connected PV system .....	26
Figure 3.16 (a) Solar irradiance, (b) PV array output voltage, (c) PV array output power, and (d) PV array output current .....	26
Figure 3.17 Measurements of (a) Boost converter duty cycle, (b) Diode current of PV array, and (c) VSC voltage.....	27
Figure 3.18 (a) Current at the utility grid, (b) Power at the utility grid .....	28
Figure 3.19 Voltage harmonic distortions at the utility grid .....	29
Figure 3.20 Current harmonic distortions at the utility grid .....	29
Figure 3.21 Multi stage PV technologies .....	30
Figure 3.22 Matlab®Simulink model of the multi stage PV inverter.....	31
Figure 3.23 Measurements at PV1 and PV2 (a) Solar irradiance, (b) Output voltage, (c) Current, and (d) Output power.....	32
Figure 3.24 Measurements of (a) Diode current of PV array, (b) Boost converter duty cycle, and (c) VSC voltage.....	33
Figure 3.25 (a) Current at the utility grid, and (b) Power at the utility grid .....	34
Figure 3.26 Voltage harmonic distortions at the utility grid .....	34



Figure 3.27 Current harmonic distortions at the utility grid .....	35
Figure 3.28 One line diagram of 12-bus power system network.....	36
Figure 3.29 Matlab®Simulink model of 12-bus power system network.....	37
Figure 3.30 (a) 11th and 13th order voltage harmonic distortions at bus 1, and (b) 11th and 13th order current harmonic distortions at bus 1 .....	38
Figure 3.31 (a) 11th and 13th order voltage harmonic distortions at bus 2, and (b) 11th and 13th order current harmonic distortions at bus 2 .....	38
Figure 3.32 (a) 11th and 13th order voltage harmonic distortions at bus 3, and (b) 11th and 13th order current harmonic distortions at bus 3 .....	39
Figure 3.33 (a) 11th and 13th order voltage harmonic distortions at bus 4, and (b) 11th and 13th order current harmonic distortions at bus 4 .....	39
Figure 3.34 (a) 11th and 13th order voltage harmonic distortions at bus 5, and (b) 11th and 13th order current harmonic distortions at bus 5 .....	40
Figure 3.35 (a) 11th and 13th order voltage harmonic distortions at bus 6, and (b) 11th and 13th order current harmonic distortions at bus 6 .....	40
Figure 3.36 (a) 11th and 13th order voltage harmonic distortions at bus 7, and (b) 11th and 13th order current harmonic distortions at bus 7 .....	41
Figure 3.37 (a) 11th and 13th order voltage harmonic distortions at bus 8, and (b) 11th and 13th order current harmonic distortions at bus 8 .....	41
Figure 3.38 (a) 11th and 13th order voltage harmonic distortions at bus 9, and (b) 11th and 13th order current harmonic distortions at bus 9 .....	42
Figure 3.39 (a) 11th and 13th order voltage harmonic distortions at bus 10, and (b) 11th and 13th order current harmonic distortions at bus 10 .....	42
Figure 3.40 (a) 11th and 13th order voltage harmonic distortions at bus 11, and (b) 11th and 13th order current harmonic distortions at bus 11 .....	43
Figure 3.41 (a) 11th and 13th order voltage harmonic distortions at bus 12, and (b) 11th and 13th order current harmonic distortions at bus 12 .....	43
Figure 3.42 Voltage harmonic distortions at the grid .....	44
Figure 3.43 Current harmonic distortions at the grid .....	44
Figure 4.1 Lithium-ion battery model .....	47
Figure 4.2 Matlab®Simulink model of the lithium-ion battery.....	48
Figure 4.3 Bidirectional battery chargers .....	49
Figure 4.4 Bi-directional DC-DC converter.....	51

Figure 4.5 Matlab®Simulink model of PHEV charger .....	52
Figure 4.6 Inverter control circuit .....	53
Figure 4.7 Bi-directional converter control circuit .....	54
Figure 4.8 Battery voltage in discharge mode .....	54
Figure 4.9 Battery current in discharge mode .....	55
Figure 4.10 Voltage at the utility grid .....	55
Figure 4.11 Current at the utility grid.....	56
Figure 4.12 Voltage harmonic distortion.....	56
Figure 4.13 Current harmonic distortion .....	57
Figure 4.14 Battery voltage in charge mode .....	58
Figure 4.15 Battery current in charge mode .....	58
Figure 4.16 Voltage at the utility grid .....	59
Figure 4.17 Current at the utility grid.....	59
Figure 4.18 Voltage harmonic distortion.....	60
Figure 4.19 Current harmonic distortion .....	60
Figure 5.1 Matlab®Simulink model of grid connected WTIG with PHEV loads.....	64
Figure 5.2 Transient voltage at WTIG-1 .....	64
Figure 5.3 Transient voltage at WTIG-2 .....	65
Figure 5.4 Transient voltage at WTIG-3 .....	65
Figure 5.5 Transient voltage at load bus 1 .....	66
Figure 5.6 Transient voltage at load bus 2 .....	66
Figure 5.7 Transient voltage at load bus 3 .....	67
Figure 5.8 Transient voltage at the grid.....	67
Figure 5.9 Voltage at the WTIG-1 .....	68
Figure 5.10 Voltage at the WTIG-2 .....	69
Figure 5.11 Voltage at the WTIG-3 .....	69
Figure 5.12 Load bus1 voltage .....	70
Figure 5.13 Load bus2 voltage .....	70
Figure 5.14 Load bus3 voltage .....	71
Figure 5.15 Voltage at the utility grid .....	71
Figure 5.16 Voltage harmonic distortion at the grid .....	72
Figure 5.17 Current harmonic distortion at the grid.....	73
Figure 5.18 Voltage harmonic distortion injected by WTIG and PHEV .....	73

Figure 5.19 Current harmonic distortion injected by WTIG and PHEV .....	73
Figure 5.20 Matlab®Simulink modeling of grid connected DG with PHEV load .....	76
Figure 5.21 Voltage at the boost converter .....	77
Figure 5.22 Voltage at the VSC .....	77
Figure 5.23 Voltage harmonic distortion.....	78
Figure 5.24 Current harmonic distortion at the utility grid .....	78
Figure 5.25 Voltage at VSC .....	79
Figure 5.26 Voltage at VSC .....	79
Figure 5.27 Three DGs connected to 12-bus power system network with 50 PHEVs .....	81
Figure 5.28 Voltage at the PV generator bus .....	82
Figure 5.29 Current at the PV generator bus .....	82
Figure 5.30 Voltage at the PV generator 1 bus .....	83
Figure 5.31 Current at the PV generator 1 bus.....	83
Figure 5.32 Voltage at the PV generator 2 bus .....	84
Figure 5.33 Current at the PV generator 2 bus.....	84
Figure 5.34 Voltage at the bus 7.....	85
Figure 5.35 Current at the bus 7 .....	85
Figure 5.36 Voltage at the bus 8.....	86
Figure 5.37 Current at the bus 8.....	86
Figure 5.38 Voltage at the bus 11.....	87
Figure 5.39 Current at the bus 11 .....	87
Figure 5.40 Current at the bus 12.....	88
Figure 5.41 Current at the utility grid.....	88
Figure 5.42 Voltage harmonic distortion at the grid .....	89
Figure 5.43 Current harmonic distortion at the grid.....	89
Figure 5.44 Grid connected distributed generation with PHEV loads .....	91
Figure 5.45 Voltage at the PV generator bus .....	91
Figure 5.46 Current at the PV generator bus .....	92
Figure 5.47 Voltage at the WTIG bus .....	92
Figure 5.48 Current at the WTIG bus.....	93
Figure 5.49 Voltage at the PV generator1 bus .....	93
Figure 5.50 Current at the PV generator1 bus .....	94
Figure 5.51 Voltage at the bus 4.....	94

Figure 5.52 Current at the bus 4.....	95
Figure 5.53 Voltage at the PV generator bus 3 .....	95
Figure 5.54 Current at the bus 3.....	96
Figure 5.55 Voltage at the PV generator bus 10.....	96
Figure 5.56 Current at the bus 10.....	97
Figure 5.57 Voltage at the PV generator bus 7 .....	97
Figure 5.58 Current at the bus 7.....	98
Figure 5.59 Voltage at the PV generator bus 11.....	98
Figure 5.60 Current at the bus 11 .....	99
Figure 5.61 Voltage harmonic distortion at the grid .....	99
Figure 5.62 Current harmonic distortion at the grid.....	99

## Abstract

### MODELING AND CHARACTERIZATION OF POWER DISTRIBUTION NETWORKS WITH INSTALLED DISTRIBUTED GENERATION AND CONNECTED PHEVs

Santhosh Basineni

Thesis Chair: Hassan El-Kishky, Ph.D., PE, MBA.

The University of Texas at Tyler

December 2012

This thesis is focused on the modeling and characterization of power distribution networks with installed distributed generation and connected plug-in hybrid electric vehicles (PHEV). A PHEV charging/discharging (bidirectional) model has been developed in MATLAB®-Simulink. Installed photovoltaic systems with varying irradiance rates are modeled and characterized. Moreover, installed wind generators with varying wind speeds are modeled and characterized. Furthermore, the charging and discharging characteristics of connected PHEV are determined. The system characteristics are determined and investigated against the PHEV battery state of charge (SOC).

# **Chapter One**

## **Introduction**

### **1.1 Energy Demand and Supply**

In general, nearly 67% of total electric energy comes from burning fossil fuels (coal, oil and natural gas), 13.4% comes from nuclear and the remaining 19.5 % comes from renewable energy resources (mainly from wind, solar, hydro) [1]. Generating the electrical energy in a remote place and transferring it long distance through transmission lines can increase power losses and cost per megawatt generation. Moreover, the use of electrical energy is increasing day by day. As a consequence, the generation of electric energy should be increased to meet growing demand.

Increasing generation is not possible all the time, because of the ratings and specifications of the generating unit, transmission line capacity, rating of the transformer, protection equipment, etc. [2]. High demand and deficiency of the fossil fuels represent obstacles against the installation of more generation units. Replacing the existing plant with new equipment may have fatal impact on financial standing of power companies.

Consumer demand can be met by improving the efficiency of the existing power system network. High Voltage Direct Current (HVDC) systems can improve the transmission line efficiency by up to 6% compared to High Voltage Alternating Current (HVAC) transmission system, GAS insulated sub-stations, super conductors (still in development stage) and wide area monitoring systems, stability of the power system will

increase by using the Flexible AC Transmission System (FACTS) devices (power electronic) [2].

Other paths to improve efficiency are distributed generation/micro grids, underground distribution lines, intelligent grid design, reduction of overall T&D (transformer and distribution) transformer MVA, energy storage devices, three phase design for distribution, ground wire loss reduction techniques. In addition, higher transmission operating voltages, voltage optimization through reactive power compensation, asset replacement schedule optimization, distribution loss reduction via distribution automation, power factor improvement, load management and power electronic transformers play a major role to improve the efficiency [2].

Plug-in hybrid electric vehicle (PHEV) is a new technology used to reduce the use of petroleum, decrease greenhouse gas emission and increase the fuel efficiency. Its potential impact highly depends on the design of energy storage system. Most of the current PHEVs and EV battery chargers are high power nonlinear devices. These chargers inject a significant amount of current harmonics into the grid. Therefore, it impacts the power quality and voltage profile of smart grids [3].

There are so many different ways to improve the efficiency of the power system. The goal of this thesis is the modeling, simulation and characterization of the dispersed generation and PHEV (plug-in hybrid electric vehicle), integration of distributed generations (DGs) to the utility grid network with PHEV loads. This thesis also investigates the power quality of the power system network while connecting PHEV loads.

## **1.2 Organization of Thesis**

This thesis is divided into six chapters; Chapter Two describes the early development of distributed generation and PHEVs. Chapter Three describes the simulation, modeling and integration of distributed generation to the utility grid. Chapter Four describes the modeling and simulation of PHEV battery connection to smart grids. Chapter Five presents the DG's and the 12-bus power system network with PHEV loads. Chapter Six presents the conclusions and directions for future work.



## **Chapter Two**

### **Background**

#### **2.1 Distributed Generation**

Distributed generation is also known as small, modular or dispersed generation depending on the power generation and size of the plant. Both the distributed generation (DGs) and large power plants are interconnected to the power system. Large power plants are connected to the transmission system far from the consumer. Whereas DGs are connected to the distribution system near to the load. For that reason, DGs are also called as on-site generators.

#### **2.2 Early Development of Distributed Generation**

The origin of DGs goes back to the invention of light bulb by Thomas Edison in 1879. The light bulb was powered by direct current. By the end of 1880s, Direct current transmission system was developed. The first commercial power plant was developed in 1882 [3]. The load voltage dropped because of high resistance DC line directly feed to the load at load voltage. Therefore, DC generators are placed at each load to keep the load voltage balanced.

This DC transmission vanished with the invention of AC transmission by Tesla and practical transformer by William Stanley in 1886 [4]. AC became more popular for transmitting electric power due to the ability to step up voltage using transformers. Transformer will step up the voltage at the generation side and step down the voltage at

the receiving side according to the load voltage. Transmission line losses were significantly reduced by using the transformer at both supply and load ends.

The life changing episode of electricity started with the development of power electronic devices [5]. Power electronics is one of the best ways to improve efficiency and reliability of the system, and control the power flow of the electricity in generation, transmission, and distribution.

Due to the following advantages distributed generation has become more popular [6].

- reduced air pollution
- reduced use of fossil fuels
- DGs reduce the cost for transmission lines (installed on-site)
- improved the power quality
- increased grid reliability

The use of DGs can improve the power quality of the network in many ways. However it also depends on the type of the DG installed. DGs can further improve the voltage stability and decrease real and reactive power losses when located near the load.

DGs have many advantages as well as some drawbacks. One of the main drawbacks of the DGs is the initial cost. Most of the alternative energy sources like wind generation [7] and PV cells [8]-[10], [17] need advanced technology. Another drawback of the DG is poor efficiency. Maximum power point tracking algorithm is used to increase the output voltage of the boost converter in the PV inverter [15], [18]. Net

metering allows the consumers to sell the excess power to the grid. Over 40 states in the U.S have net metering.

### **2.3 Plug-in Hybrid Electric Vehicle Technology**

The first stage of development in electrical vehicles started in 1832 [14]. Approximately electric vehicles have been in use from 1832 to 1920 [14]. Lack of adequate horse power, demand of long range and availability of petroleum resulted in the disappearance of electric vehicles. The second stage of development in electric vehicles started in 1966 [14]. In 1966, the U.S congress encouraged the production of the electric vehicles to reduce greenhouse gas emission [14].

There are two types of plug-in electric vehicles (PEV) that are available in the market, Plug-in hybrid electric vehicles (PHEVs) and battery electric vehicles (BEV). Plug-in hybrid electric vehicle have two power systems. One is an internal combustion engine (IC) and the other is the battery energy storage system [14]. Battery electric vehicles have only one energy storage system. Both PEVs use the energy supplied from the grid. In the long run, vehicles cannot use only the battery power to run the vehicles because of the size and capacity limitations of the battery. PHEV is best suited for the vehicles because of both battery energy storage system and IC engine [11]-[13]. So, the vehicle will run either in electric mode or in the IC engine mode [14]. PHEV is a great way to integrate the transportation sector and electric sector [16]. The use of PHEVs is expected to significantly increase in the future and hence, large numbers of PHEVs may connect to the grid at a time. Some of the vehicles will be charging and some vehicles will be discharging at the same time. Better charger will be able to decrease injected

harmonics into the grid. The battery should support either charging or discharging according to the condition of battery and the power grid.

Integration of DGs to the utility grid is one of the advanced technologies to improve the power quality and to reduce the greenhouse gas emissions. Generally, most of the PHEVs will connect to the power grid at distribution side. Suitable battery charger for the PHEVs will decrease the losses into the grid. DGs and PHEVs together will improve the efficiency and reliability of the system as well as reduce the fuel consumption rate of both systems [19], [20].

## **Chapter Three**

### **Grid Connected Distributed Generations**

#### **3.1 Introduction**

In this chapter a grid connected wind turbine induction generator, centralized photovoltaic (PV) cell, Multi string PV technology and 12-bus power system network were modeled in Matlab®Simulink. The specifications and ratings of the machines were selected according to the standard guidelines to design the distributed generators. All the models are tested under different weather and load conditions.

#### **3.2 Grid Connected Wind Turbine Induction Generators (WTIGs)**

In most of the cases, distribution systems are unbalanced due to the asymmetrical line spacing and unbalanced loads. Therefore, all power network components are represented by a three phase system. The test power system network includes three squirrel-cage wind turbine induction generators. The stator of each generator is connected to a 60Hz three phase distribution network. The output voltage is regulated by controlling the pitch angle of the rotor. The pitch angle can control the nominal output voltage if the wind speed exceeds 8m/s [7].

One line diagram of the test power system network shows a 132KV, 60 Hz sub transmission network with short circuit capacity of 2500MVA feeding a 33KV distribution system with 132/33KV step down transformer.

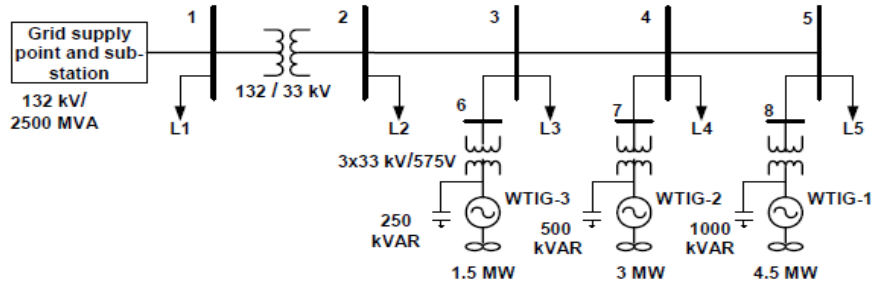


Figure 3. 1 One line diagram of the distribution system with WTIG

Three WTIG generators rated at 1.5MW, 3MW and 4.5MW, respectively under normal operating condition, and capacitive banks of 250KVar, 500KVar, and 1000KVar are connected at each generator to compensate the reactive power from WTIG to grid or grid to WTIG. The generators are connected to the distribution network through 575/33KV step-up transformer [7].

### 3.3 Modeling and Simulation of Test Power System Network

A three phase positive sequence grid network with 2.5MVA SSC was developed. Loads L1, L2, L3, and L4 are assumed to be constant. The 575/33KV step-down transformer and the 132/33KV step-down transformer are modeled by using the SimPowerSystems toolbox provided in the Matlab@Simulink.

#### 3.3.1 Wind Turbine Induction Generator

Wind turbine model was developed based on study state power characteristics. The output power ( $P_m$ ) of the wind turbine can be given as follows.

$$P_m = C_p(\lambda, \beta) \frac{\rho A}{2} v_{wind}^3 \quad (3.1)$$

Where  $A$  is turbine swept area ( $m^2$ ),  $\rho$  is air density ( $\frac{kg}{m^3}$ ) and  $C_p$  is the Performance coefficient of the turbine,  $v_{wind}$  is wind speed (m/s),  $\lambda$  is tip speed ratio of the rotor blade tip speed to wind speed,  $\beta$  is blade pitch angle. Wind turbine shaft is connected to the synchronous generator. Stator of the induction generator is connected to the three phase distribution network as shown in the Figure 3.1.

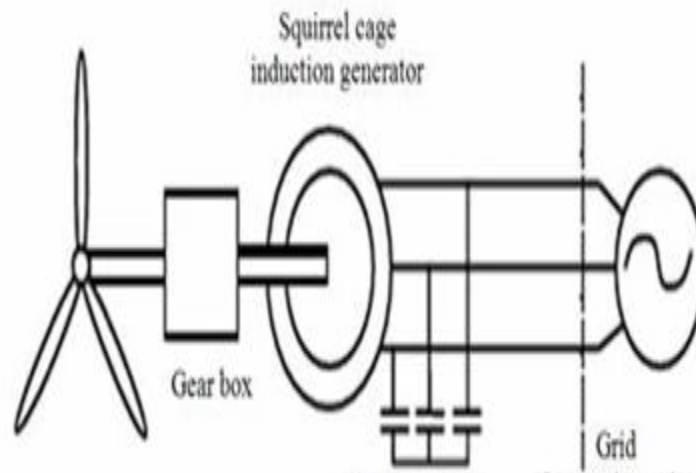


Figure 3.2: Block diagram of wind turbine induction generator

Figure 3.2 shows a schematic diagram of the wind turbine induction generator. Squirrel cage type induction generator is used in this study to design the wind turbine induction generator. Rotor of induction generator is driven by variable pitch wind turbine and stator of induction generator is connected to 3- $\phi$  grid. Figure 3.3 shows the Matlab®Simulink model of the wind turbine induction generator. The data acquisition block read will acquire all output signals generated from the wind turbine induction generator (WTIG).

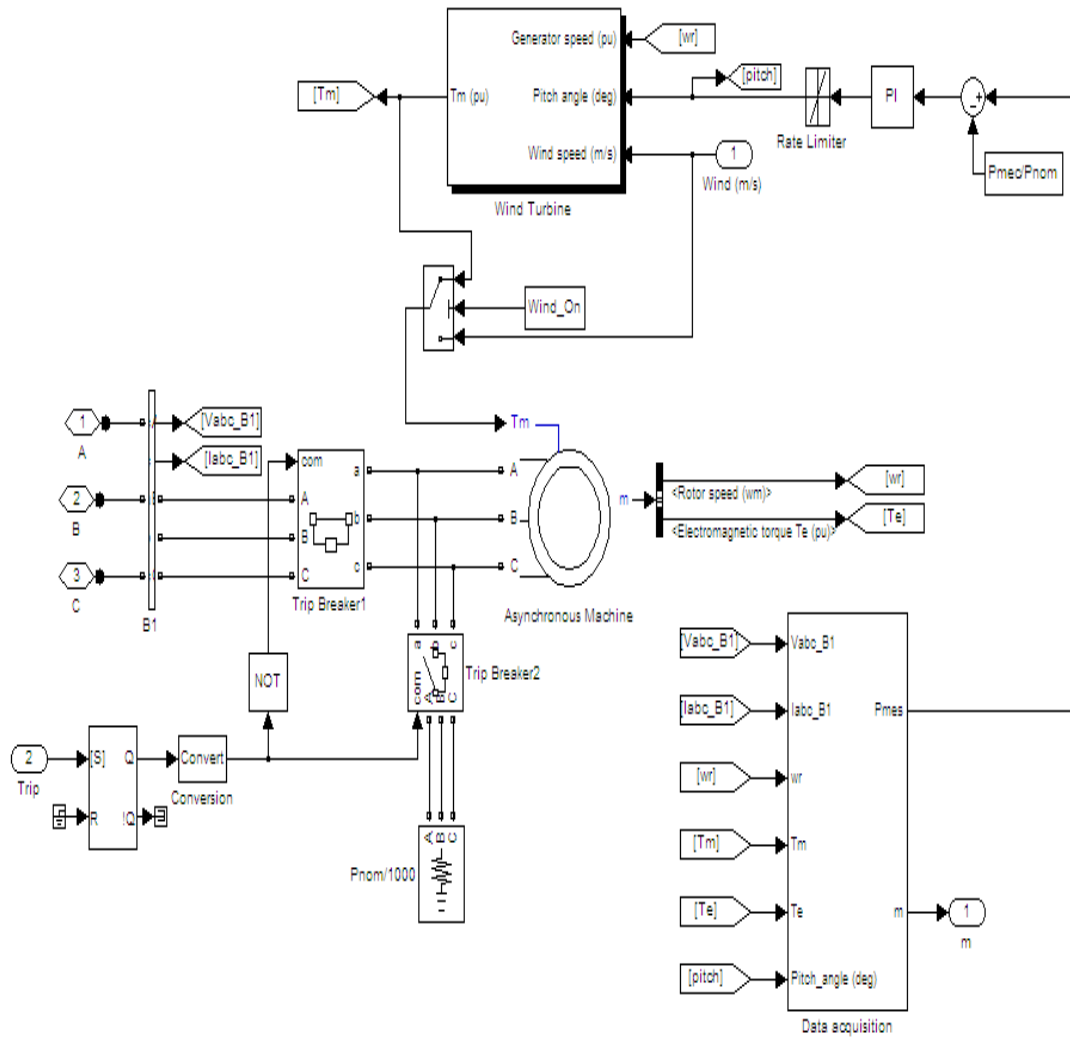


Figure 3.3: Matlab@Simulink model of wind turbine induction generator

### 3.3.2 Matlab@Simulink Model of the Test Power System Network

Figure 3.4 shows the Matlab@Simulink diagram of the test power system network presented in Figure 3.1. The power system network was modeled in the phasor simulation. Grounding transformer should limit the fault current of the network. The data acquisition blocks acquire the data from the various buses in the network. Those blocks are connected to scope to measure the output waveform at each bus.



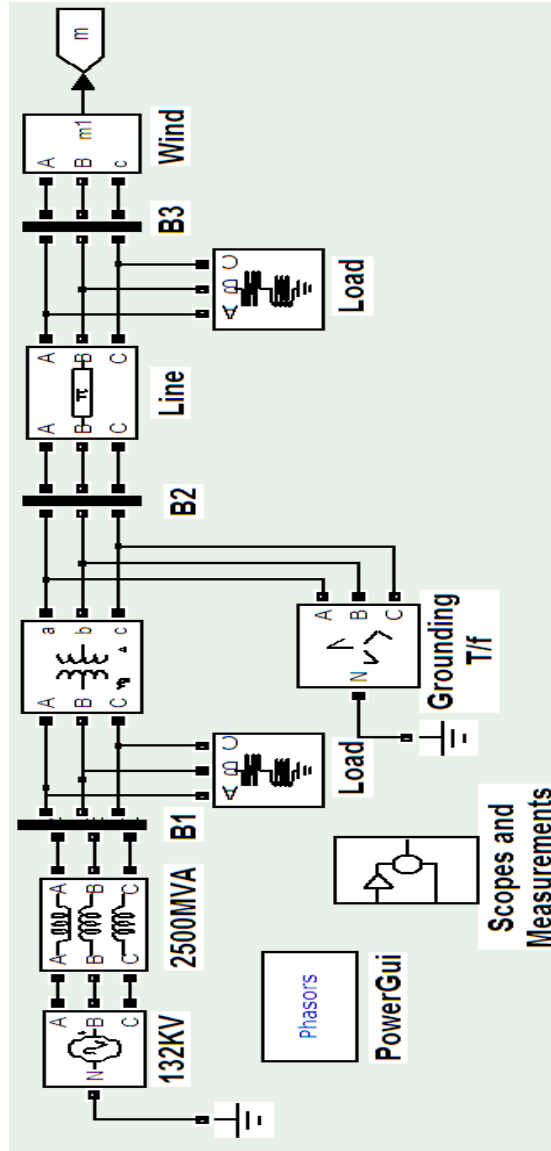


Figure 3.4 Matlab®Simulink model of the test power system network

Figure 3.5 shows a sub-system of the wind farm shown in the figure 3.4. WTIGs are connected to buses 6, 7 and 8 (Figure 3.1) through step up transformers and those buses are connected to the buses 3, 4 and 5 through  $\pi$ -section transmission line models. Three loads L2, L3 and L4 are shown in the network. Shunt capacitances are provided at each bus to provide necessary reactive power compensation to the network. AC positive

sequence voltage and current protections are enabled for the WTIG to protect against unwanted disturbances.

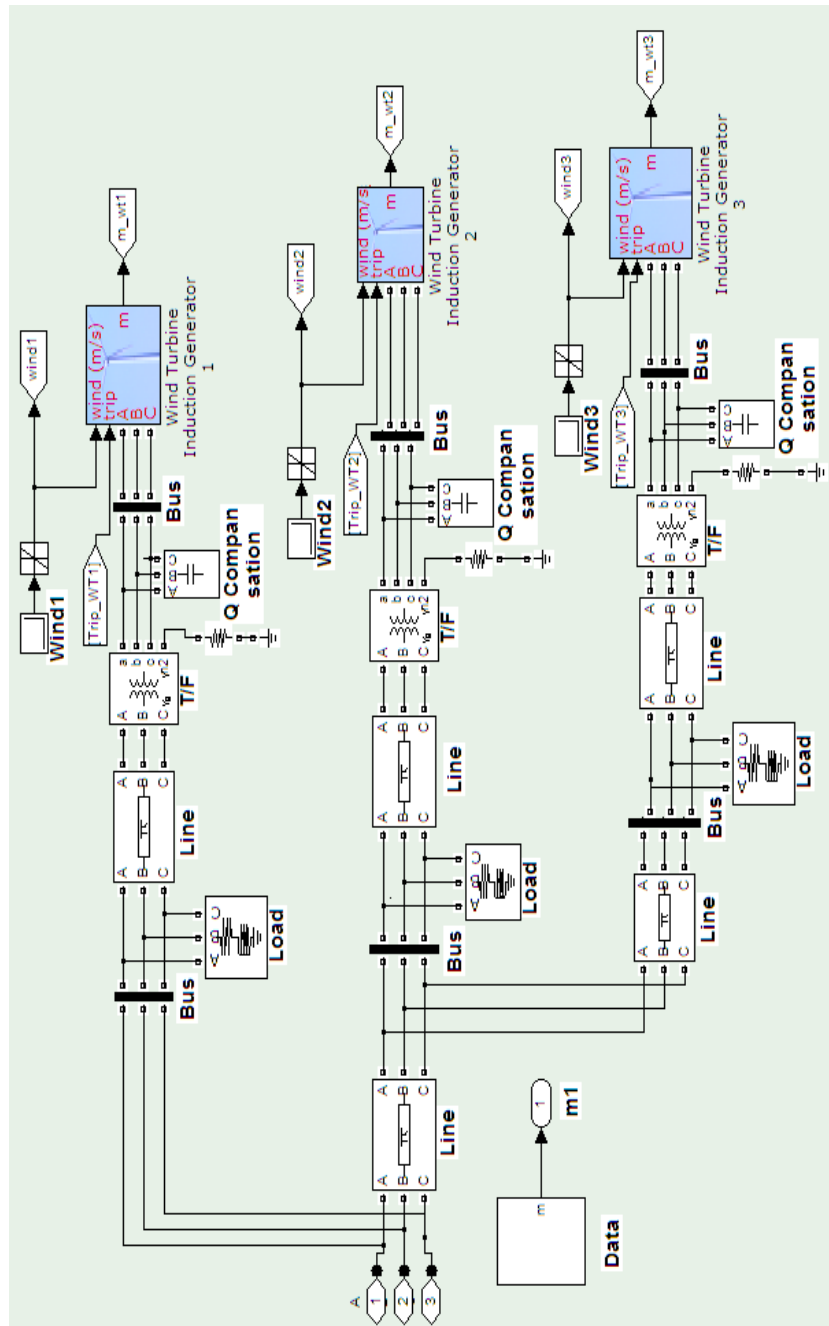


Figure 3.5 Matlab®Simulink model of the distribution network connected to WTIG

### 3.4 Simulation Results

The dynamic behavior of the WTIG, active and reactive power drawn/injected into the grid during the wind speed change is analyzed for constant wind speed and linear wind speed.

#### 3.4.1 Constant Wind Speed

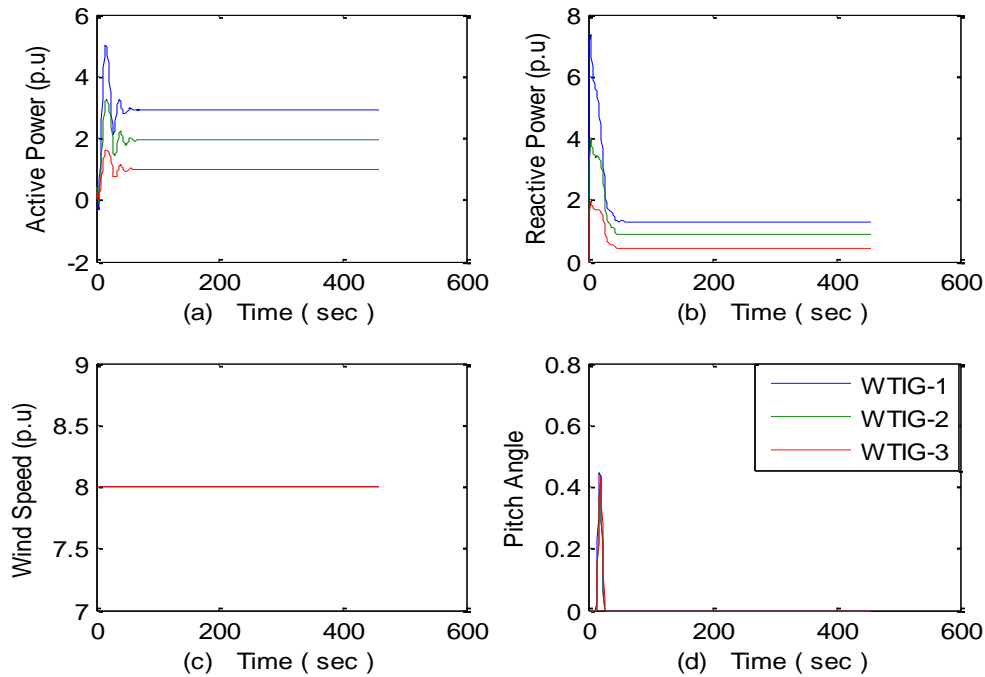


Figure 3.6 (a) Active power, (b) Reactive powers, (c) Wind speed, and (d) Pitch angel of the WTIG at constant speed

Figure 3.6 shows the active and reactive power generated by the WTIGs at bus 6, 7, and 8. A constant wind speed of 8m/s is applied to WTIGSs. The active power and reactive power generation of WTIGs are shown in the figure 3.5. WTIG-1 rated power is 4.5MW at wind speed of 9m/s, generates 2.91MW at constant wind speed of 8m/s. The negative reactive power generation indicates that WTIG absorbs 1.291MVAR of reactive power at constant wind speed of 8m/s. WTIG-2 rated power is 3.0MW at wind speed of

9m/s, generates 1.94MW, and observes 0.86VARs. WTIG-3 rated power is 1.5MW at wind speed of 9m/s, generates 0.98MW, and observes 0.43VARs. The pitch angle is controlled in order to limit the output voltage to its nominal value. Total power generated from the WTIG at 8m/s is less than the total load of the system. So the remaining power is observed from the grid.

### **3.4.2 Linear Wind Speed**

In this case-study linear change of wind speed is applied to the WTIGs. This type of wind speed change enables the WTIGs to inject active power into a network ranging from a minimum to a maximum value in a manner slow enough not to induce unwanted oscillations.

Figure 3.7 shows the real and reactive power generations of WTIGs for a linear change of wind speed 8m/s to 11m/s. At a lower wind speed of 8m/s, the real power generation and reactive power consumption of WTIG-1 are 2.91MW and 1.29MVAR, respectively. However at a wind speed 11m/s, the real and reactive powers are 4.5MW and 2.19MVAR, respectively. Hence if the wind speed increases, the real and reactive power increases. The corresponding values for WTIG-2 and WTIG-3 for wind speed 8m/s to 11m/s are 1.94MW, 1.01MVAR and 0.98MW, 0.43MVAR, respectively. Moreover, for wind speed 11m/s, the corresponding values are 3MW, 1.46MVAR and 1.5MW, 0.73MVAR. The pitch angle was varied in order to limit the power to its nominal value as shown in Figure 3.7.

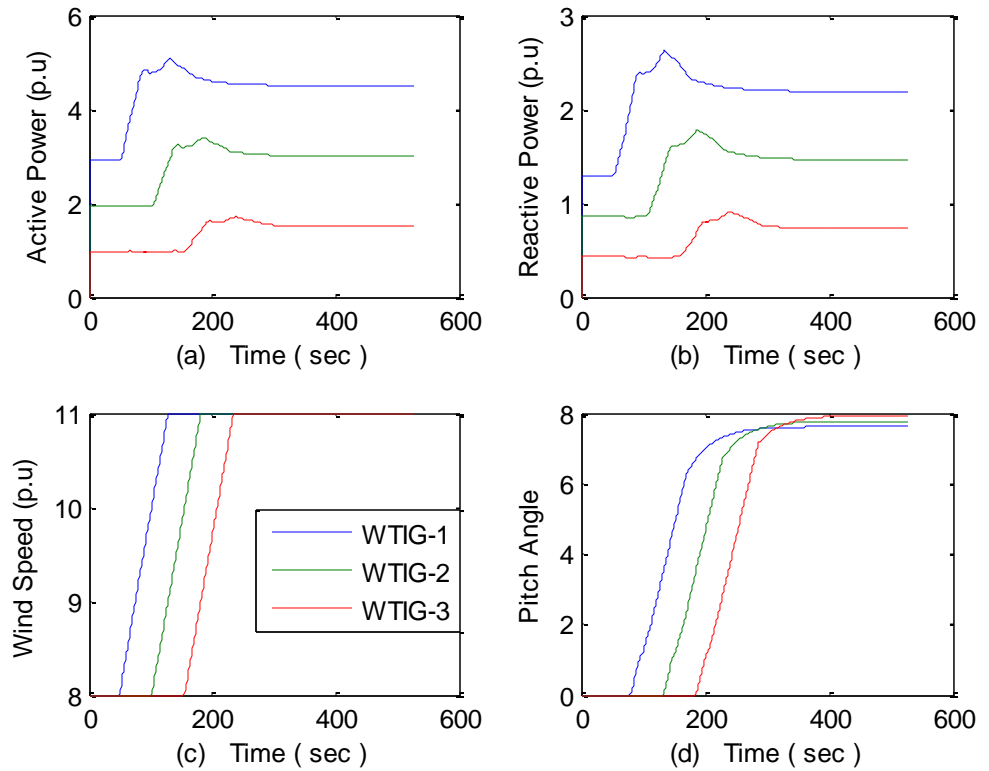


Figure 3.7 (a) Active power, (b) Reactive powers, (c) Wind speed, and (d) Pitch angle of the WTIG at linear change of wind speed

### 3.5 Modeling and Simulation of Photovoltaic Generation

#### 3.5.1 Photovoltaic Cells

Generally, photovoltaic cells (PV) convert solar energy into electricity. PV cells are made of semiconductor materials. The materials used in PV cells are mono-crystalline silicon, poly-crystalline silicon and Gallium Arsenide (*GaAs*), Cadmium Telluride (*CdTe*) and copper indium Diselenide (*CuInSe<sub>2</sub>*). Mono-crystalline silicon is the best model using one diode where the poly-crystalline silicon modeled by using two diode equivalent circuit. A typical PV cell generates voltage in the range of 0.5V for an input irradiance of 1 W/m<sup>2</sup> at 25<sup>o</sup>c [8]. The power producing by a one PV module is not sufficient to meet a required commercial or residential load. Several PV cells are

integrated and connected together, called PV modules. Parallel modules will increase the output current and series modules will increase the output voltage. Practically, several PV modules will have to be connected in series and parallel to increase the output power, called PV array. First, PV cells are connected in series to produce the output voltage and then all the PV modules are connected in parallel to allow the system to produce more current. A typical PV cell module is made up of around 36 or 72 cells connected in series.

### 3.5.2 Characteristics of PV Cell

Figure 3.8 shows an equivalent model of a typical PV cell, where,  $I_{pv,cell}$  is the PV cell current,  $R_{sh}$  is the equivalent parallel resistance and  $R_s$  is equivalent series resistance. The equivalent circuit of an ideal PV cell is represented by a current source in parallel with a diode. The output of the current source is directly proportional to the light falling on the PV cell [9].

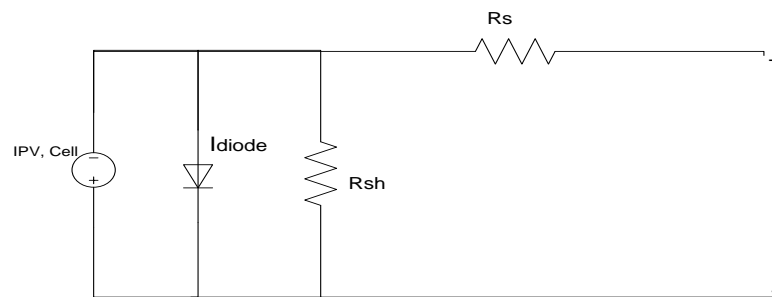


Figure 3.8 Equivalent circuit of a PV cell

Applying Kirchhoff's law to the above circuit, under ideal conditions;

Series and parallel resistance are zero in ideal condition [9].

$$I = I_{PV,CELL} - I_{diode} \quad (3.2)$$

$$I = I_{PV,CELL} - I_{0,cell} \left[ \exp\left(\frac{q*V}{\alpha*k*T}\right) - 1 \right] \quad (3.3)$$

Where,

$I_{PV,CELL}$ : The current generated by the solar irradiance [A].

$I_{diode}$ : The Shockley diode equation [A].

$I_{0,cell}$ : The reverse saturation or leakage current of the diode [A].

q: Electron charge [ $1.602 * 10^{-19}$ C].

T: Temperature of the p-n junction diode in Kelvins

$\alpha$ : The diode ideality constant which lies between 1 and 2 for mono-crystalline silicon.

Equation 3.3 is for idea conditions. It does not represent the I-V characteristics of practical PV array. A practical circuit composed of several PV modules will require the addition of series resistance ( $R_s$  or  $r_s$ ) and parallel resistance ( $R_p$  or  $R_{sh}$ ). Adding of  $R_s$  and  $R_p$  the equation 3.3 becomes [9]

$$I = I_{PV} - I_0 \left[ \exp\left(\frac{V+R_s*I}{\alpha*Vt}\right) - 1 \right] - \frac{V+R_s*I}{R_p} \quad (3.4)$$

The current generated by the solar module is dependent on the solar irradiance and it also depends on the temperature

$$I_{PV} = (I_{PV,n} + K_t \Delta T) \frac{G}{G_n} \quad (3.5)$$

Where  $K_t$  is the temperature coefficient of  $I_{SC}$ ,  $G$  is the irradiance in  $W/m^2$  and  $G_n$  is irradiance at standard operating condition.

Diode saturation current can be expressed as

$$I_0 = \frac{I_{sc,n} + K_I \Delta T}{\exp\left[\frac{V_{oc,n} + K_V \Delta T}{V_t * \alpha}\right] - 1} \quad (3.6)$$

' $V_{oc,n}$ ' is open circuit voltage,  $I_{sc,n}$  is the short circuit current,  $V_t = N_s * kT/q$  is the thermal voltage of the module with  $N_s$  cells connected in series.

If the cells are composed of  $N_s$  series connections of PV modules, then

$$I_{PV} = I_{PV,module} * N_p \quad (3.7)$$

$$I_o = I_{o,module} * N_p \quad (3.8)$$

If the cells are composed of  $N_p$  parallel connections of PV modules, then

$$R_s = R_{s,module} * \left(\frac{N_s}{N_p}\right) \quad (3.9)$$

$$R_p = R_{p,module} * \left(\frac{N_s}{N_p}\right) \quad (3.10)$$

All practical PV cells have higher values of  $R_p$  and lower values of  $R_s$  for giving more output power and fill factor [17].

Fill factor in PV inverter is defined for "judgment of efficient cell operation" [16].

$$FF = \frac{P_{max}}{V_{oc} * I_{sc}} \quad (3.11)$$



### 3.5.3 Efficiency of PV Cell

The efficiency of a PV cell is defined as the ratio of peak power to input solar power. Where,  $V_{mp}$  is the voltage at peak power  $I_{mp}$  is current at peak power,  $I$  is solar irradiance, and  $A$  is the area on which solar irradiance falls.

$$\eta = \frac{V_{mp} \cdot I_{mp}}{I \left( \frac{KW}{m^2} \right) \cdot A(m^2)} \quad (3.12)$$

### 3.5.4 Maximum Power Point Tracking (MPPT)

When a PV array is directly connected to a load, the operating point is seldom at the MPPT. Generally a power converter is needed to adjust the power flow from PV array to load. Different types of algorithms are used to perform the MPPT like perturb and observe algorithm and incremental conductance algorithm etc. [15].

PV array is connected to the grid by an inverter. Whenever the output power of the PV array is less than the load, then the grid supplies power to the load. If the PV array output power is greater than the load, then it can supply the power to the load and excess power will be delivered to the grid. PV system can be used as stand-alone, installed on site, or grid connected system.

### 3.5.5 Types of PV Inverters

There are three important inverter technologies are shown below [10]

1. single power processing inverter
2. dual power processing inverter
3. multi stage inverter

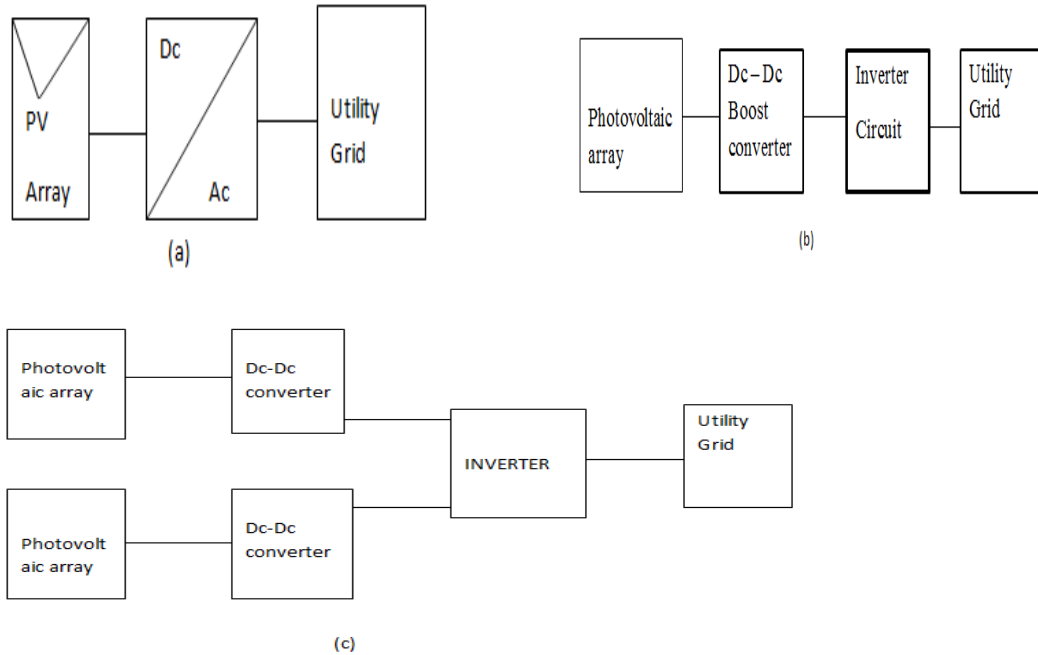


Figure 3.9 Types of PV inverters

Figure 3.9 (a) shows a single power processing stage inverter. It handles MPPT, voltage amplification, as well as grid current control. Figure 3.9(b) shows a dual power processing inverter, where the DC-DC converter handles the MPPT and DC-AC inverter handles the grid current control. Voltage amplification is handled in both converters. Figure 3.9 (c) shows a multi stage inverter, where each PV string is connected to a separate DC-DC converter and the output of both converters connected to DC-AC inverter. Grid voltage is controlled by DC-AC inverter and MPPT is controlled by DC-DC converters. Voltage amplification is handled in all the converters.

### 3.6 Matlab@Simulink Modeling of PV Technology

#### 3.6.1 PV Array

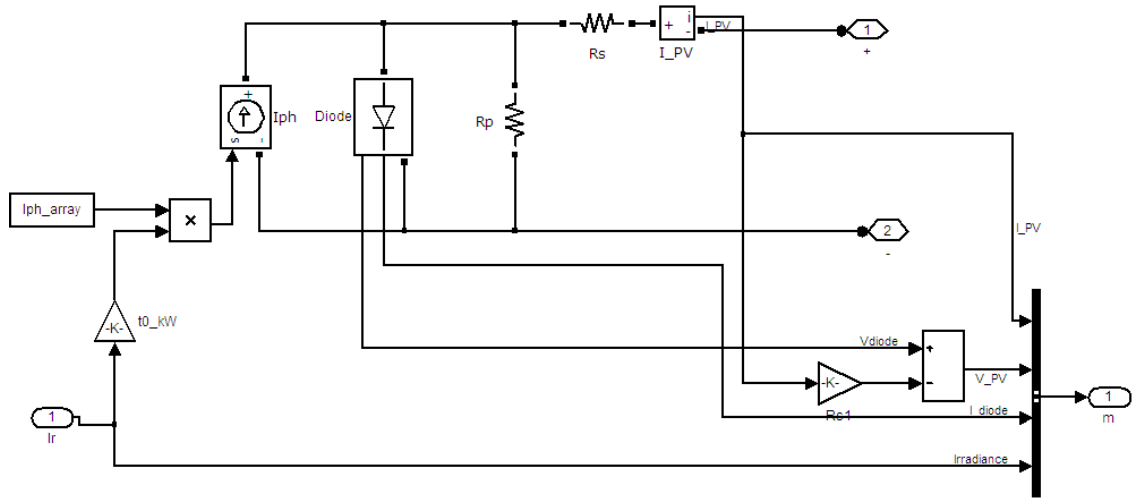


Figure 3.10 Mathematical model of photovoltaic cell

A Photovoltaic cell module was developed based on equations 3.1 to 3.9. The model shows current source in parallel with a diode, series resistance ( $R_s$ ) and parallel resistance ( $R_p$ ) represents a single PV cell, Fig. 3.10.

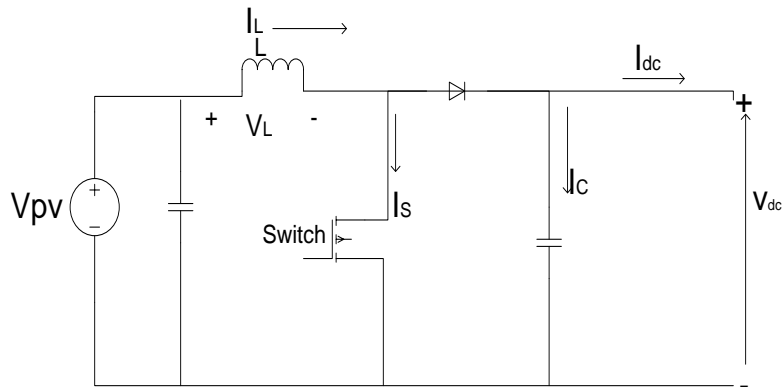


Figure 3.11 Circuit diagram of the boost converter

Figure 3.11 shows the circuit diagram of the boost converter. The output of PV array is connected to a boost converter to boost the voltage from normal unregulated DC voltage to a fixed DC voltage. The output voltage of the boost converter can control by controlling the duty cycle of the IGBT switch [18].

In this model, the incremental conductance algorithm [15] is used to track the maximum power output. The output of the MPPT algorithm was subtracted from initial duty cycle, which is given to IGBT gate through PWM generator. The gate drive circuit is as shown in the Figure 3.12.

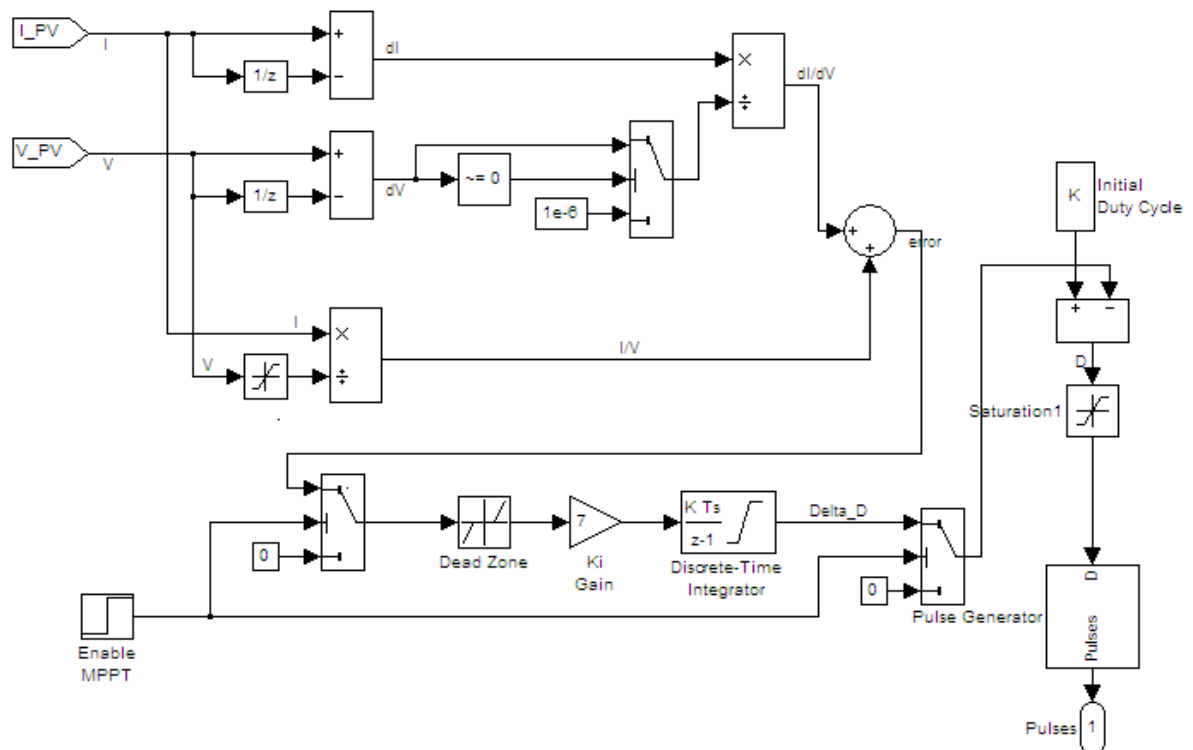


Figure 3.12 Gate control circuit of IGBT converter

The output of boost converter is fed to a 3-phase, three level voltage source inverter by a DC link. The DC link capacitor acts as a buffer between the input DC power and output inverter. DC link voltage is kept constant all the time. The DC link voltage will subtract from a fixed value, and a PI controller is used to control the DC link voltage.

Figure 3.13 shows, a 3- $\Phi$  three level voltage source inverter. Figure 3.14 shows, a gate control circuit of 3- phase bridge inverter. Power factor correction (PFC), DC voltage regulator and current regulator are modeled for gate control of the inverter. PWM generator is used to control the switching time of the gate control circuit. The output of the inverter is connected to the 60Hz utility grid via a 3 phase step up transformer.

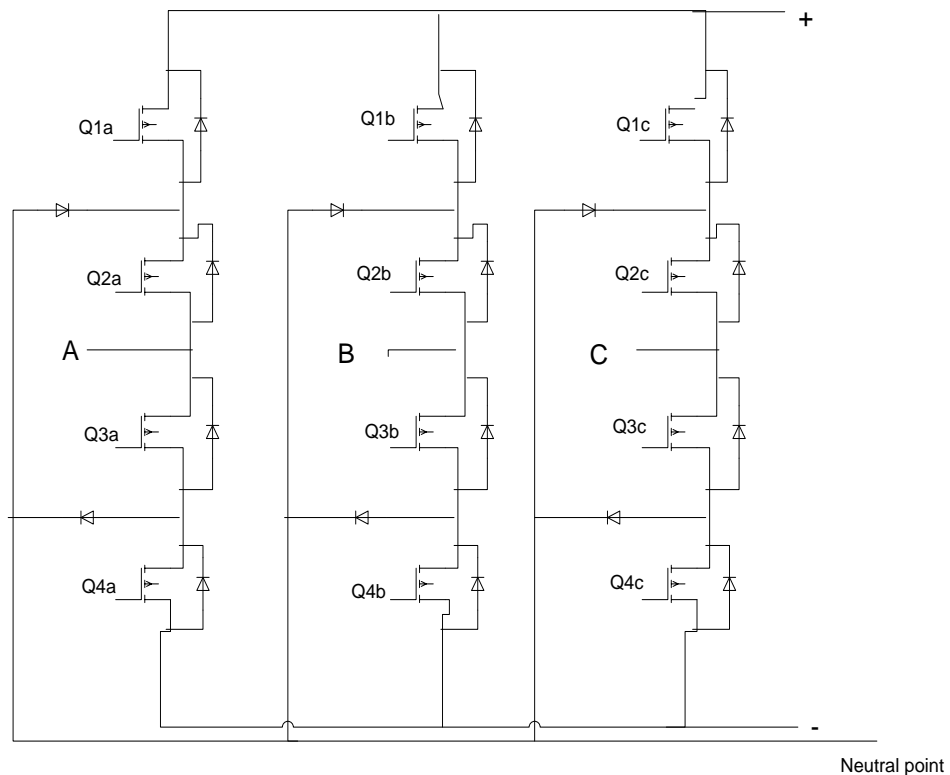


Figure 3.13 3-  $\Phi$  three level bridge inverter

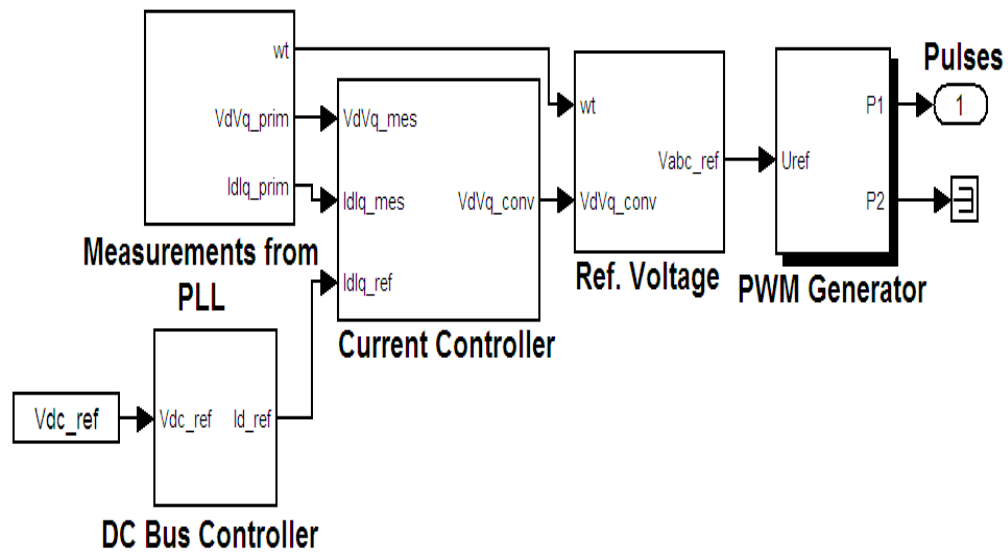


Figure 3.14 Gate control circuit of inverter

PV cell input current varies based on input solar irradiance. The output of PV array is connected to a boost converter, where the gate circuit of the boost converter is controlled by MPPT (incremental conductance) algorithm. A DC link is placed between boost converter and the 3-phase bridge inverter. The gate control circuit of the inverter circuit is controlled by a voltage regulator, a current regulator, and a PFC. Finally, the output of the inverter is connected to the utility grid via step up transformer.

Figure 3.15 shows, a Simulink diagram of PV array connected to the utility grid. The simulation was developed using the discrete simulation tool provided in the Matlab®Simulink toolbox. All scopes are shown in the scopes and measurements block.

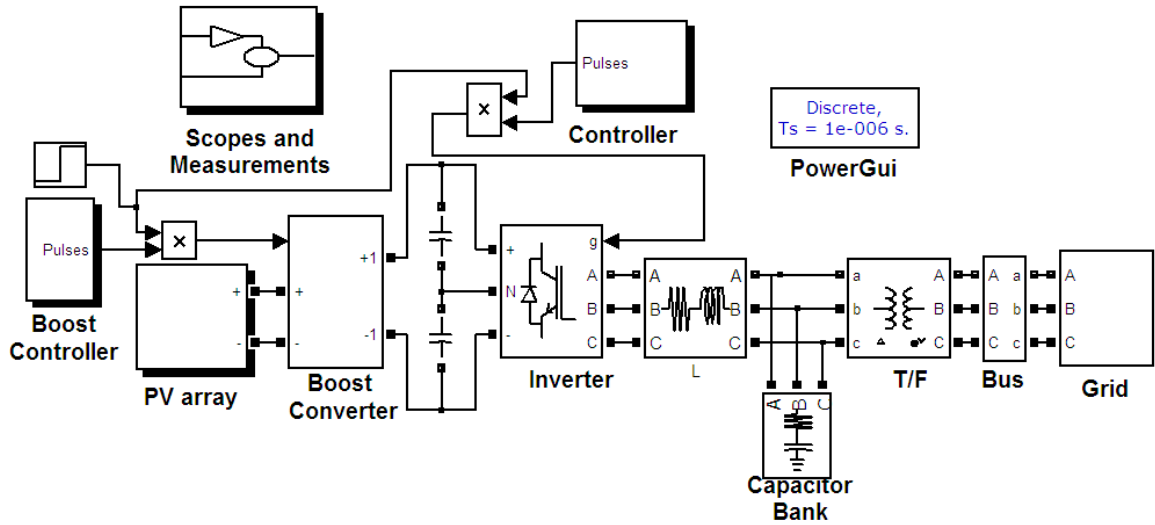


Figure 3.15 Simulink diagram of the grid connected PV system

### 3.6.2 Simulation Results

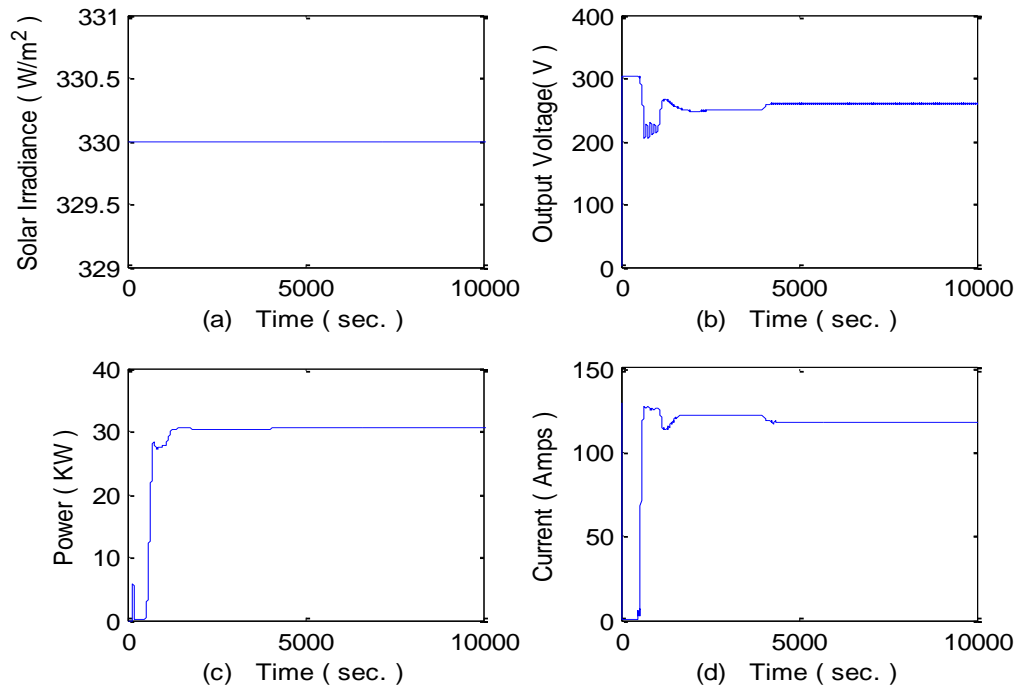


Figure 3.16 (a) Solar irradiance, (b) PV array output voltage, (c) PV array output power, and (d) PV array output current

Figure 3.16 shows, the simulation results of solar irradiance, PV array output voltage, output current and power. Initially, output voltage of PV array is zero. Constant irradiance of 330 W/m<sup>2</sup> is applied to the PV array. The output voltage and current is increase from zero to maximum. The output power of PV array is increased with respect to the voltage and current. PV array is generating 30KW of power.

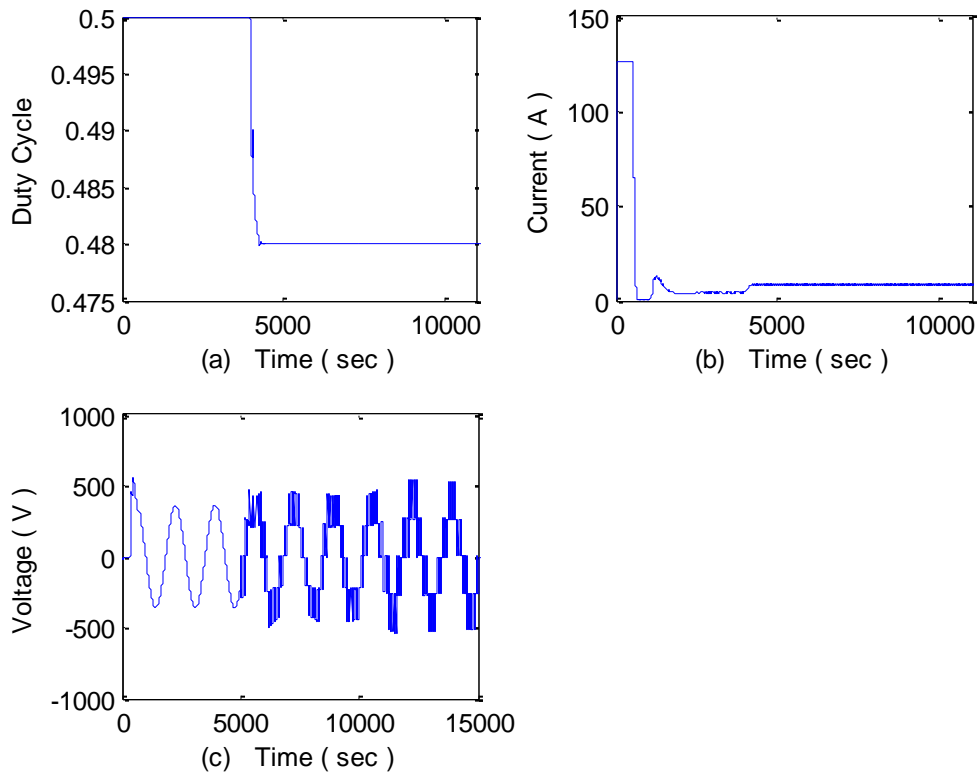


Figure 3.17 Measurements of (a) Boost converter duty cycle, (b) Diode current of PV array, and (c) VSC voltage

Figure 3.17 shows the duty cycle of the boost converter, the diode current of PV array, and voltage at the voltage source converter. Initially, the duty cycle of the boost converter is taken as 0.5. The MPPT algorithm calculated the necessary correction for the



duty cycle i.e. 0.48, to get the maximum output from the boost converter. The output voltage of VSC is increased at the duty cycle 0.48.

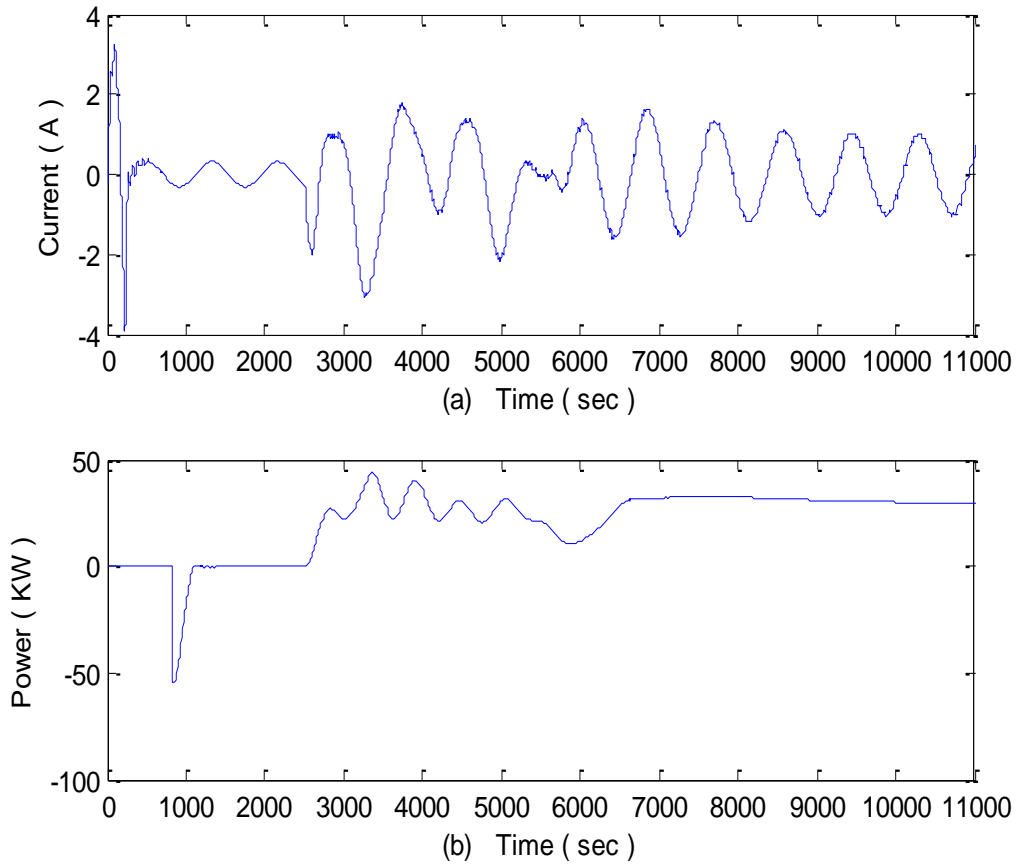


Figure 3.18 (a) Current at the utility grid, (b) Power at the utility grid

Figure 3.18 shows simulation outputs of the current and power at the utility grid. 30KW, 20KV power is transferring from PV inverter to the grid. Initially, output power of PV array is zero. Voltage Source Converter (VSC) is absorbing power from the grid, after few seconds PV array starts generating power with the applied irradiance, and transferring power to the utility grid. Current transients will present in the initial stage of

simulation as shown in Figure 3.18 (a). The harmonics will reduce, when the PV array starts generating power at MPPT.

### Voltage Harmonic Distortion

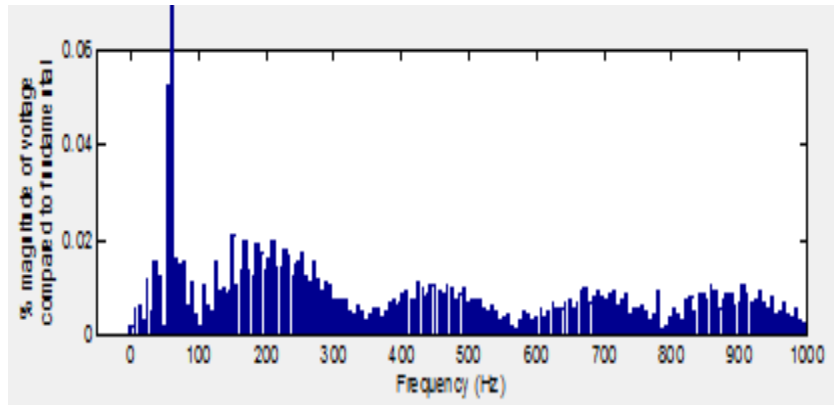


Figure 3.19 Voltage harmonic distortions at the utility grid

### Current Harmonic Distortion

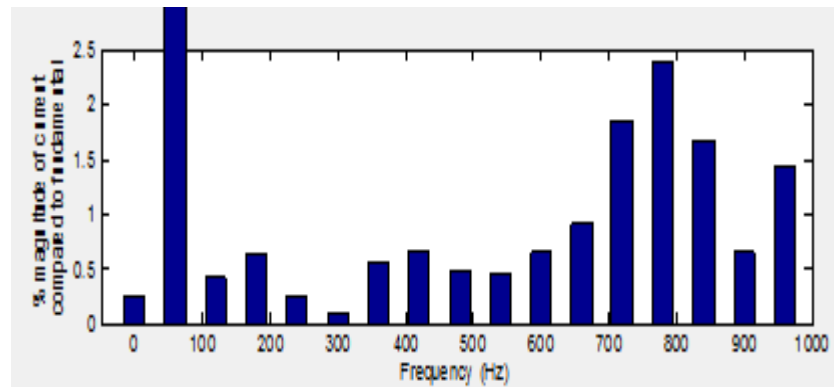


Figure 3.20 Current harmonic distortions at the utility grid

Figures 3.19, and 3.20 show the voltage harmonic distortion and the current harmonic distortion at the utility grid. PV array injected 0.04% of voltage harmonic distortion and 5.79% of current harmonic distortions into the utility grid.

### 3.7 Simulation of PV Array with Multi Stage Inverter

The block diagram of multi stage inverter PV technology is shown in Figure 3.21. The outputs of two PV arrays are connected to separate DC-DC converters, and the converters are connected in parallel. The Perturbs & observes technique is used to control the gate circuit of boost converters. The output of DC-DC converter is connected to an inverter by a DC link. The output of DC-DC converter is connected to an inverter by a DC link.

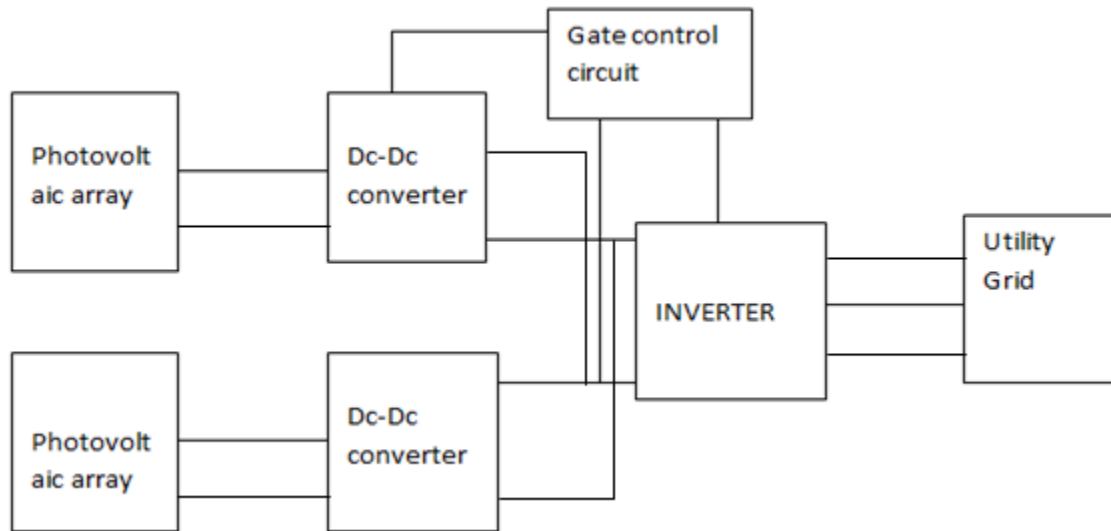


Figure 3.21 Multi stage PV technologies

#### 3.7.1 Matlab®Simulink Modeling of Multi Stage PV Technology

Figure 3.29 shows the Matlab®Simulink model of a Multi stage PV inverter. Measurements and scopes sub-system shows, scope of PV converter, inverter, grid voltages and currents. The simulation was developed by using the discrete simulation tool provided in the Simulink. Capacitor banks are used to control the reactive power flow and voltage stability at the utility grid.

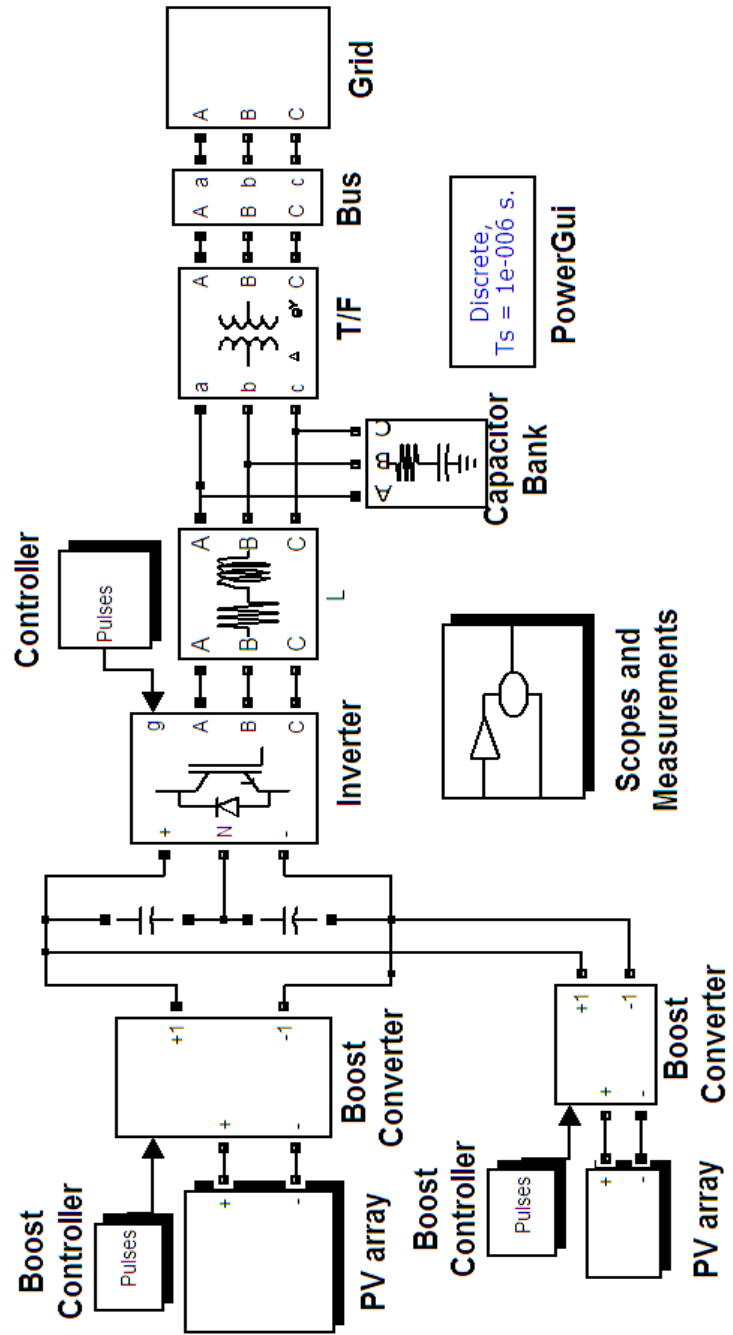


Figure 3.22 Matlab@Simulink model of the multi stage PV inverter

### 3.7.2 Simulation Results

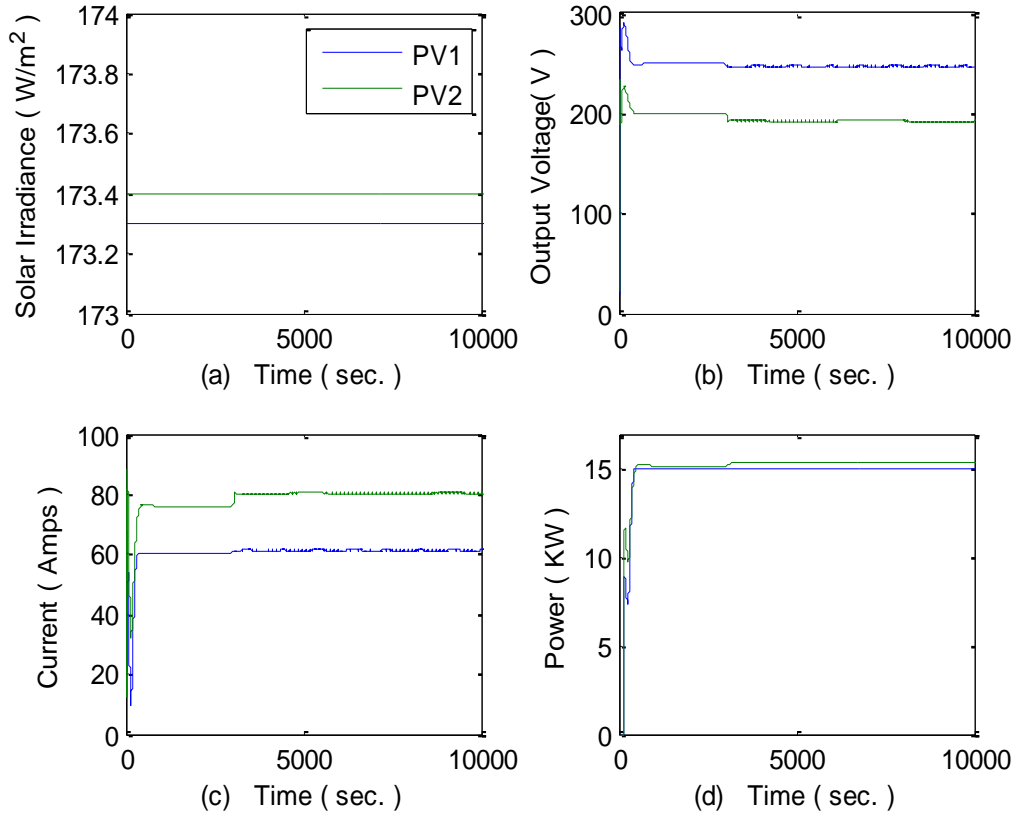


Figure 3.23 Measurements at PV1 and PV2 (a) Solar irradiance, (b) Output voltage, (c) Current, and (d) Output power

Figure 3.23 shows, the simulation results of solar irradiance, PV1 and PV2 output voltage, output current and power. Initially, output voltage of PV1 and PV2 is zero. Constant irradiance of 173.3 and 173.4 W/m<sup>2</sup> is applied to the two PV arrays. The output voltage and current is increase from zero to maximum. The output power of PV1 and PV2 is increased with respect to the voltage and current. PV1 is generating power of 15KW at 260V and PV2 is generating power of 15KW at 195V.

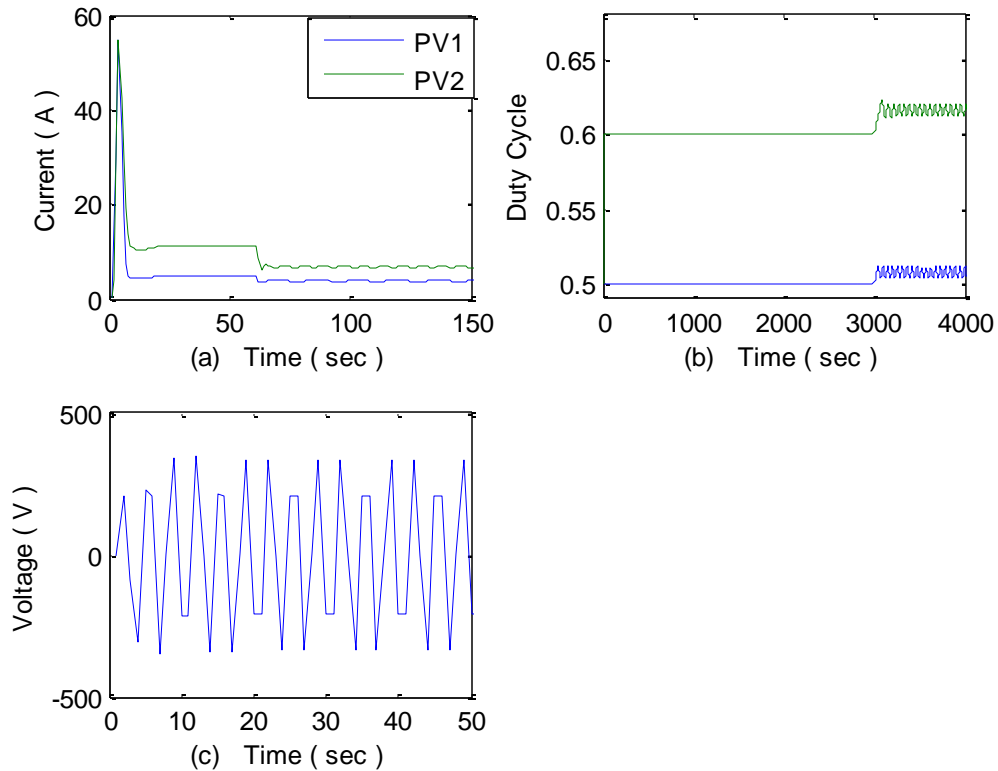


Figure 3.24 Measurements of (a) Diode current of PV array, (b) Boost converter duty cycle, and (c) VSC voltage

Figure 3.24 shows the duty cycle of the boost converters, the diode current of PV array, and voltage at the voltage source converter. Initially, the duty cycle of the boost converters are taken as 0.5 and 0.6. The MPPT algorithm calculated the necessary correction for the duty cycle i.e. 0.51 and 0.52, to get the maximum output from the boost converter. The output voltage of VSC is increased at after correcting the duty cycle of the boost converter.

Figure 3.25 shows the current, and power at the utility grid. 30KW at 260V is transferring from PV inverter to the utility grid. Initially, output power of PV1 and PV2 is zero. Transients will present in the initial stage of simulation as shown in Figure 3.25 (a). The harmonics will reduce, when the PV array starts generating power at MPPT.

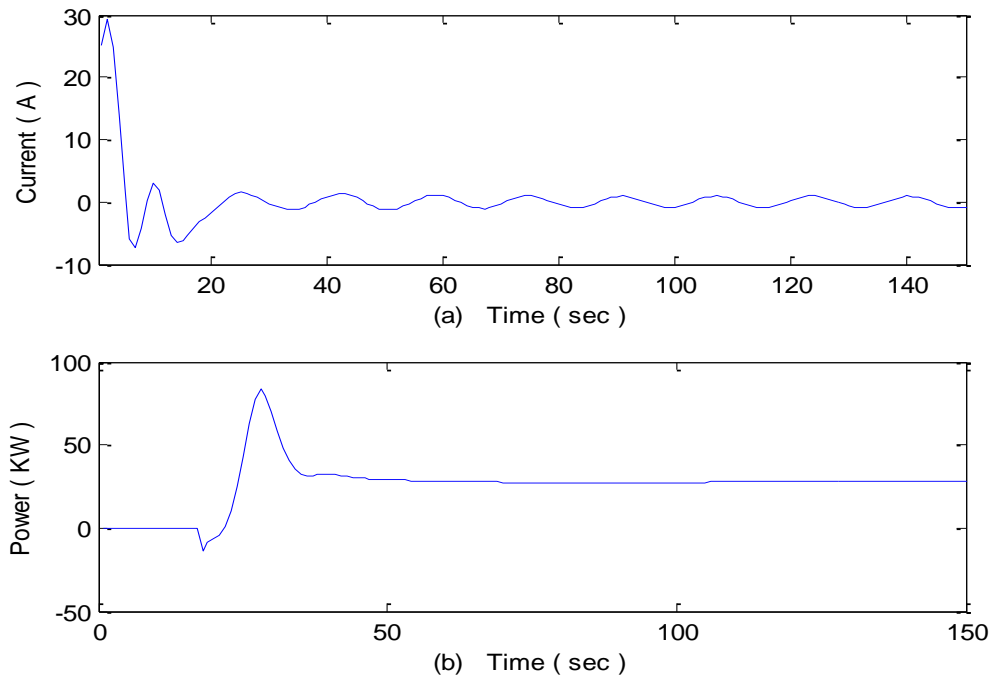


Figure 3.25 (a) Current at the utility grid, and (b) Power at the utility grid

The voltage harmonic distortion at the utility grid is as shown in Figure 3.26. PV1 and PV2 are injecting 3.02% of total voltage harmonics into the grid. Figure 3.27 shows the current harmonic distortion at the utility grid, 4.37% of current harmonic distortions are injected by the PV1 and PV2.

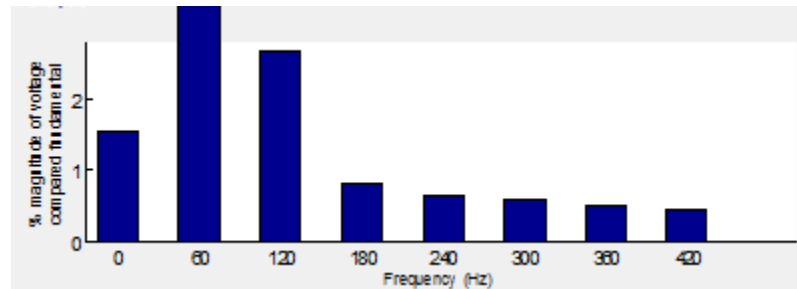


Figure 3.26 Voltage harmonic distortions at the utility grid

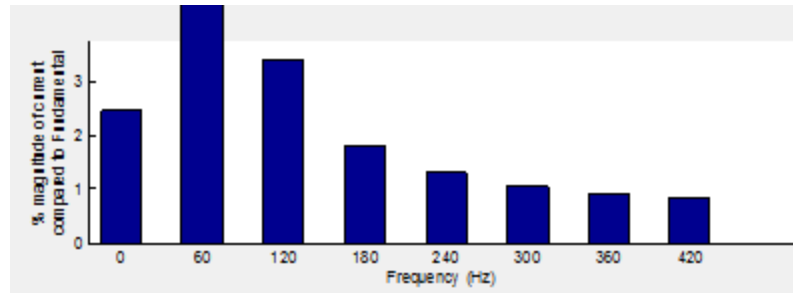


Figure 3.27 Current harmonic distortions at the utility grid

### 3.8 12-Bus Power System Network

A one line diagram of 12-bus power system network is as shown in Figure 3.28 [20]. It consists of three distribution generators at bus 5, 6, 9, and loads at bus 2, 5, 6 and 9. PV inverters are connected to the utility grid via step down transformer. Three PV inverters supply power to the loads. If the power of three PV generators is less than the total load, then utility grid will supply power to the load. Three PV generators supply power back to the grid when total generation is greater than the load demand.

Load changing and power electronics switches inject harmonics into grid, affecting the power quality. Throughout the simulation, loads are assumed to be constant, input solar irradiation is assumed constant, and initially the system voltage is stable. Distribution line parameters and load details are shown in table 3.1 and 3.2.

Table 3.1 Distribution line details

line	Distance in (Km)	Voltage (kv)	Power Rating (KVA)
B1-B2	20	120	250
B2-B4	10	25	100
B2-B4	10	25	100
B2-B12	15	25	100
B4-B6	10	25	100
B3-B5	10	25	100
B9-B10	10	25	100
B10-B11	25	25	100
B11-B12	25	25	100

Table 3.2 Load details

Bus no.	RloadKW	Q (KVAR)
Bus 2	200	30 L load
Bus 5	10	10 C load
Bus 6	10	10 C load
Bus 7	4.00E+01	20 L load
Bus 8	40	20 L load
Bus 9	10	10 C load



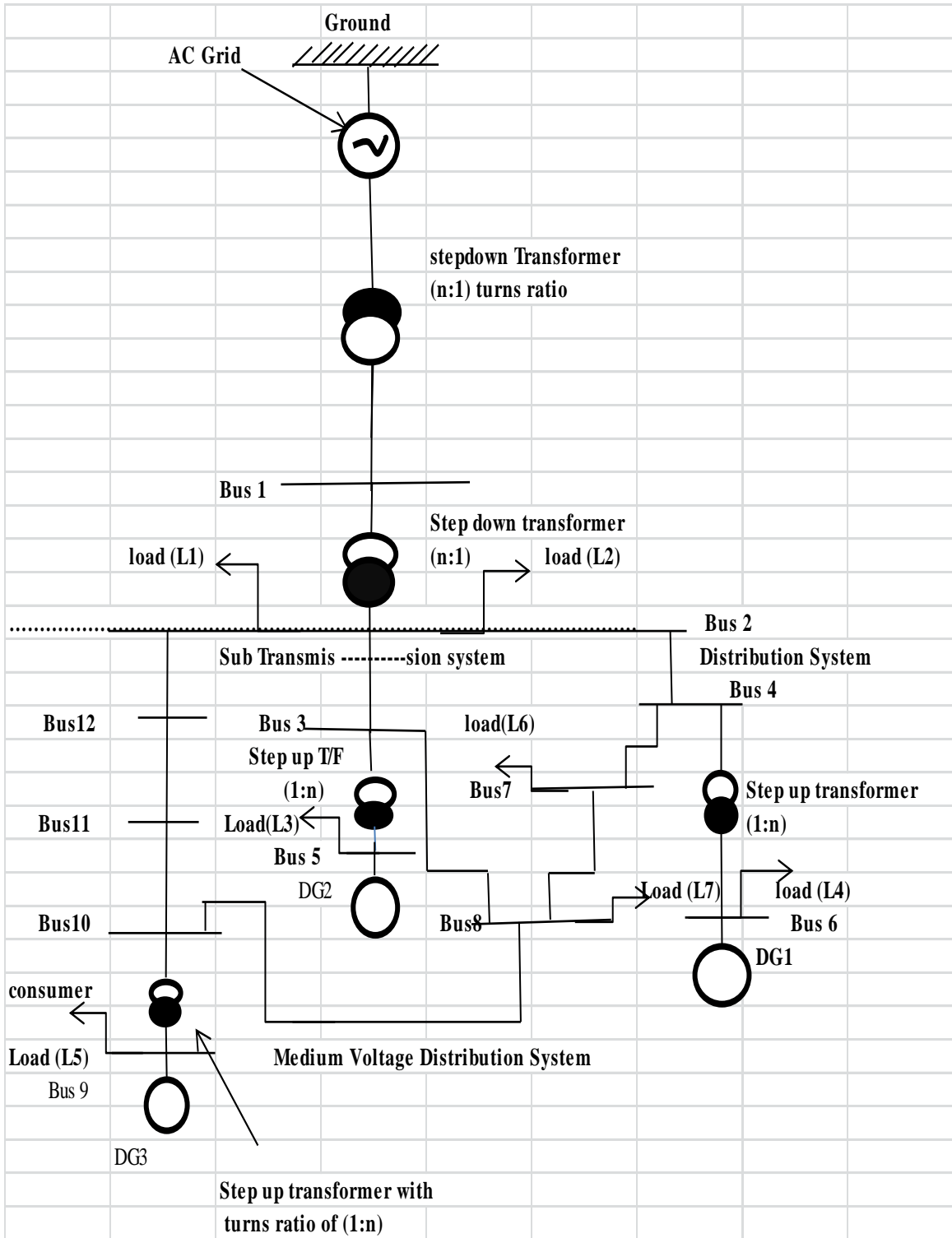


Figure 3.28 One line diagram of 12-bus power system network

### 3.8.1 Matlab®Simulink Model of the 12-bus IEEE Test Power System Network

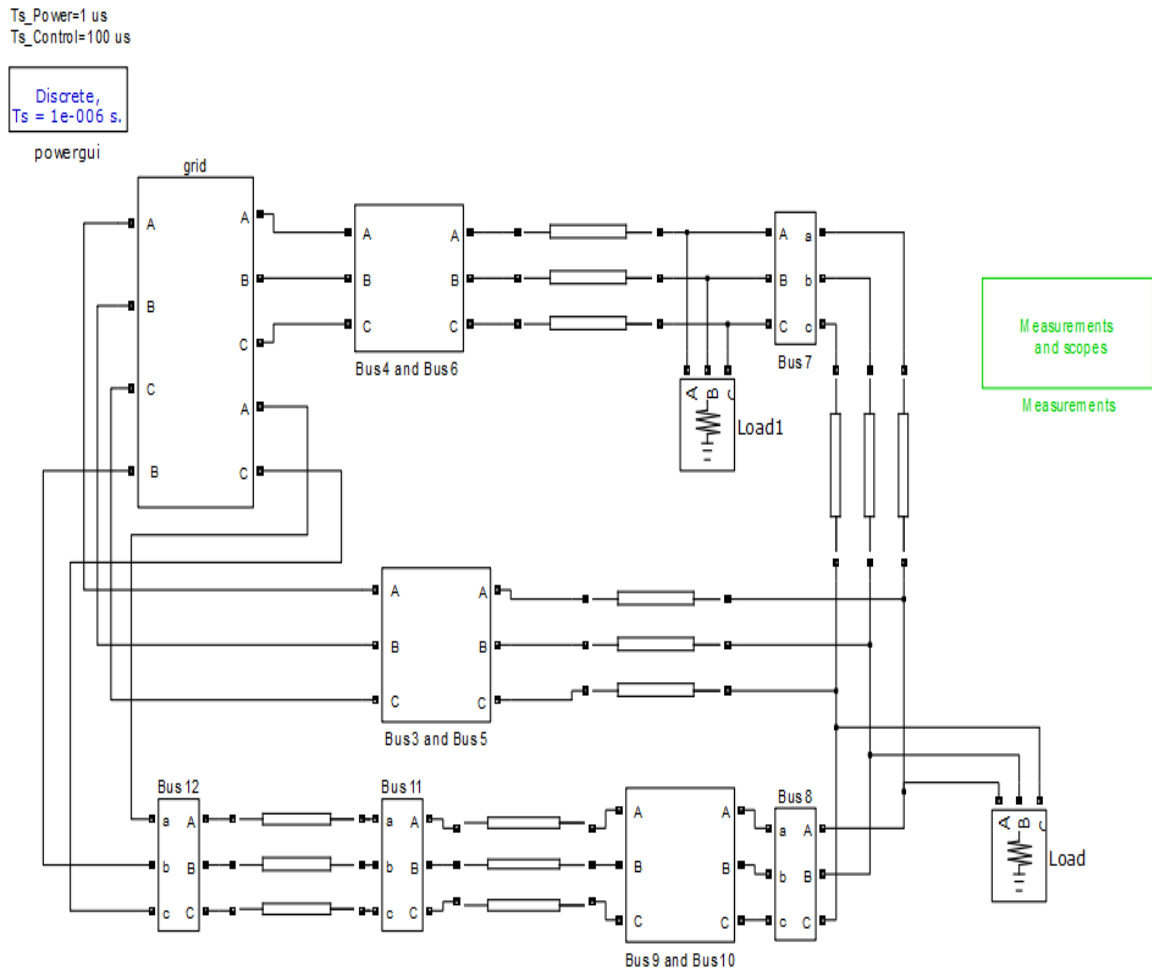


Figure 3.29 Matlab®Simulink model of 12-bus power system network

Figure 3.29 shows, Matlab®Simulink model of the 12-bus test power system network. The simulation was performed by using discrete simulation tool. T-section lines are considered to model distribution network. Measurements and scopes sub-system shows all scopes generates in the simulation. Simulation results are shown in section 3.8.2.

### 3.8.2 Simulation Results

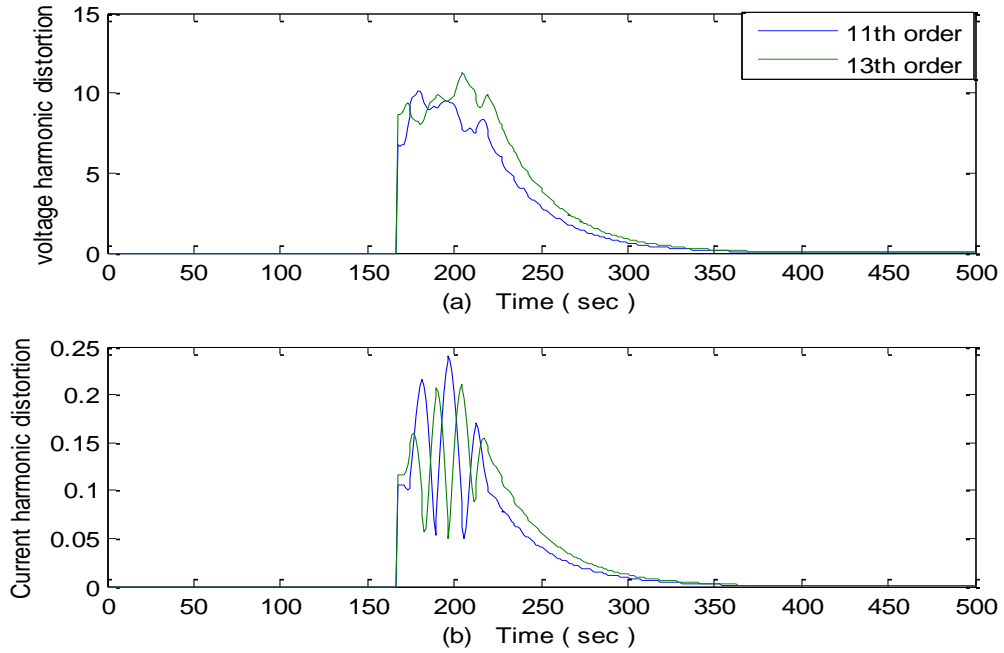


Figure 3.30 (a) 11<sup>th</sup> and 13<sup>th</sup> order voltage harmonic distortions at bus 1, and (b) 11<sup>th</sup> and 13<sup>th</sup> order current harmonic distortions at bus 1

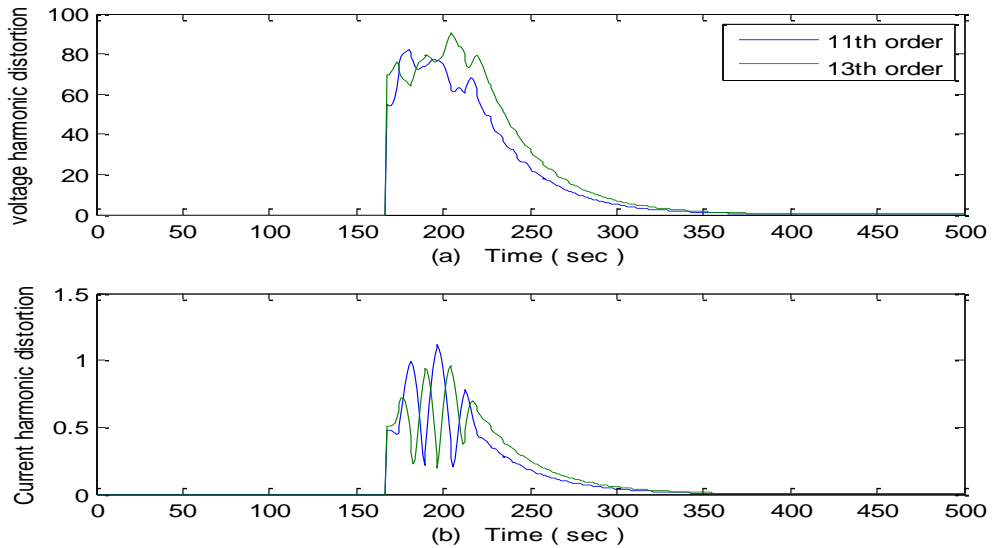


Figure 3.31 (a) 11<sup>th</sup> and 13<sup>th</sup> order voltage harmonic distortions at bus 2, and (b) 11<sup>th</sup> and 13<sup>th</sup> order current harmonic distortions at bus 2

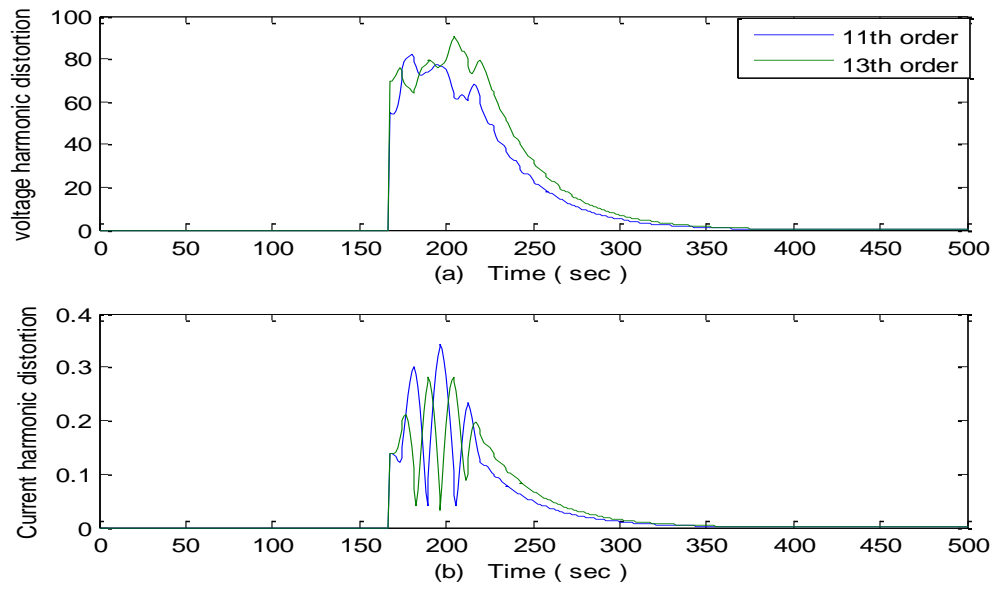


Figure 3.32 (a) 11<sup>th</sup> and 13<sup>th</sup> order voltage harmonic distortions at bus 3, and (b) 11<sup>th</sup> and 13<sup>th</sup> order current harmonic distortions at bus 3

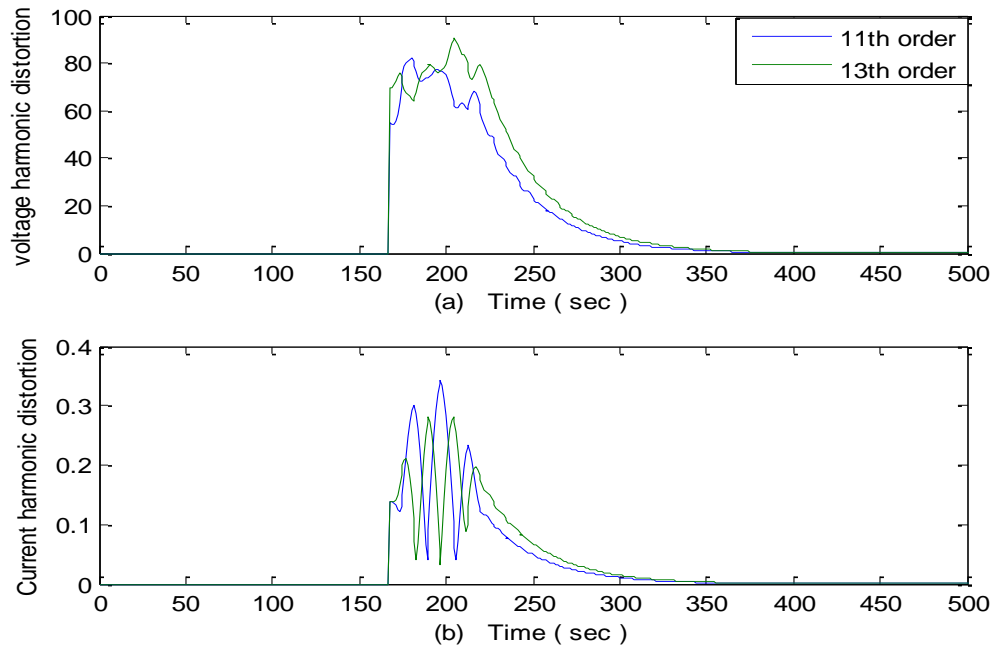


Figure 3.33 (a) 11<sup>th</sup> and 13<sup>th</sup> order voltage harmonic distortions at bus 4, and (b) 11<sup>th</sup> and 13<sup>th</sup> order current harmonic distortions at bus 4

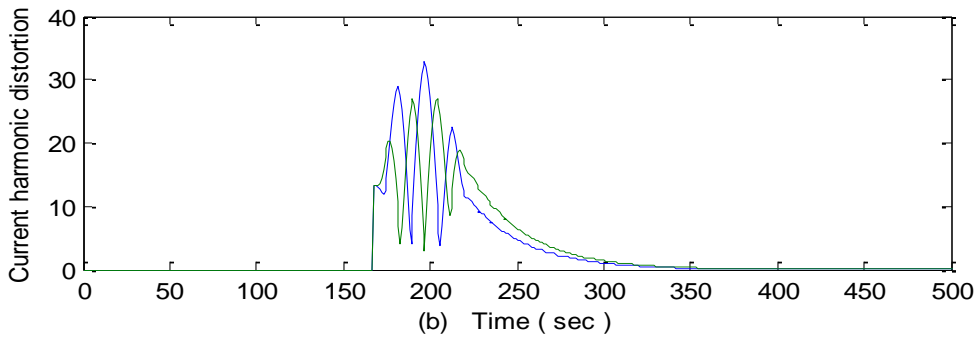
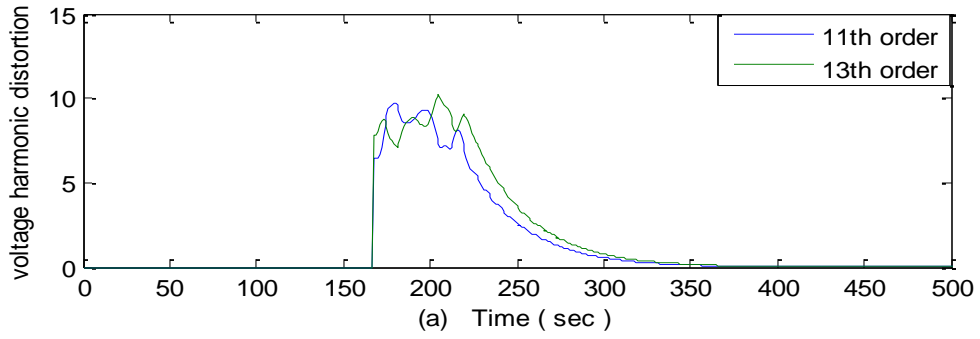


Figure 3.34 (a) 11<sup>th</sup> and 13<sup>th</sup> order voltage harmonic distortions at bus 5, and (b) 11<sup>th</sup> and 13<sup>th</sup> order current harmonic distortions at bus 5

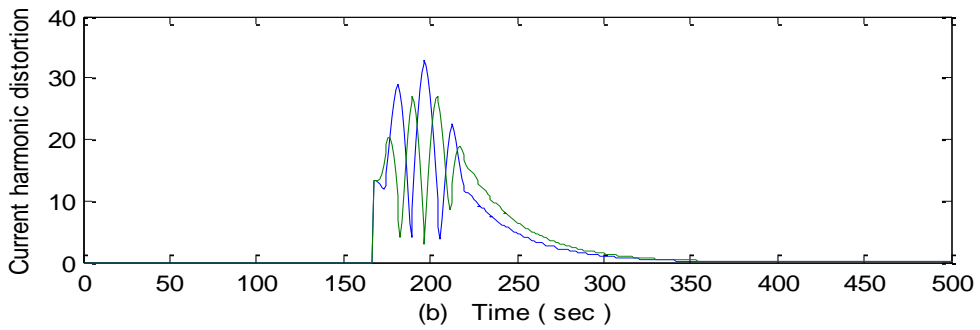
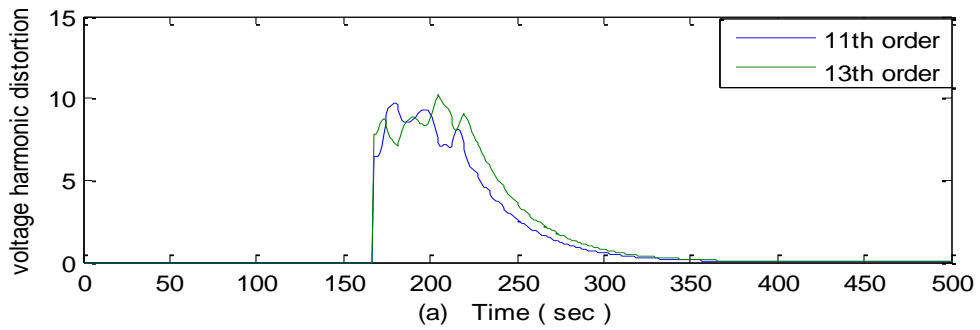


Figure 3.35 (a) 11<sup>th</sup> and 13<sup>th</sup> order voltage harmonic distortions at bus 6, and (b) 11<sup>th</sup> and 13<sup>th</sup> order current harmonic distortions at bus 6

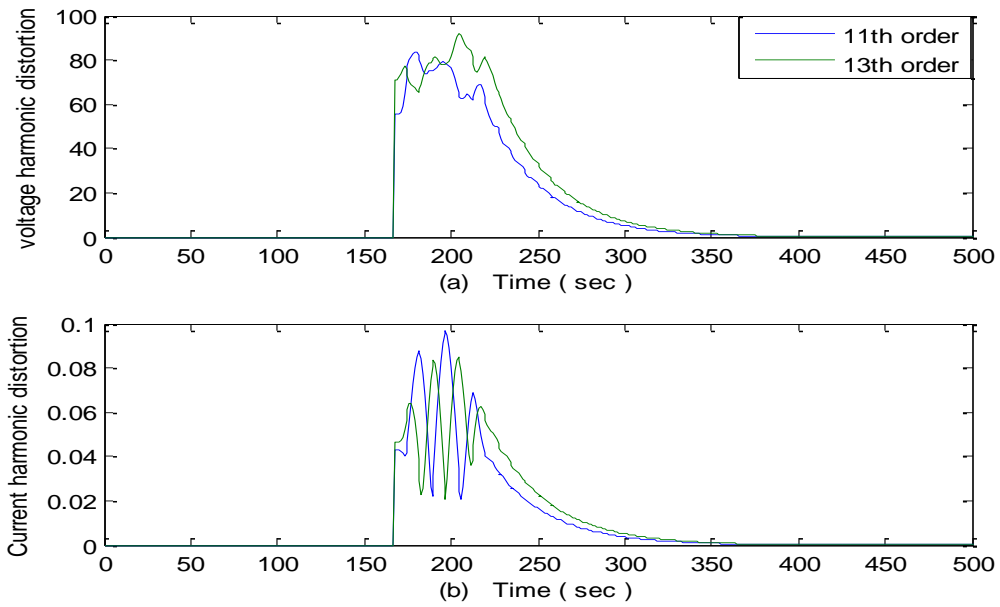


Figure 3.36 (a) 11<sup>th</sup> and 13<sup>th</sup> order voltage harmonic distortions at bus 7, and (b) 11<sup>th</sup> and 13<sup>th</sup> order current harmonic distortions at bus 7

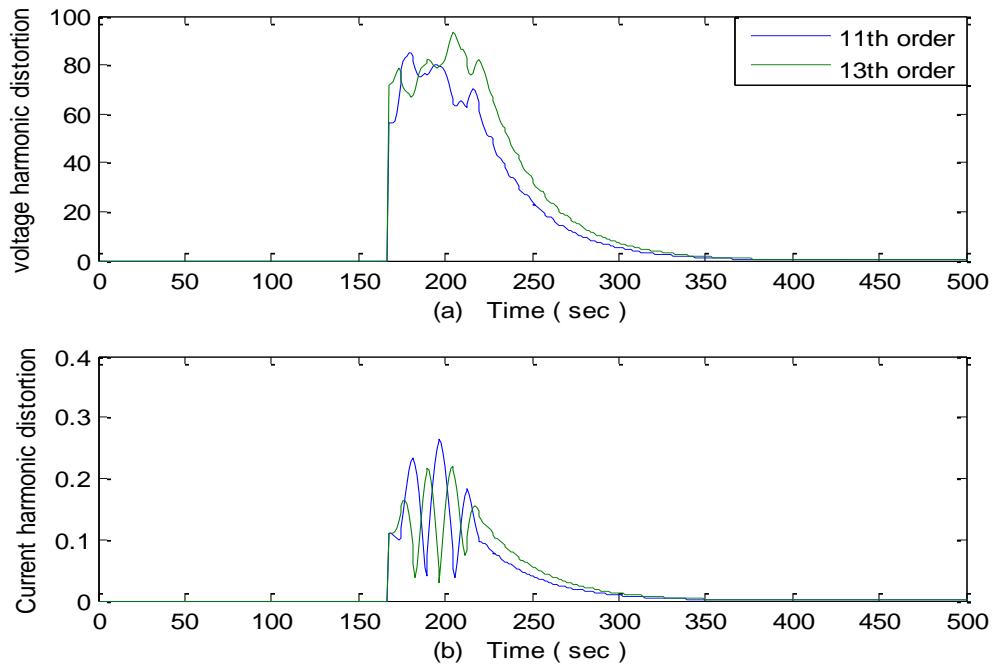


Figure 3.37 (a) 11<sup>th</sup> and 13<sup>th</sup> order voltage harmonic distortions at bus 8, and (b) 11<sup>th</sup> and 13<sup>th</sup> order current harmonic distortions at bus 8

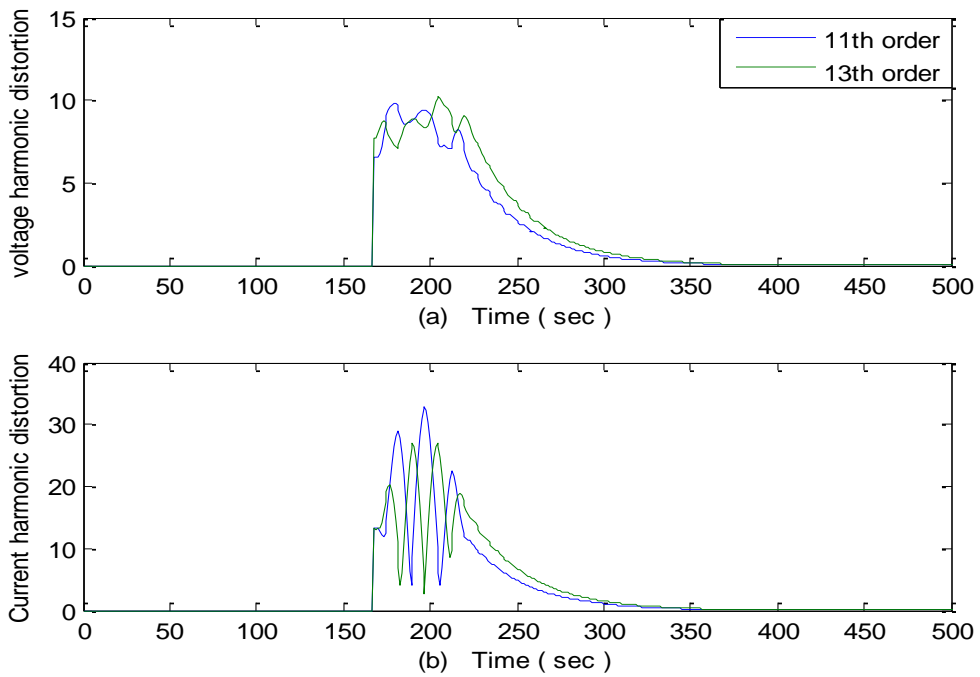


Figure 3.38 (a) 11<sup>th</sup> and 13<sup>th</sup> order voltage harmonic distortions at bus 9, and (b) 11<sup>th</sup> and 13<sup>th</sup> order current harmonic distortions at bus 9

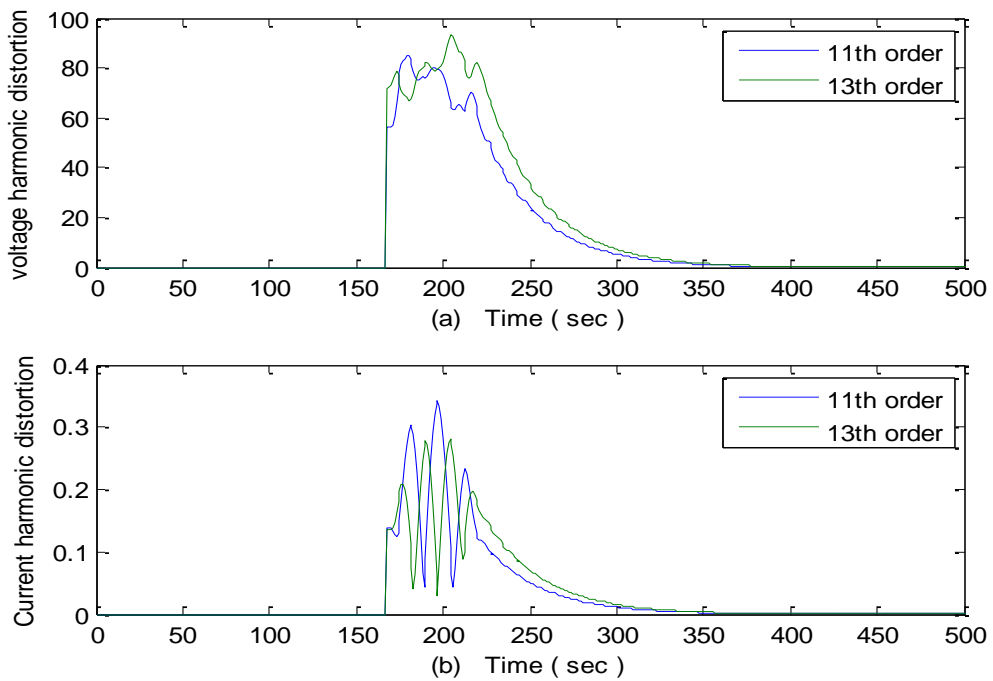


Figure 3.39 (a) 11<sup>th</sup> and 13<sup>th</sup> order voltage harmonic distortions at bus 10, and (b) 11<sup>th</sup> and 13<sup>th</sup> order current harmonic distortions at bus 10

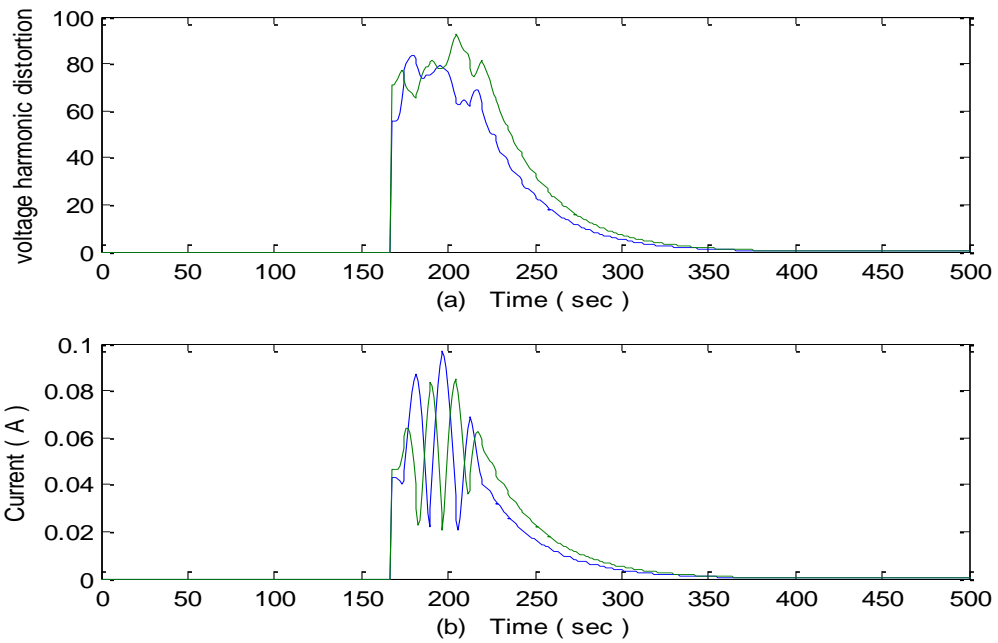


Figure 3.40 (a) 11<sup>th</sup> and 13<sup>th</sup> order voltage harmonic distortions at bus 11, and (b) 11<sup>th</sup> and 13<sup>th</sup> order current harmonic distortions at bus 11

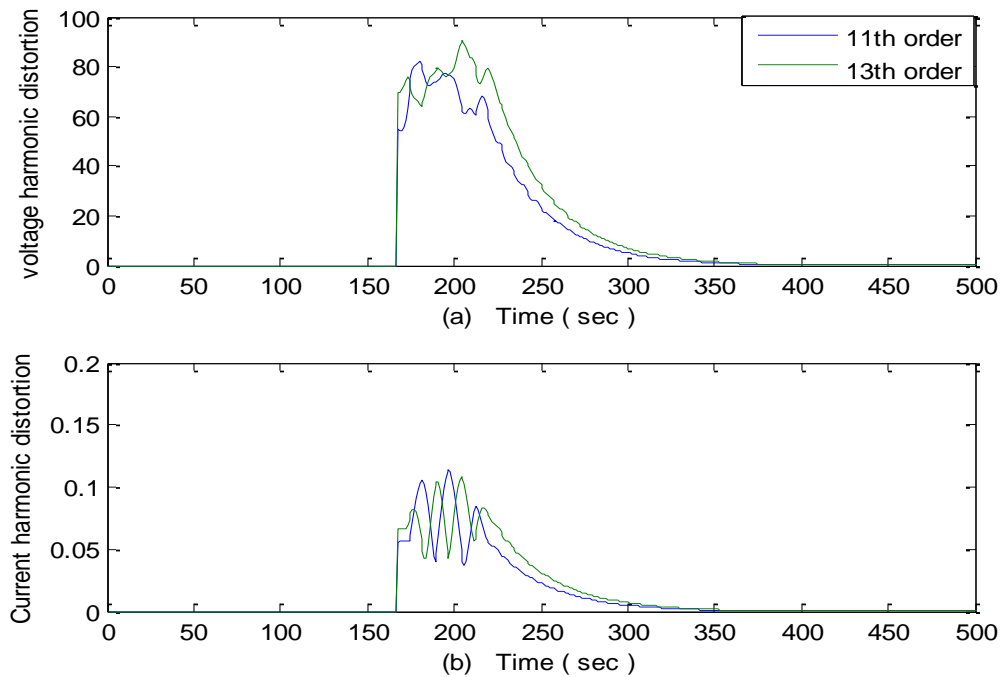


Figure 3.41 (a) 11<sup>th</sup> and 13<sup>th</sup> order voltage harmonic distortions at bus 12, and (b) 11<sup>th</sup> and 13<sup>th</sup> order current harmonic distortions at bus 12



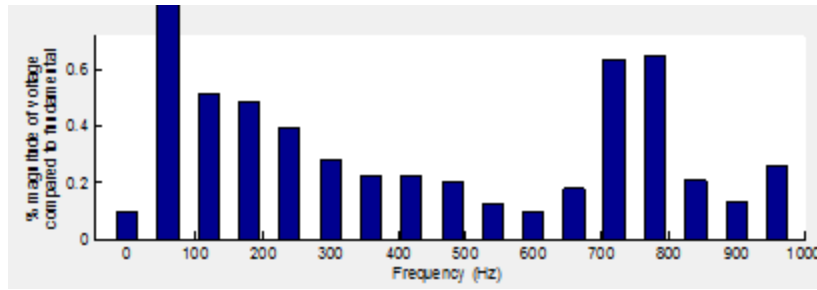


Figure 3.42 Voltage harmonic distortions at the grid

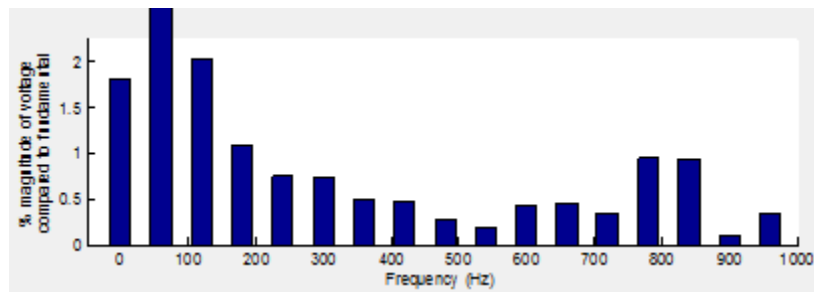


Figure 3.43 Current harmonic distortions at the grid

The grid is observing power of 260KW from the distribution network. The grid can supply any amount of power, if the distribution system needed. If the power generated by the DGs greater than the connected loads, then it can supply power back to the grid. Bus 2 is transferring power of 10KW from distribution system to the grid. PV generators are connected to bus 5, 6 and 9. Each PV inverter is generating power of 100KW. Bus 3, 4 and 10 are transferring power from the PV inverter to the distribution network. Bus 7 is observing power of 30KW and bus 8 is observing power of 90 KW. Bus 11 and 12 are transferring power of 10KW from distribution system to the grid.

Voltage and current harmonic distortions for 12-buses are shown in the Figure 3.30 to 3.41. Initially the system is in transient state; high voltage and current harmonic

distortions are presented at the generator buses. Capacitive bank are connected at the generator buses to improve the voltage stability and provide reactive power support to distribution system. High voltage harmonic distortions are presented at the load buses 2, 7 and 8. After few seconds, the system comes into stable state.

Figure 3.42 and Figure 3.43 shows total voltage and current harmonic distortion at the utility grid. Simulation results shows, voltage harmonic distortion at the grid is 1.42% and current harmonic distortion at the grid is 4.69%. Maximum 5% of harmonics are allowed to connect distributed generation to the grid. When the grid is off, distributed generation will supply power to the load. So, the system reliability will improve.

## **Chapter Four**

### **Electric Vehicle Battery Charger for Smart Grids**

#### **4.1 Introduction**

Most of the U.S oil products are imported from other countries. Nearly, 93% of petroleum, 3% of natural gas and 4% of renewable energy was used in the transportation system in 2011. The domestic production of petroleum continuously decreases while the use steadily increases. Using alternative fuels such as renewable energy resources can greatly reduce the use of petroleum.

Hybrid electric vehicle (HEV) technology is a great way to improve the fuel economy. HEV's use battery based energy storage system to store the energy generated during regenerative braking. A typical HEV can reduce gas consumption by 30% compared to conventional vehicles [11]. Plug-in hybrid electric vehicle (PHEV) is a hybrid electric vehicle with the ability to charge the energy storage system from the utility grid. The main advantage of the PHEV is that the vehicle will no longer depend on only one fuel. PHEV is an advanced technology which will integrate the energy and transportation system together to improve the efficiency, reduce fuel usage and improve the system reliability [16]. The usage of PHEV is expected to increase; the success of PHEV however will depend on both grid and the charging equipment.

The charging equipment plays a significant role in the PHEV technology. Energy Storage System (ESS) must charge or discharge without affecting the power quality of the utility grid. Another important issue is the time required to charge the battery where it

depends on the amount of energy stored in the ESS. A lithium-ion battery pack provides good operating characteristics under various operating conditions and the charger should provide or receive balanced, constant and fast power flow to or from the grid [13]. This in turn contributes to improve the voltage stability of the system.

In this chapter, a 3-phase bi-directional battery charger is developed for PHEV connected to the grid. A control strategy is developed and applied to a simple system configuration to verify whether it allows bi-directional power flow from/to the grid. The power should flow from Grid to Vehicle (G2V) when the battery is charging and from the Vehicle to Grid (V2G) when it is discharging. Throughout the operation, the voltage stability and the power quality should be maintained. ESS can act as an energy storage system to the grid. It will charge in the off-peak times and deliver power to the grid in the peak times (if needed!).

## 4.2 Battery Models

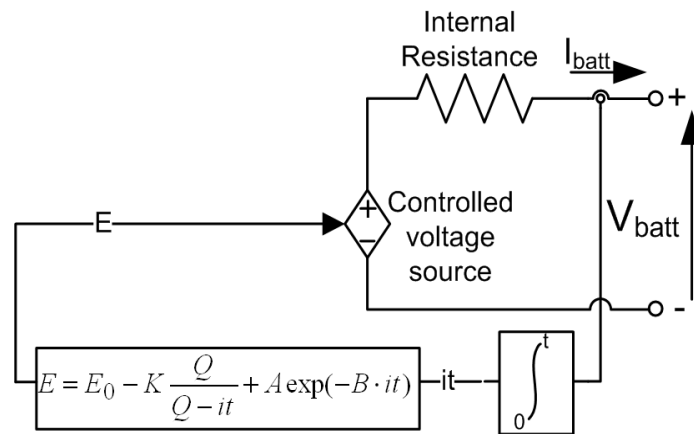


Figure 4.1 Lithium-ion battery model

A lithium-ion battery is considered to model the ESS for a PHEV. Lithium-ion battery has low self-discharge characteristics, highly reliable and requires low maintenance [12]. The circuit diagram of the lithium-ion battery is as shown in the Figure 4.1.

#### 4.2.1 Matlab®Simulink Model of the Lithium-ion Battery

Figure 4.2 shows the Simulink model of a lithium-ion battery.

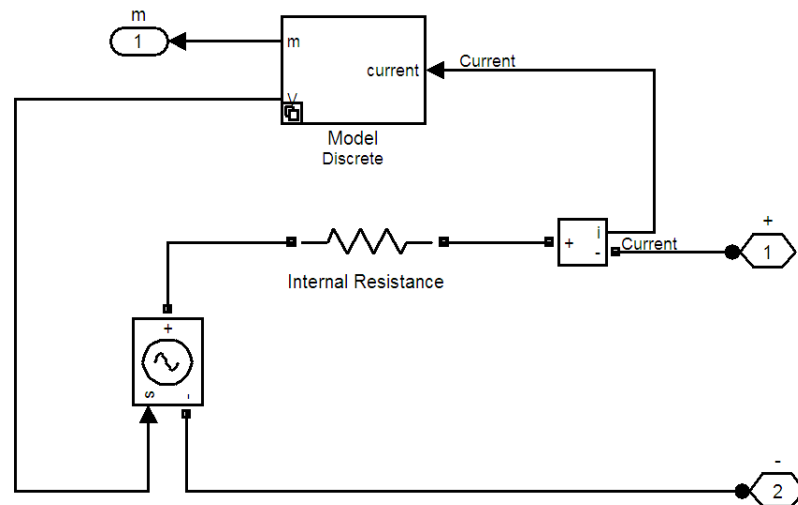


Figure 4.2 Matlab®Simulink model of the lithium-ion battery

Some assumptions were made to develop an accurate battery model. The internal resistance ( $R$ ) of the battery is assumed constant during charging and discharging and it doesn't vary with the amplitude of the current. The parameters calculated from the discharge curve are assumed constant during charging mode. Capacity of the battery does not change with the amplitude of the current [11].

The minimum voltage of the battery is 0V and maximum voltage of the battery is  $2 \cdot E_0$  (nominal battery voltage). The minimum capacity of the battery is 0Ah and maximum current of the battery is  $Q_{max}$  [11].

Experimental validation of the battery model shows a peak error of 5% (when State Of Charge (SOC)) in between 10% to 100%) for charge and discharge dynamics [11].

### 4.3 Bi-directional Battery Charger

The bi-directional battery charger used in this study is developed as shown in the figure 4.1 [13].

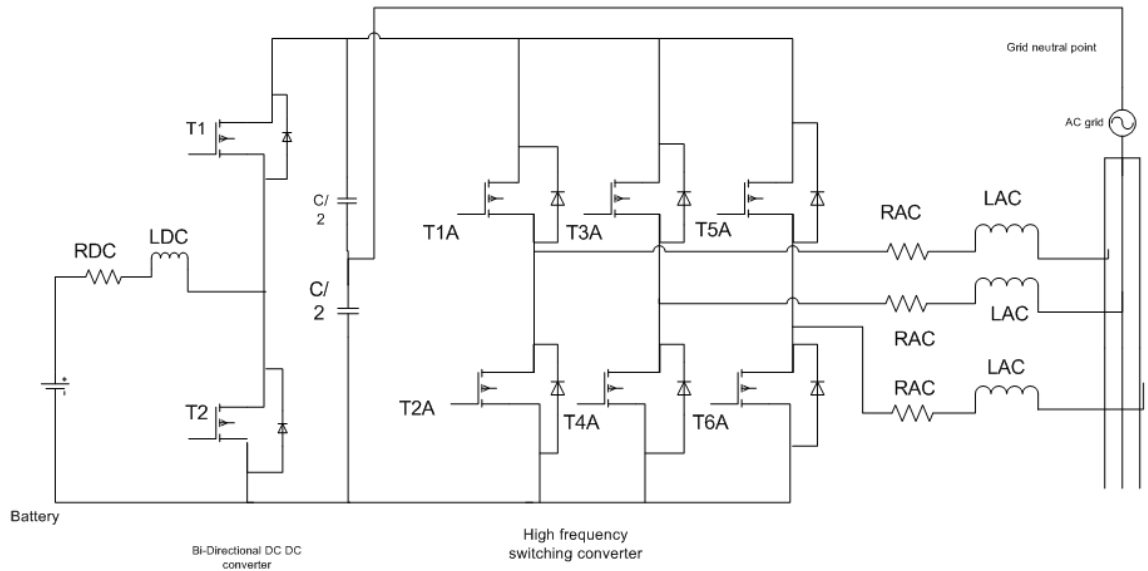


Figure 4.3 Bidirectional battery chargers

Figure 4.3 shows a bi-directional battery charger for plug-in hybrid electric vehicles. The battery draws power from the grid during off-peak times and delivers

power to the grid during the peak times. A DC link is placed between the DC-DC converter and inverter.

The DC-DC converter converts the battery output voltage to a suitable input voltage for the inverter, i.e. the DC link voltage is fixed at one particular value that's independent of the battery output voltage. The inverter converts constant DC values to suitable AC values to inject the sinusoidal currents and voltage into the grid with in the vehicle to grid operation (V2G) mode. The inverter in a reverse mode converts sinusoidal AC values to DC values, and then DC-DC converter converts fixed unregulated DC output of the inverter to regulated DC to charge the battery in grid vehicle operation (G2V) mode [13].

There are two modes developed according to charging and discharging of the battery.

1. Charging: the power will flow from grid to the vehicle (G2V).
2. Discharging: the power will flow from vehicle to grid (V2G).

A bi-directional DC-DC converter is as shown in the Figure 4.4. Charging and discharging of the ESS can be determined based on the direction of the current. The battery will discharge when it's current is positive ( $I_{bat}>0$ ) and it will charge when current is negative ( $I_{bat}<0$ ).

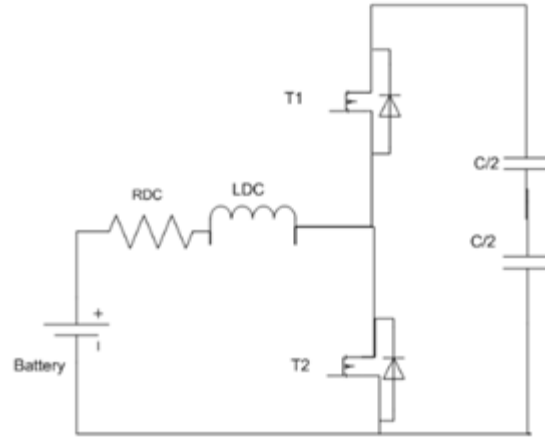


Figure 4.4 Bi-directional DC-DC converter

#### 4.4 Control Strategy

The control strategy used in this study is explained below

The instantaneous output power  $P(t)$  is

$$P(t) = U_{an}I_{an} + U_{bn}I_{bn} + U_{cn} \quad (4.1)$$

Where  $U_{an}$ ,  $U_{bn}$  and  $U_{cn}$  are the output sinusoidal voltage and  $I_{an}$ ,  $I_{bn}$  and  $I_{cn}$  are the instantaneous sinusoidal currents [13]

$$I_{inv,ref} = \frac{U_{bat}I_{bat}}{U_{an1}^2 + U_{bn1}^2 + U_{cn1}^2} \begin{bmatrix} U_{an1} \\ U_{bn1} \\ U_{cn1} \end{bmatrix} \quad (4.2)$$

Where  $I_{inv,ref}$  is the reference current for the control strategy and  $U_{an1}^2$ ,  $U_{bn1}^2$  and  $U_{cn1}^2$  are the positive sequence fundamental voltages, and  $U_{bat}$ ,  $I_{bat}$  are the battery voltage and current.

The duty cycle of the DC-DC converter is calculated from Figure 4.4.



$$U_{dc} * D_{dc} = U_{bat} - I_r * R_{dc} - \frac{i_{mes,dc} - i_{ref,dc}}{T_c} * L_{dc} \quad (4.3)$$

Solving the equation in the DC-DC converter, the duty cycle of the converter can be given by;

$$D_{dc} = \left[ U_{bat} - I_r * R_{dc} - \frac{i_{mes,dc} - i_{ref,dc}}{T_c} * L_{dc} \right] * \frac{1}{U_{dc}} \quad (4.4)$$

#### 4.5 Matlab@Simulink Modeling of Bi-directional Converter

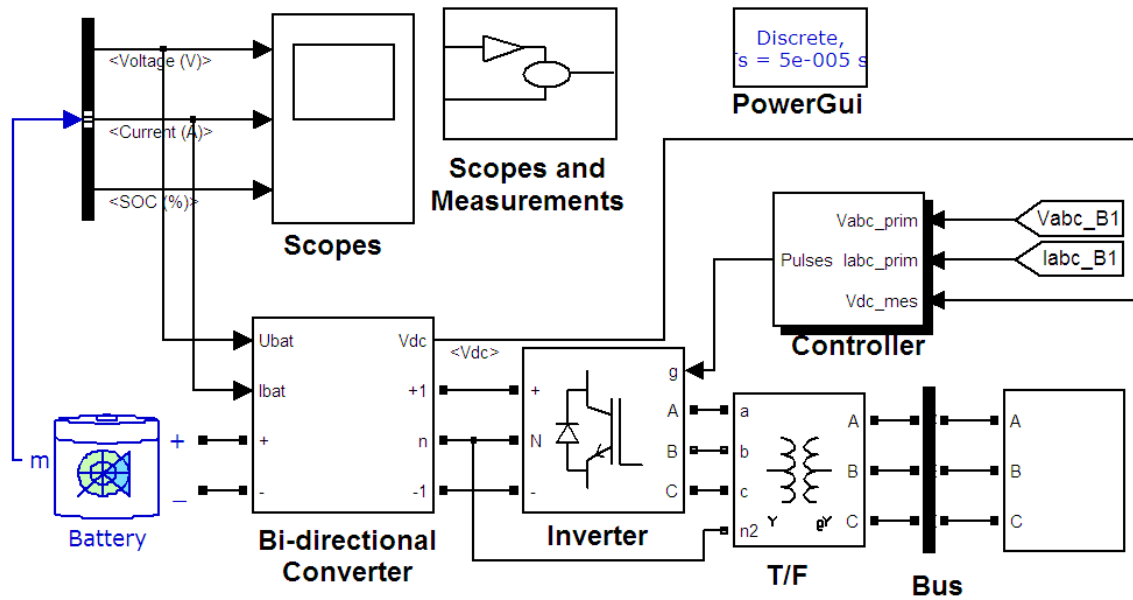


Figure 4.5 Matlab@Simulink model of PHEV charger

Figure 4.5 shows, a Simulink model of PHEV battery charger for grid connected electric vehicles. A battery is connected to the grid through bi-directional converter and inverter topology. Measurements and instrumentations are shown in the bottom portion of Figure 4.5.

The control strategies developed for the bi-directional converter, inverter circuit is as shown in the Figure 4.6 and Figure 4.7.

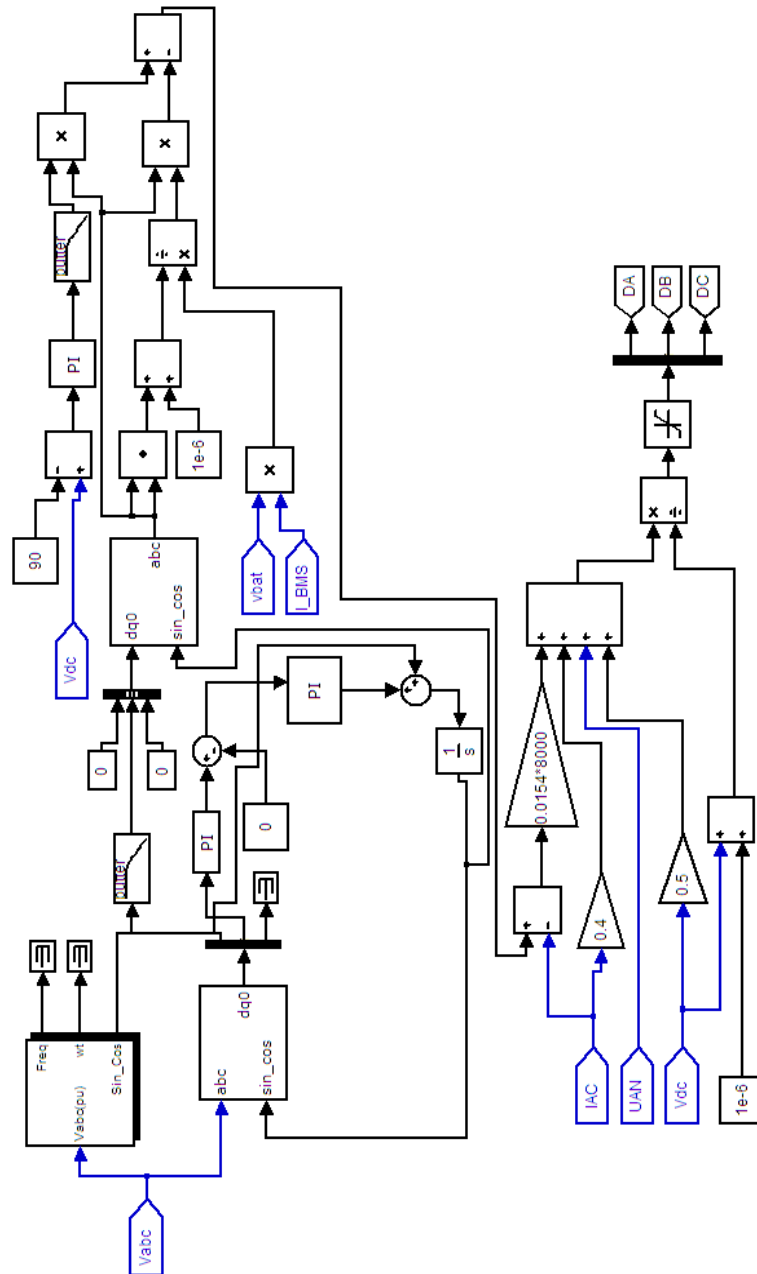


Figure 4.6 Inverter control circuit

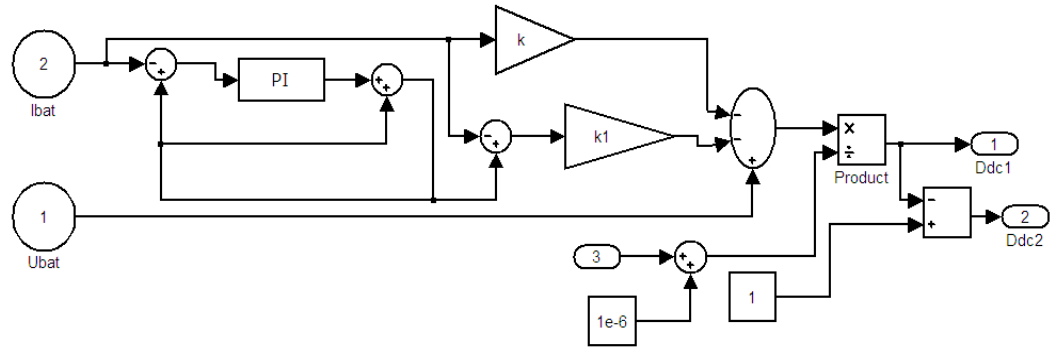


Figure 4.7 Bi-directional converter control circuit

Current controller, voltage controller, and PFC techniques are applied in this study to reduce the voltage and current harmonic distortions in the grid.

#### 4.6 Simulation Results

The simulation results show the charging and discharging characteristics of the simulated PHEVs connected to the grid.

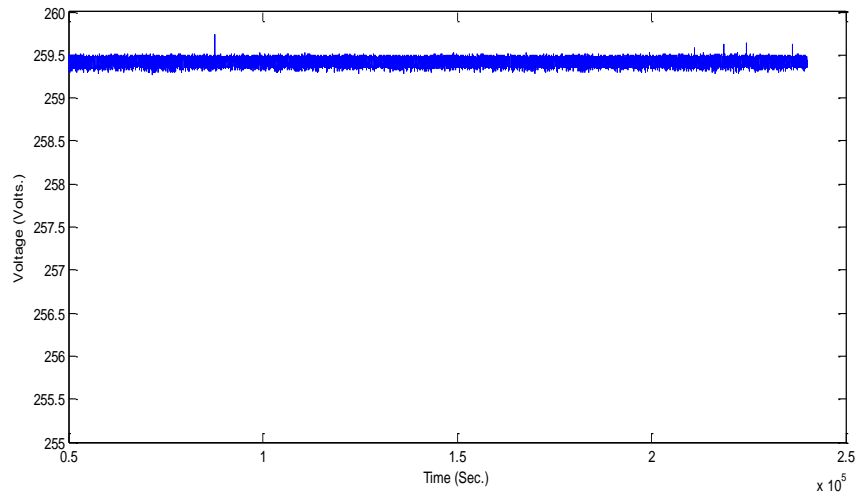


Figure 4.8 Battery voltage in discharge mode

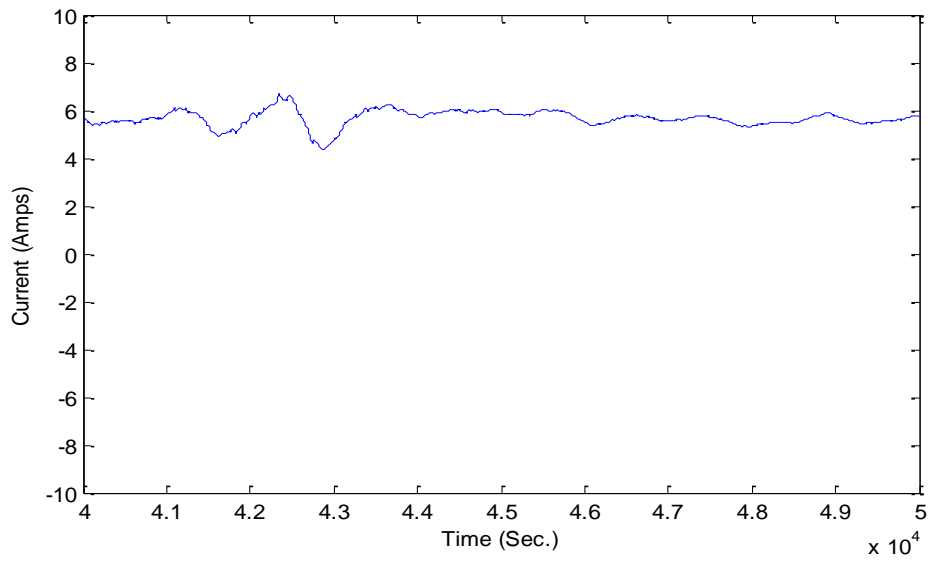


Figure 4.9 Battery current in discharge mode

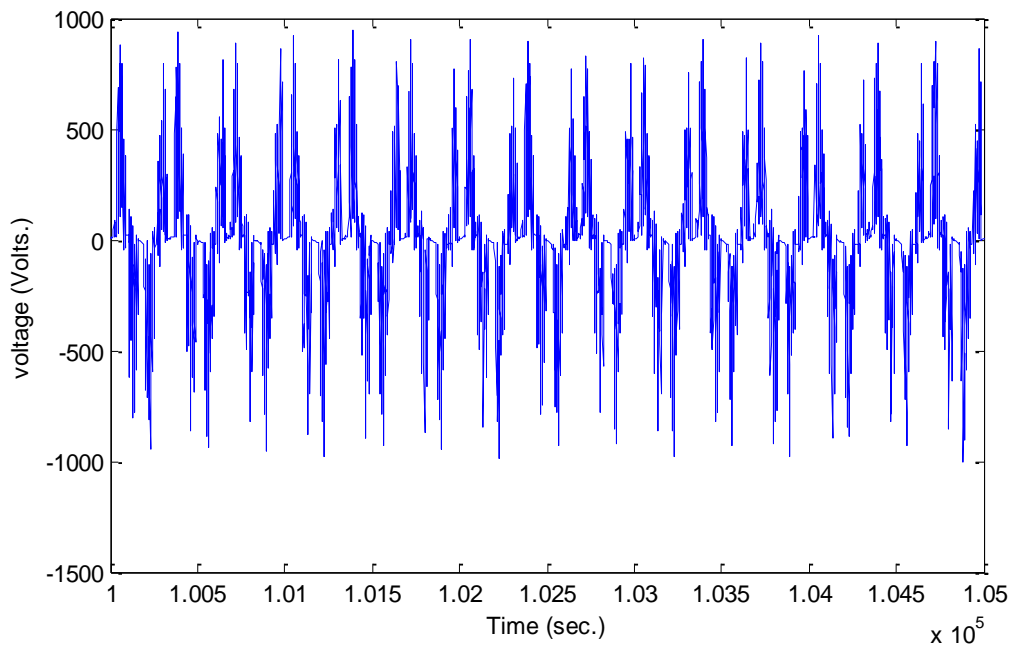


Figure 4.10 Voltage at the utility grid

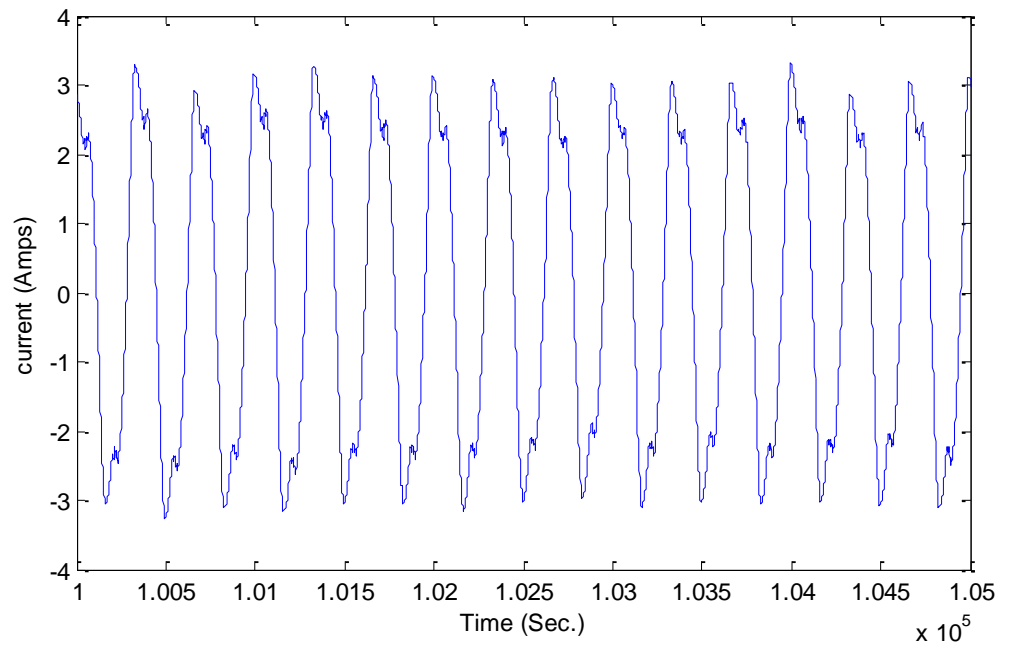


Figure 4.11 Current at the utility grid

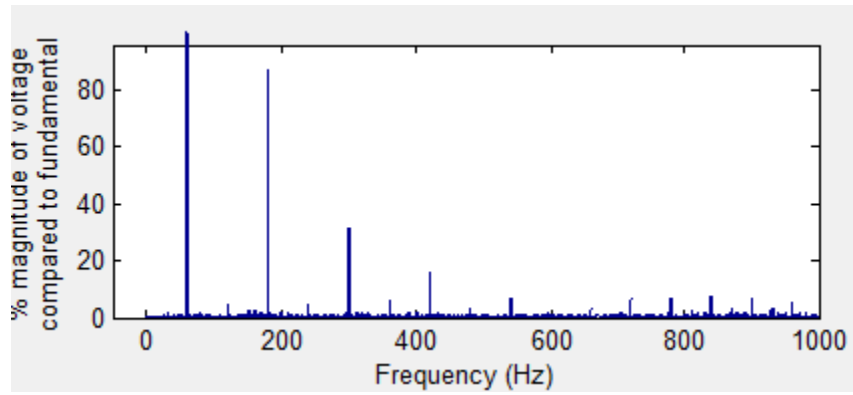


Figure 4.12 Voltage harmonic distortion

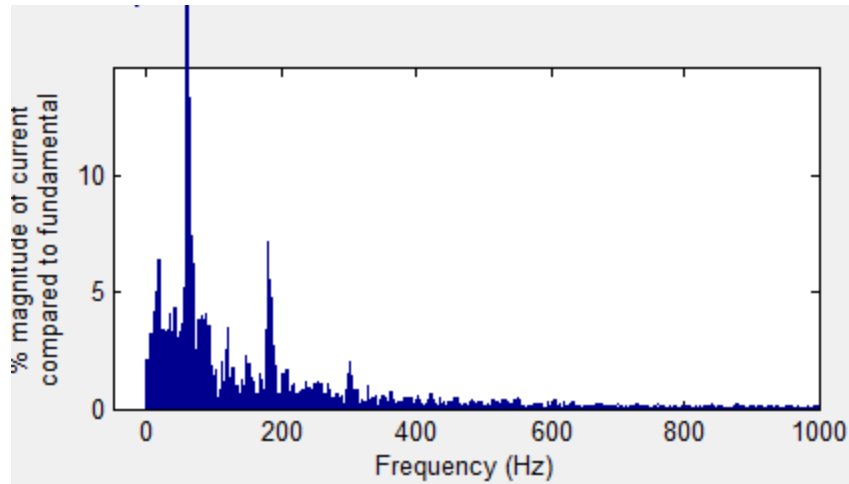


Figure 4.13 Current harmonic distortion

Battery discharge mode voltage and current is shown in Figure 4.8 and Figure 4.9. The battery is discharging power into the grid at current 5.8Amps with the voltage of 259.5Volts. Voltage and current at the grid is as shown in the Figure 4.10 and 4.11. Voltage and current are in phase in the grid to vehicle operation mode. In the vehicle to grid operation, the battery is injecting high voltage and current harmonics into the grid as shown in the Figure 4.12 and 4.13.

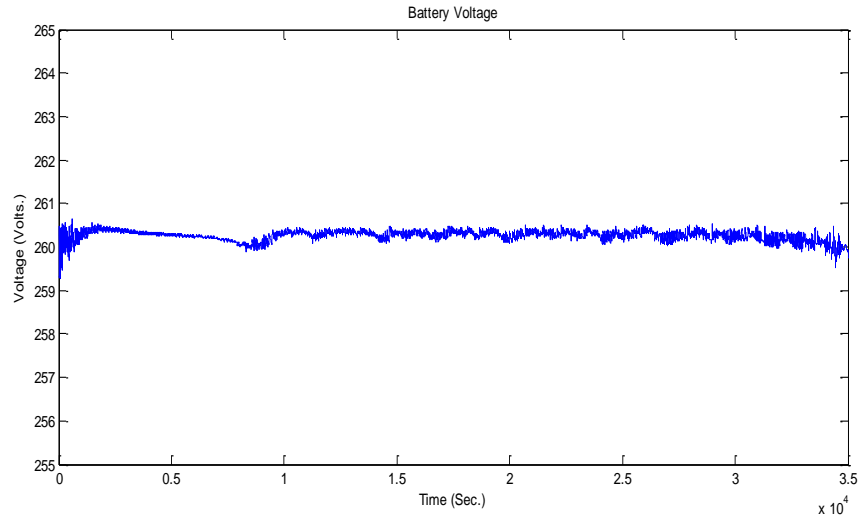


Figure 4.14 Battery voltage in charge mode

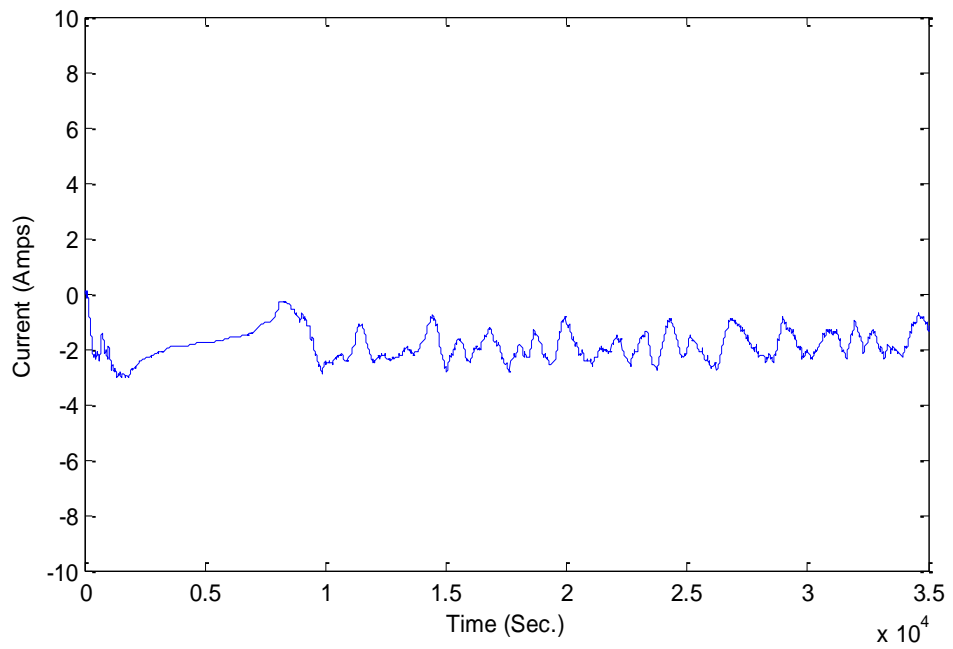


Figure 4.15 Battery current in charge mode

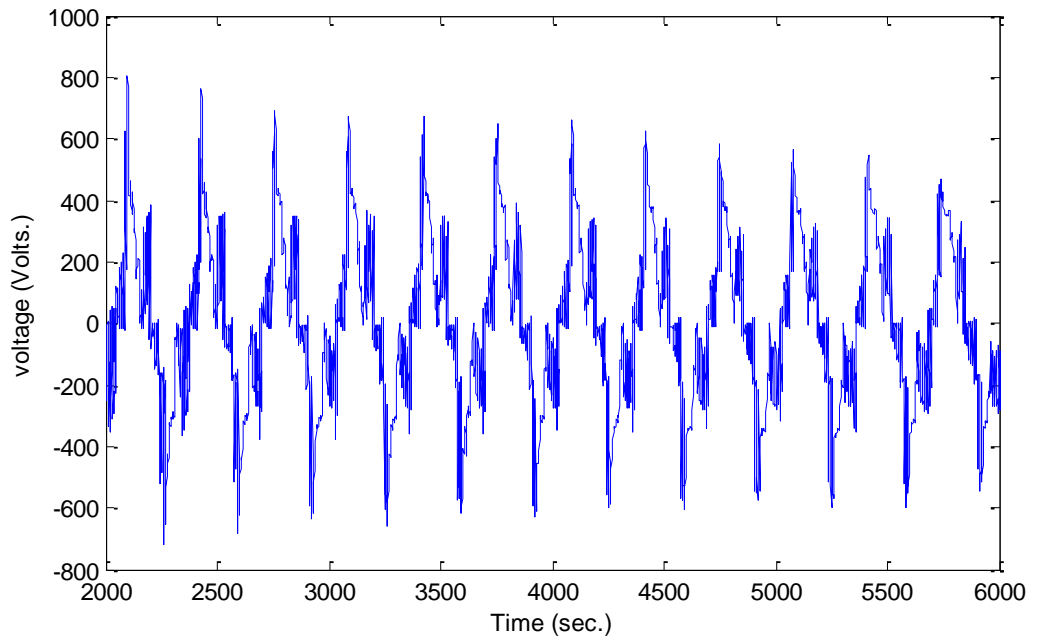


Figure 4.16 Voltage at the utility grid

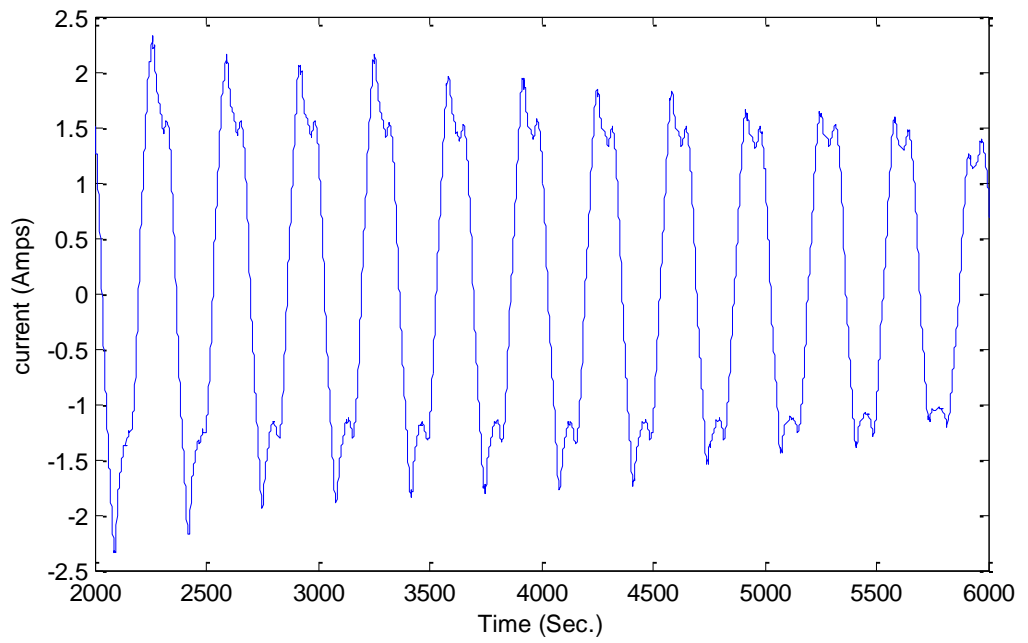


Figure 4.17 Current at the utility grid



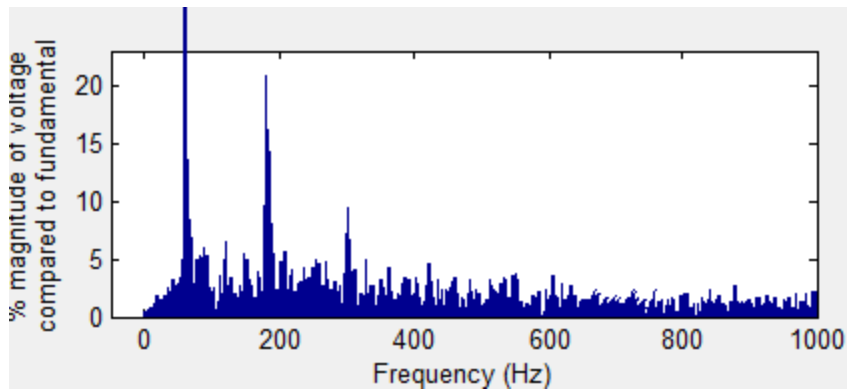


Figure 4.18 Voltage harmonic distortion

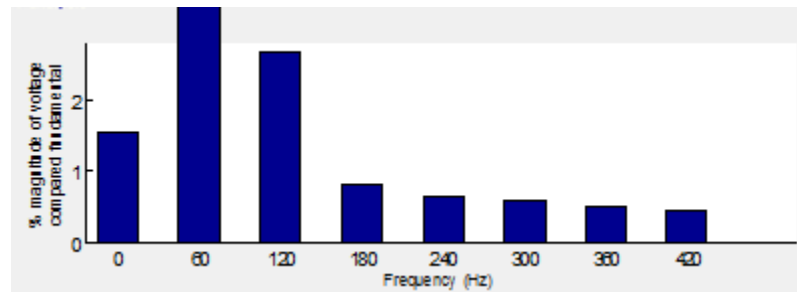


Figure 4.19 Current harmonic distortion

Battery charge mode voltage and current is shown in Figure 4.14 and 4.15. The battery is charging from the grid at current -2.3Amps with the voltage of 260Volts. Voltage and current at the grid is as shown in the Figure 4.16 and 4.17. Grid voltage and current are out of phase in charging operation mode. In the grid to vehicle mode, voltage and current harmonics injected by the battery is as shown in Figure 4.18 and 4.19. The battery is injecting 26.62% of voltage harmonics and 8.14% of current harmonics into the grid.

## **Chapter Five**

### **Grid Connected Distributed Generation with PHEV Loads**

#### **5.1 Introduction**

This chapter discusses power quality and voltage stability of the utility grid with multiple PHEV connected loads. Two test power system network models were simulated and presented in this chapter. The first model is a photovoltaic array supply power to the grid with a single PHEV load connected at the bus. The second model is a 12-bus test power system network with three DGs and PHEV loads connected to the utility grid. Both models are developed and simulated in the Matlab®Simulink environment as shown in sections 5.2, 5.3 and 5.4.

If the generating power of the DG is greater than the load of the system, then the PHEV can act as an energy storage system. If the generation of the PV is greater than the consumer load demand, then the consumer can sell power to the grid. Due to the non-linear behavior of the power electronic switches, when a large number of PHEV's are connected to the utility grid, a significant increase in harmonics in the system is measured. The battery charger model plays a vital role in the integration of grid and transport system. The general model for a PHEV battery charger given in chapter four is considered here to test the multiple PHEVs at various conditions.

## **5.2 Power Quality of Power System**

Large power generation units will inject pure sinusoidal waveforms into the grid. Distribution networks are fed to the power system through transmission lines. Reactive power imbalance, voltage fluctuations, voltage transients, power electronic converters and harmonics will disturb the power quality of power system. Voltage transients and harmonic distortions are discussed in this thesis to find the power quality of power system. Distributed generation and PHEVs are connected to distribution network.

Distributed wind generation and PV inverter was designed to provide active power support to the grid. Reactive power support was provided at the distribution generation. PHEV loads are connected at various buses to observe the power flow from grid to vehicle and vehicle to grid. Power quality evaluation of distribution system with installed distribution generation and PHEV loads was observed under two different conditions. First, it is observed under normal operating (steady state) condition. Second, it is observed under transient condition.

### **5.2.1 Steady-state Voltage Problems**

The steady-state voltage problems involve over voltage or under voltage problems. Typically, the nominal voltage is 10% above or below rated voltage under this condition. Distributed generation is connected to the grid via a common bus. For proper operation, the voltage and frequency should keep constant at the nominal value. Reactive power support provided for distributed wind generation to control the voltage to its nominal value.

### **5.2.2 Transients in Power System**

Transients can be defined as disturbance in the AC waveform evidenced by a sharp discontinuity in the output waveform. This may be additive or subtracted from the nominal waveform. Transients are short duration events, and it occurs when there is a sudden change in the voltage or current in a power system network.

### **5.2.3 Harmonic Distortion**

Harmonic distortion is the change in the supply wave form when compared with the fundamental waveform. Voltage harmonic distortions and current harmonic distortions will affect the power quality. Power electronic converts are the main reason for harmonics when subjected to distributed generation and PHEVs.

## **5.3 Grid Connected Wind Turbine Induction Generator with PHEV load**

Grid connected wind turbine induction generator with PHEV loads was modeled to investigate voltage transients and harmonics injected by both wind turbine induction generator and PHEVs into the grid. Here the battery state of charge is considered for charging and discharging operation. If the battery state of charge is greater than 95%, then it deliver power to the grid, else it can absorb power from the grid.

Initially, the battery state of charge was considered as 90%, so the grid is supplying power to the Battery Energy Storage System (BESS). One line diagram of test power system network was shown in Figure 3.1 (Chapter 3). PHEV loads are connected at bus 4 and 5. Simulink diagram of grid connected WTIG with PHEV loads is as shown in Figure 5.1.

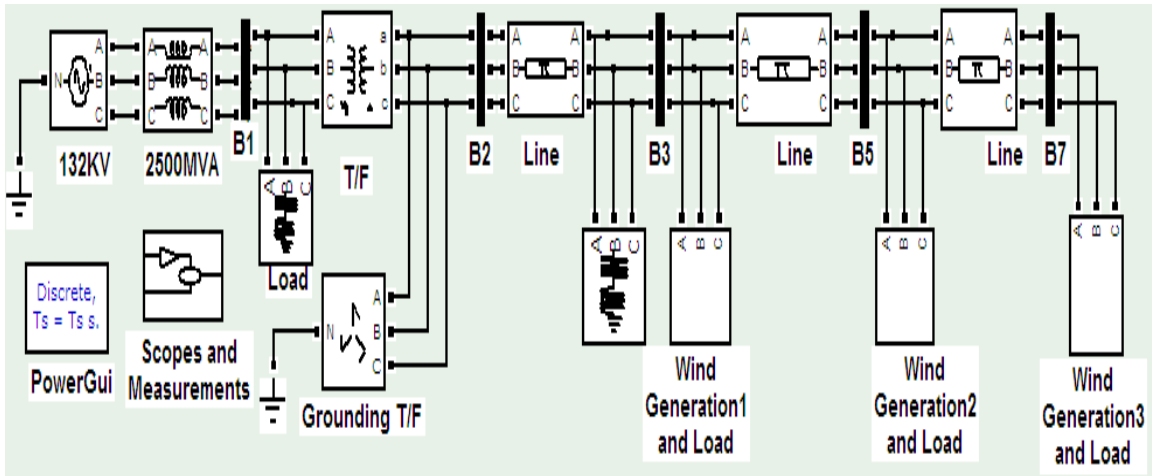


Figure 5.1 Matlab®Simulink model of grid connected WTIG with PHEV loads

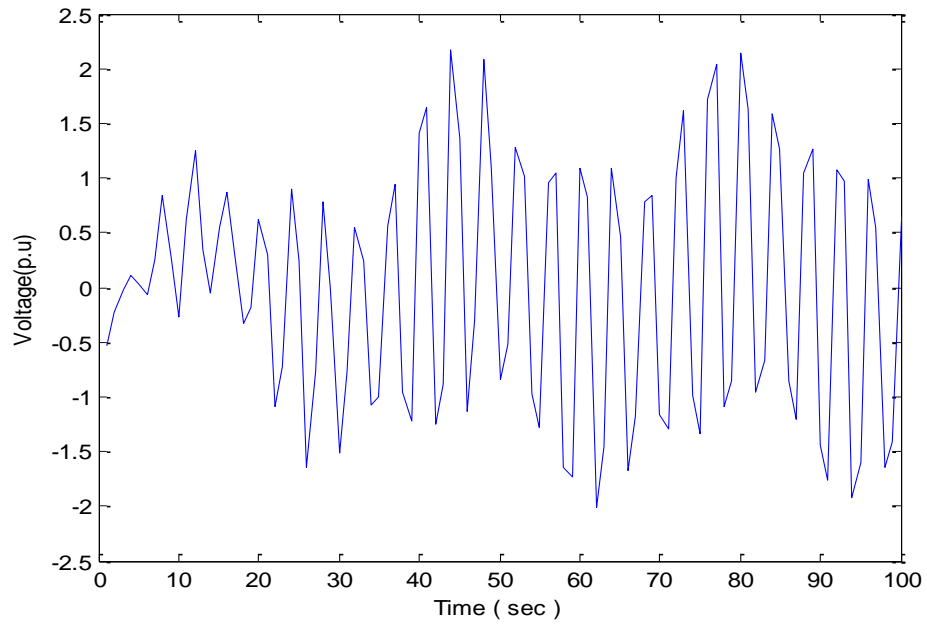


Figure 5.2 Transient voltage at WTIG-1

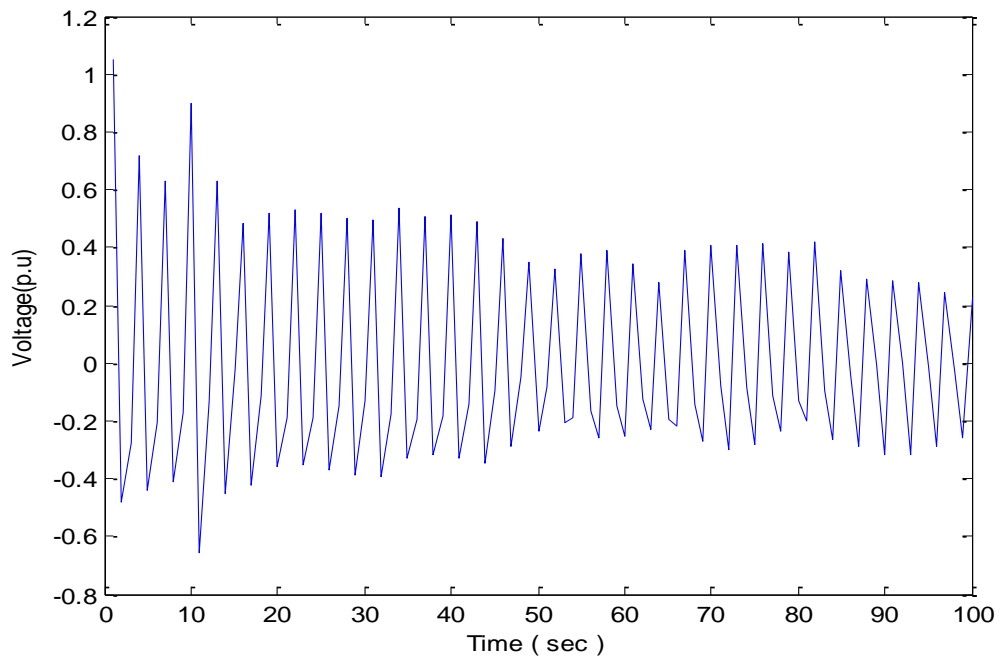


Figure 5.3 Transient voltage at WTIG-2

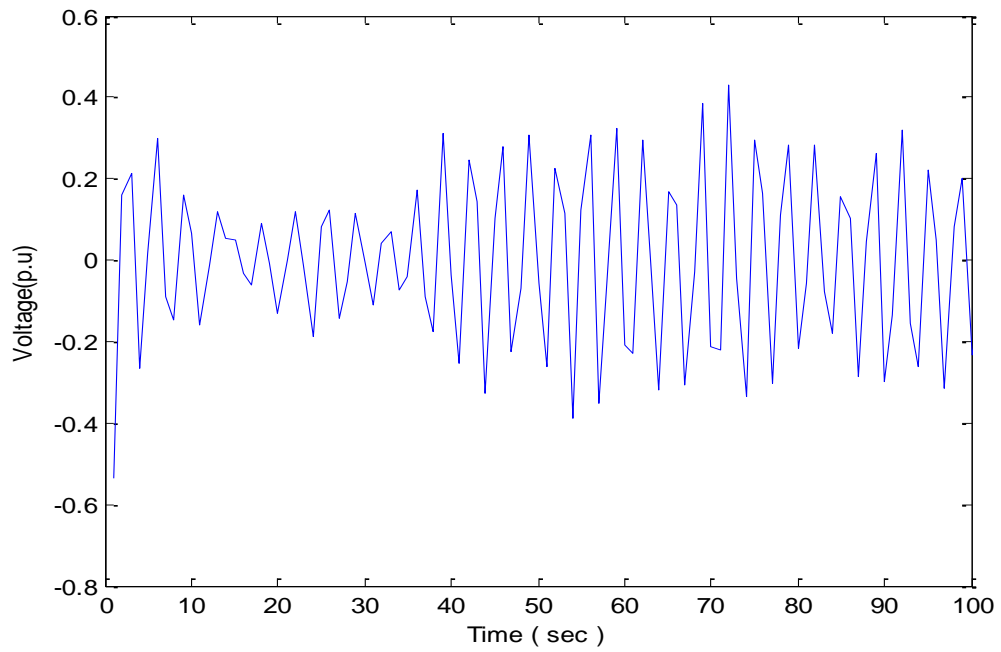


Figure 5.4 Transient voltage at WTIG-3

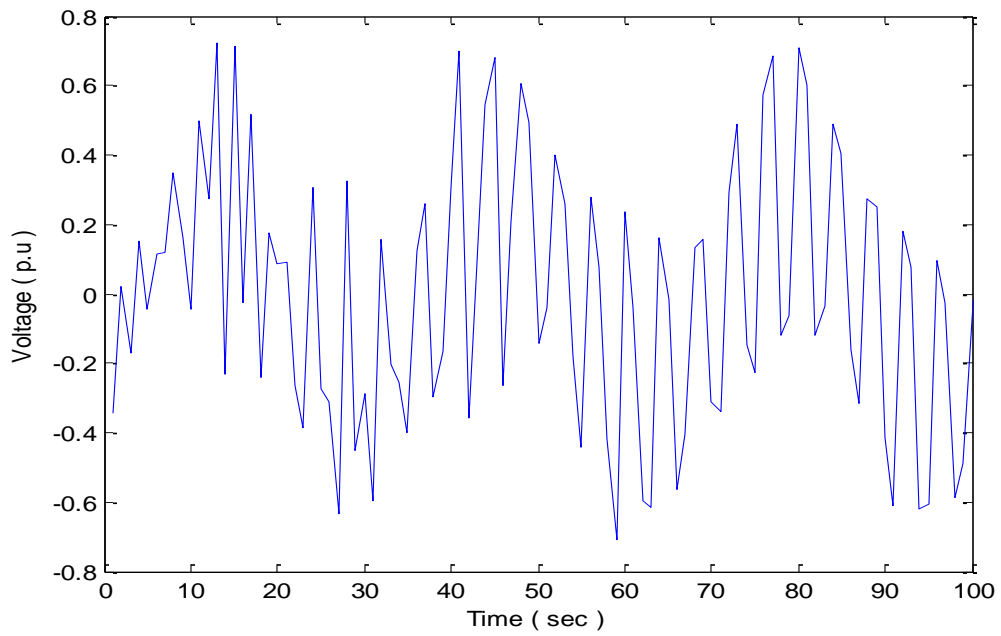


Figure 5.5 Transient voltage at load bus 1

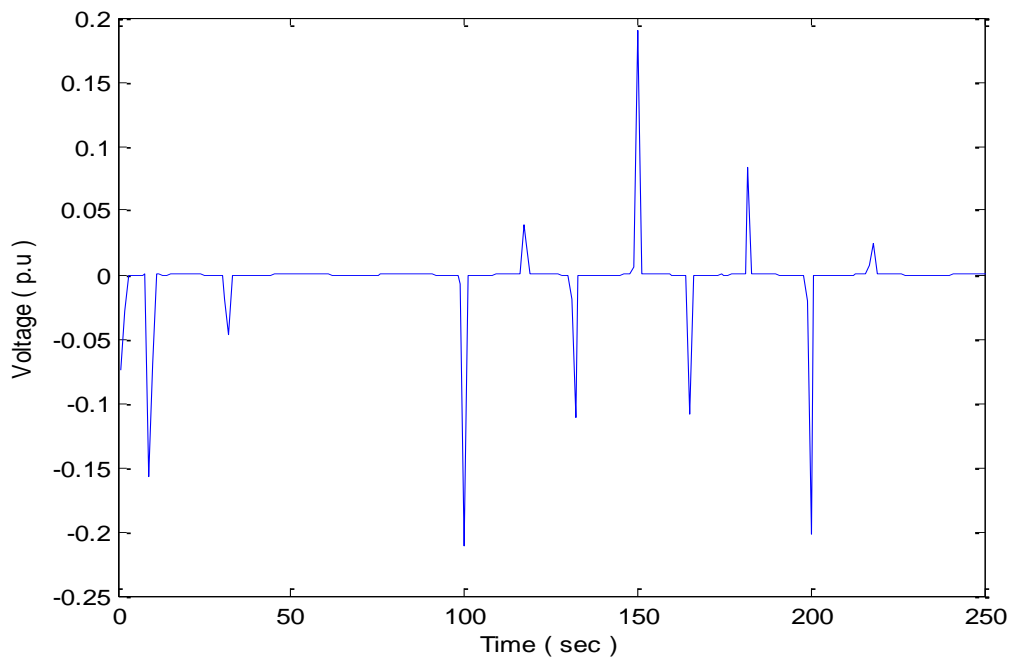


Figure 5.6 Transient voltage at load bus 2

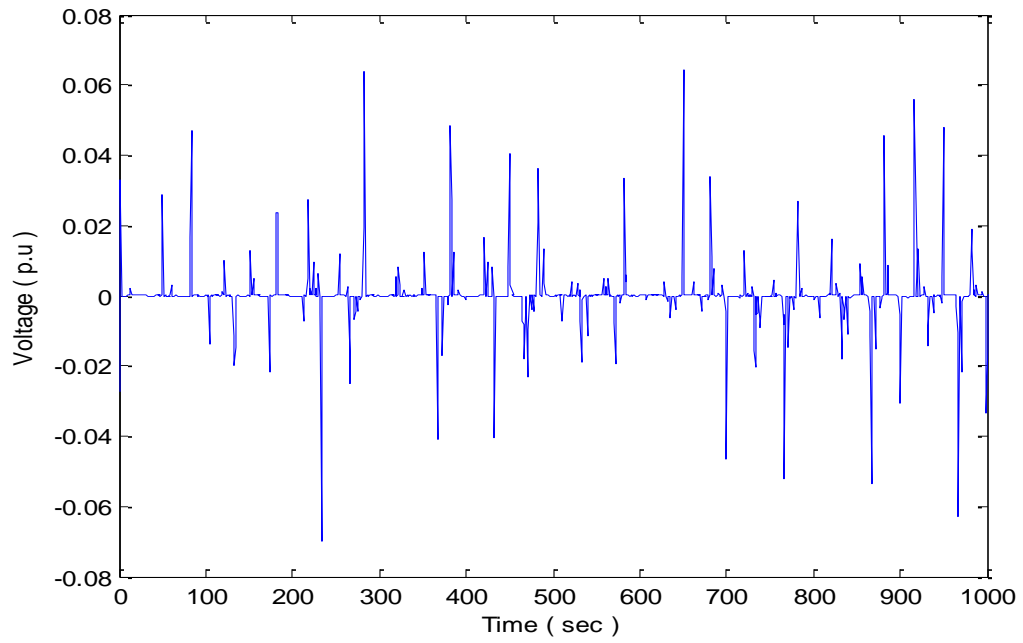


Figure 5.7 Transient voltage at load bus 3

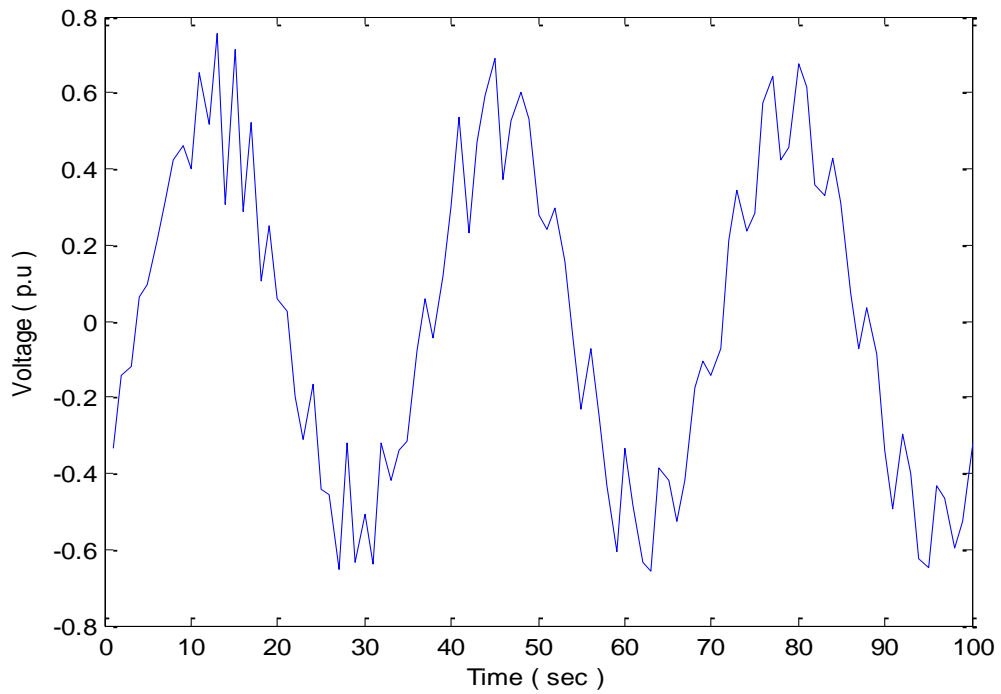


Figure 5.8 Transient voltage at the grid



Initial voltage transients at wind turbine induction generator, PHEV loads and grid is as shown in Figure 5.2 to 5.8. Initial operating characteristics and switching of reactive power compensator are the main reason for Voltage transients at the WTIG for first few seconds. Voltage at load bus1 shows the bus voltage without PHEV load, the voltage sags are because of high current will flow through the network in the starting stage. Load bus voltage at bus2 and bus3 shows the bus voltage with PHEV load. DC component and switching of high frequency power electronic converters are main reason for the voltage transients at the load buses. Resulting, voltage transients at the grid is as shown.

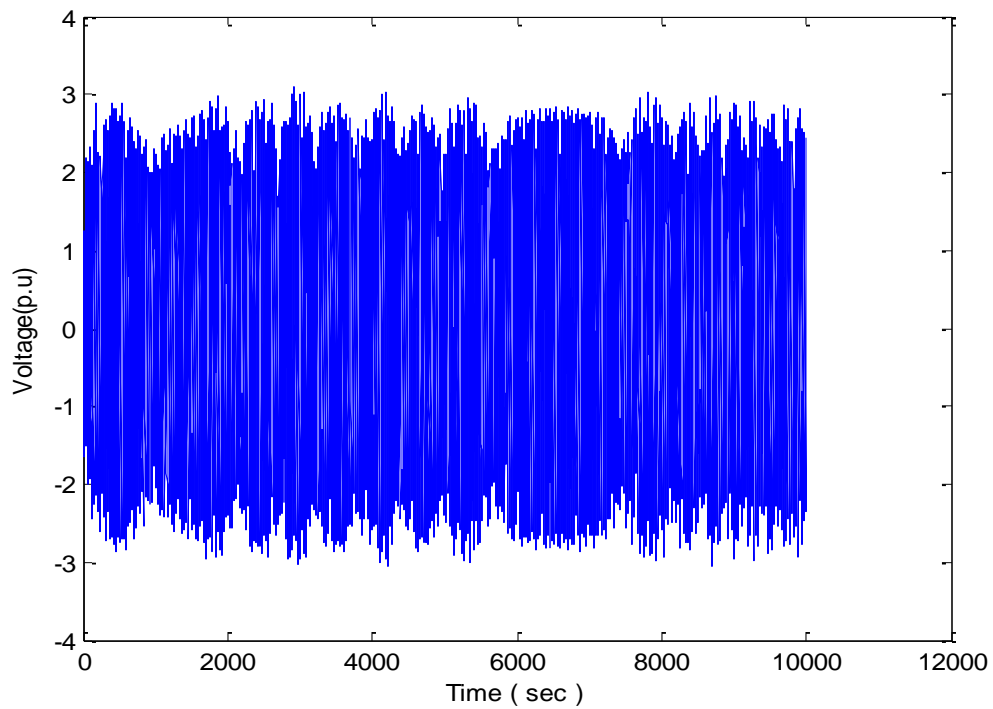


Figure 5.9 Voltage at the WTIG-1

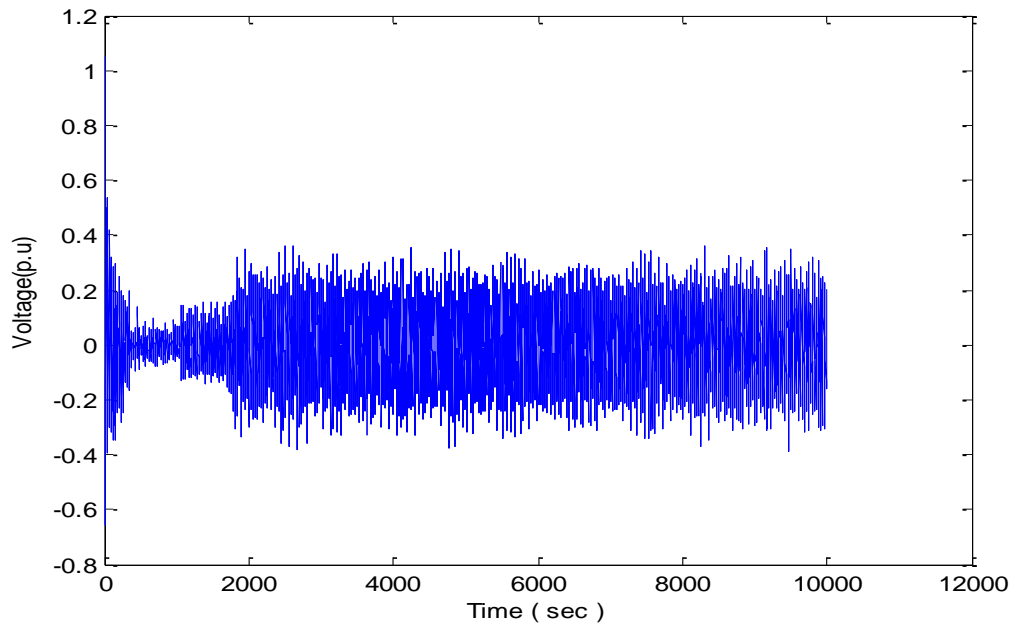


Figure 5.10 Voltage at the WTIG-2

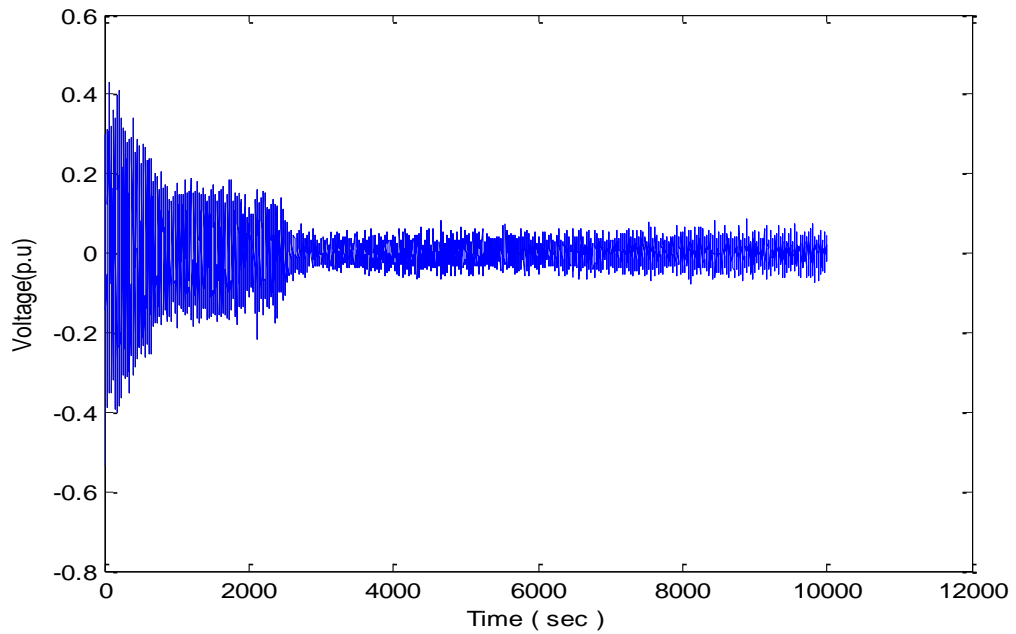


Figure 5.11 Voltage at the WTIG-3

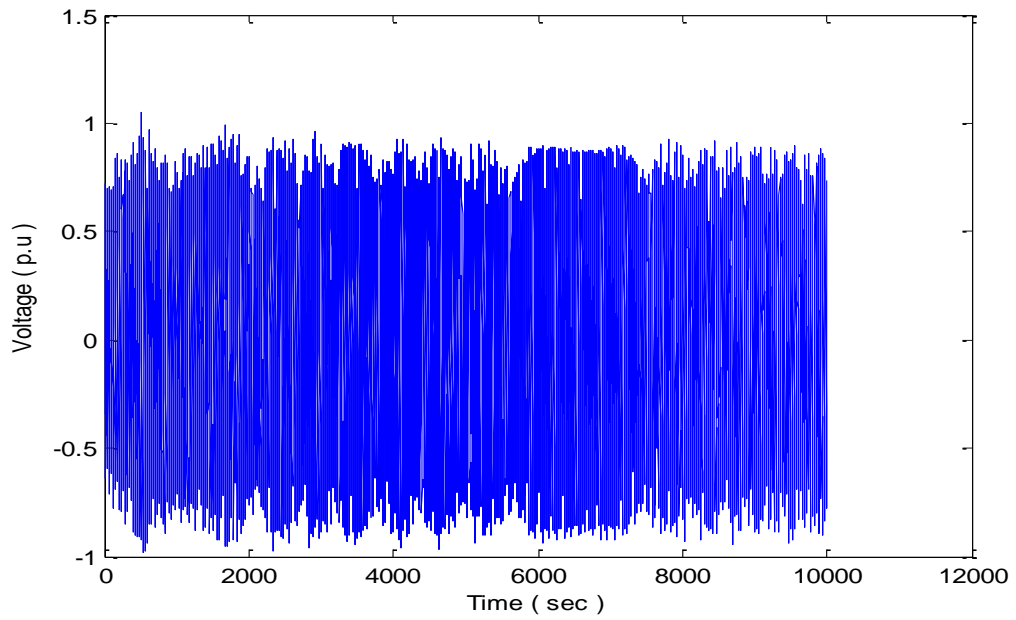


Figure 5.12 Load bus 1 voltage

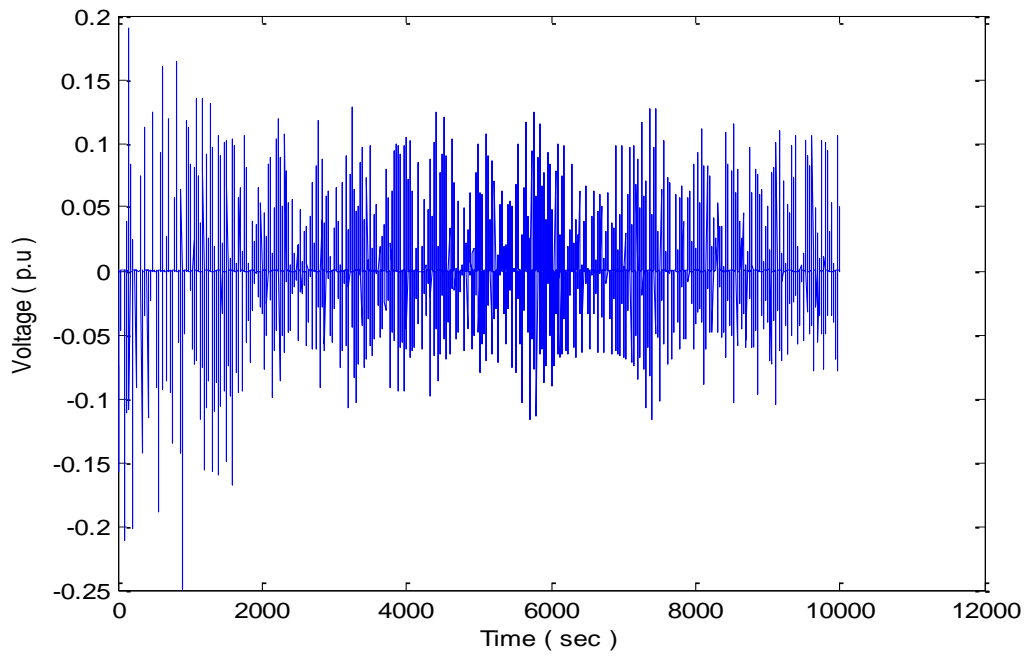


Figure 5.13 Load bus 2 voltage

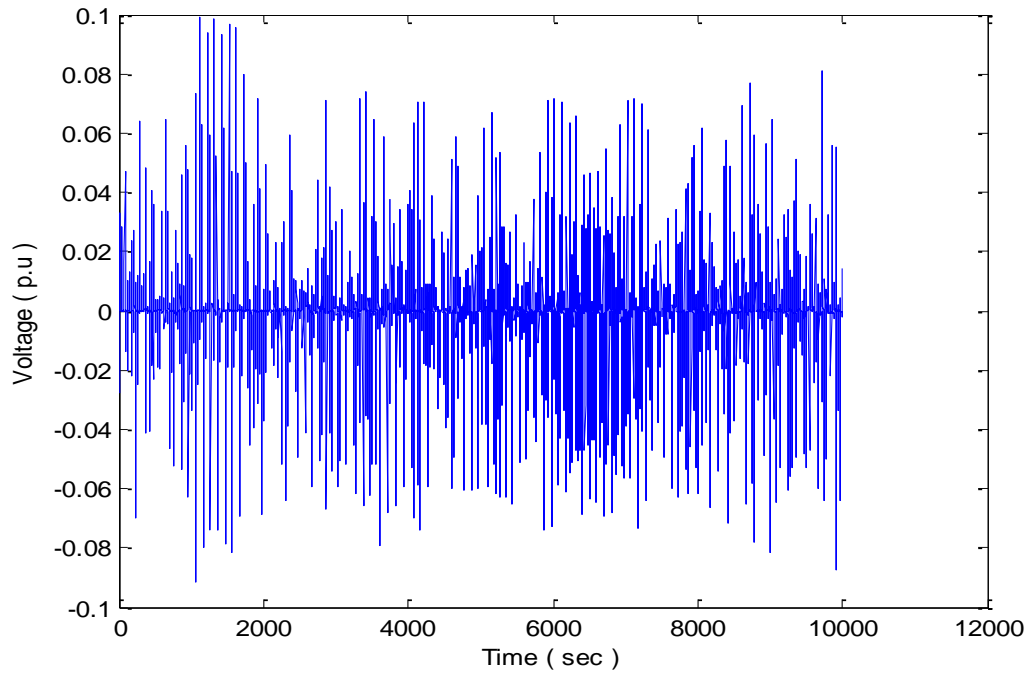


Figure 5.14 Load bus 3 voltage

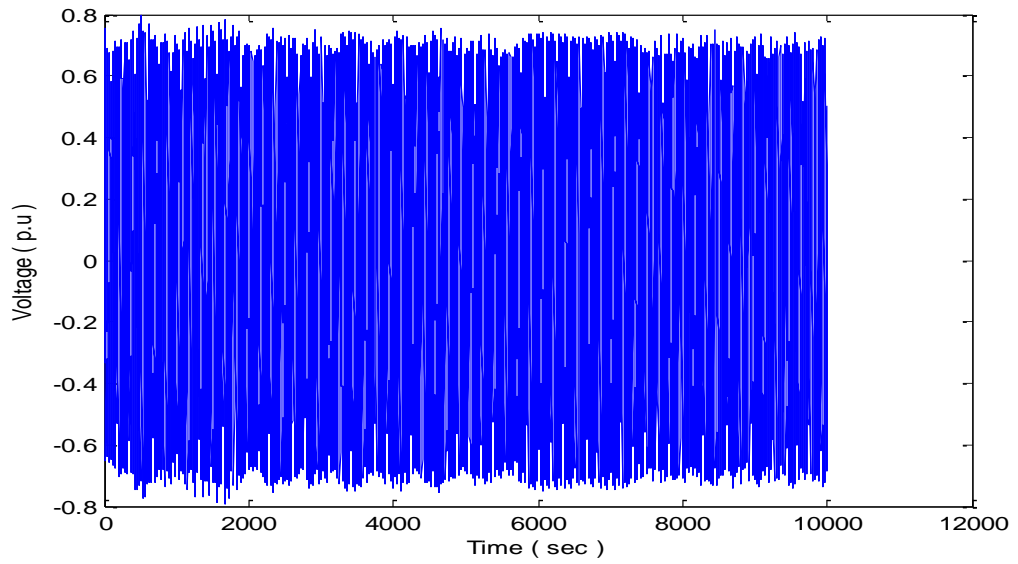


Figure 5.15 Voltage at the utility grid

After a few seconds of starting operation, the system will come into stable operating condition. The steady state voltages at various buses are shown in Figure 5.9 to 5.15. High voltage harmonics are presented at PHEV buses because of 8KHZ power electronic converters are connected to the system for charging and discharging operation of PHEV.

WTIGs and PHEVs are injecting significant amount of voltage and current harmonics into the grid. These harmonics will disturb the power quality. Totally, both are injecting 81.11% of voltage harmonics and 69.61% of current harmonics into the power system (Figure 5.18 and 5.19). The distribution system is injecting voltage harmonic distortion of 4.29% and current harmonic distortion of 5.29% into the grid. The respective plots for voltage and current harmonic distortion are shown in Figure 5.16 to 5.17.

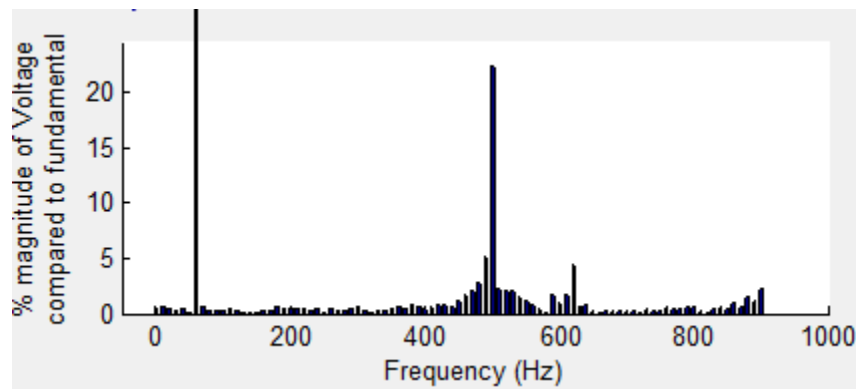


Figure 5.16 Voltage harmonic distortion at the grid

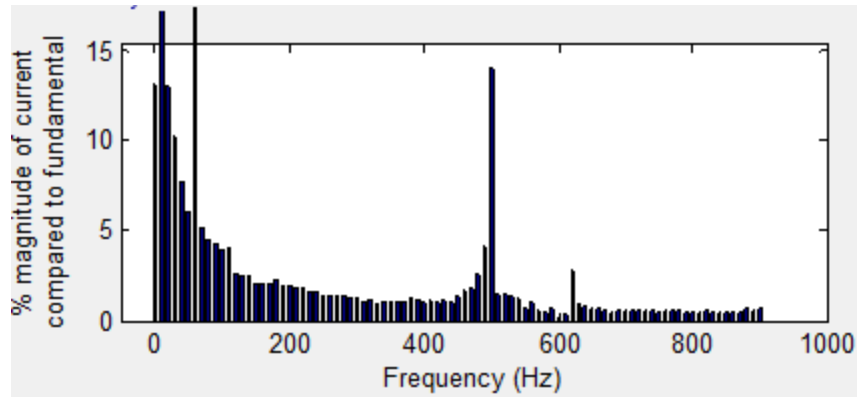


Figure 5.17 Current harmonic distortion at the grid

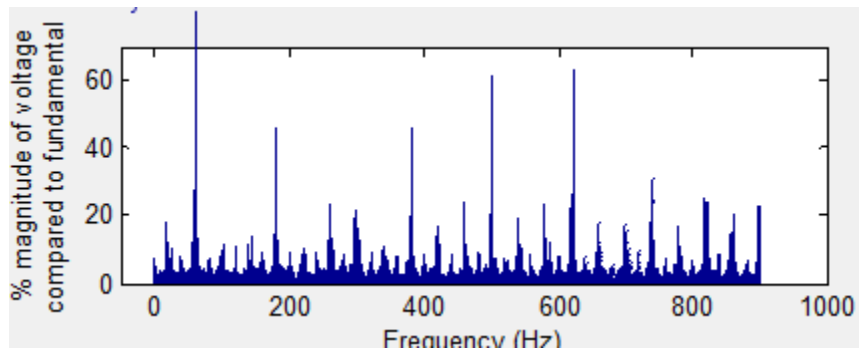


Figure 5.18 Voltage harmonic distortion injected by WTIG and PHEV

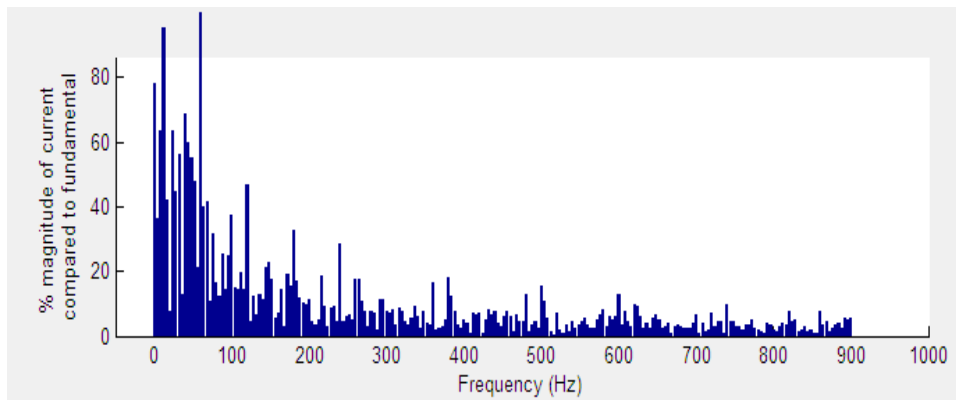


Figure 5.19 Current harmonic distortion injected by WTIG and PHEV

#### 5.4 Grid Connected PV Inverter with PHEV load

A 100KW distributed generation and a PHEV load is connected to the utility grid.

The output of the PV cell will vary with respect to the solar irradiance. Based on the output characteristics of PV and state of PHEV five cases are studied here [19].

Case study 1: Generally during the night times, early morning times and during inclement weather or abnormal conditions the output power of PV is zero, and then the grid will supply power to the load.

$$P_{pv}=0 \quad (5.1)$$

Case study 2: If  $P_{pv}$  is greater than zero and less than the minimum value and SOC of the PHEV is greater than the threshold value then the PV and PHEV will supply power to the load.

$$P_{pv} > 0 \ \& \ P_{pv} < P_{pv} |_{min} \quad (5.2)$$

$$SOC > T_{soc} \quad (5.3)$$

Case study 3: If the  $P_{pv}$  is greater than zero and less than the minimum value and if the SOC of the PHEV is less than the threshold value then the PV and grid will supply power to the PHEV connected load.

$$P_{pv} > 0 \ \& \ P_{pv} < P_{pv} |_{min} \quad (5.4)$$

$$SOC < T_{soc} \quad (5.5)$$

Case study 4: The PV power varies from minimum to maximum during day time so the PV can supply power to the connected load.

$$P_{pv} > 0 \ \& \ P_{pv} |_{min} < P_{pv} < P_{pv} |_{max} \quad (5.6)$$

Case study 5: If the power of the PV is greater than the maximum value, then PV will supply power to the load.

$$P_{pv} > P_{pv} |_{max} \quad (5.7)$$

The above five conditions are shown in table 5.1

**Table 5.1 Case study**

Case	Condition	State of PV	State of PHEV	State of Grid
1	$P_{pv} = 0$	OFF	OFF	ON
2	$P_{pv} > 0 \ \& \ P_{pv} < P_{pvmin} \ \& \ SOC > T_{soc}$	ON	ON	OFF
3	$P_{pv} > 0 \ \& \ P_{pv} < P_{pvmin} \ \& \ SOC < T_{soc}$	ON	OFF	ON
4	$P_{pvmin} < P_{pv} < P_{pvmax}$	ON	OFF	OFF
5	$P_{pv} > P_{pvmax}$	ON	OFF	OFF

### 5.5 Matlab@Simulink Model of Grid Connected PHEV

A 45Ah, 240V nominal voltage battery is considered to model the PHEV battery.

The control circuit for bi-directional converter was modeled in chapter 4. The input irradiance of PV will vary from 0 W/m<sup>2</sup> to 1000W/m<sup>2</sup>. The control circuit for photovoltaic system was modeled in chapter 3. Figure 5.20 shows the Matlab@Simulink models of the DG connected to the utility grid with PHEV load.



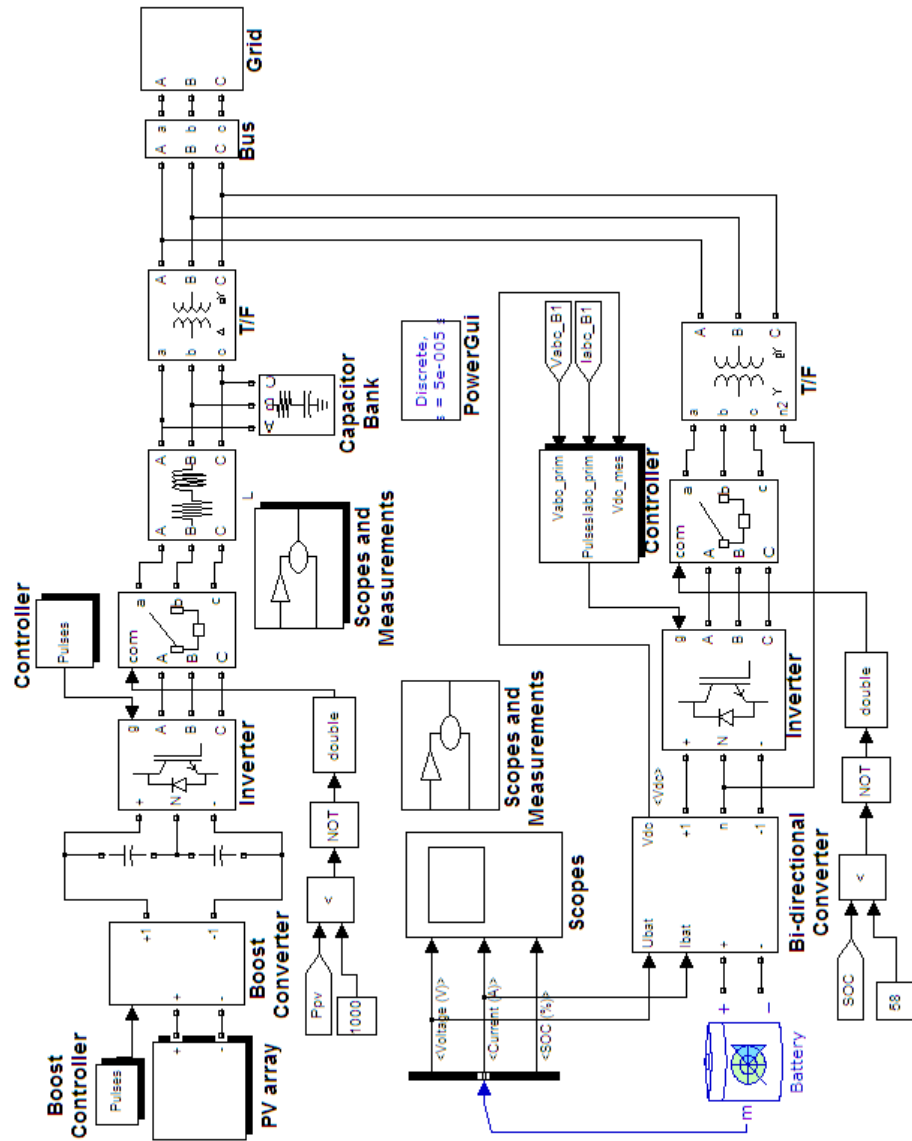


Figure 5.20 Matlab@Simulink modeling of grid connected PV with PHEV load

## 5.6 Simulation Results

Case study 1: Grid supplying power to the load.

In this case PV and PHEV are not injecting any harmonics into the grid

Case study 2: PV and PHEV supplying power to load.

PV array output power is not enough to supply the load, so both PV and PHEV are supplying power to the load.

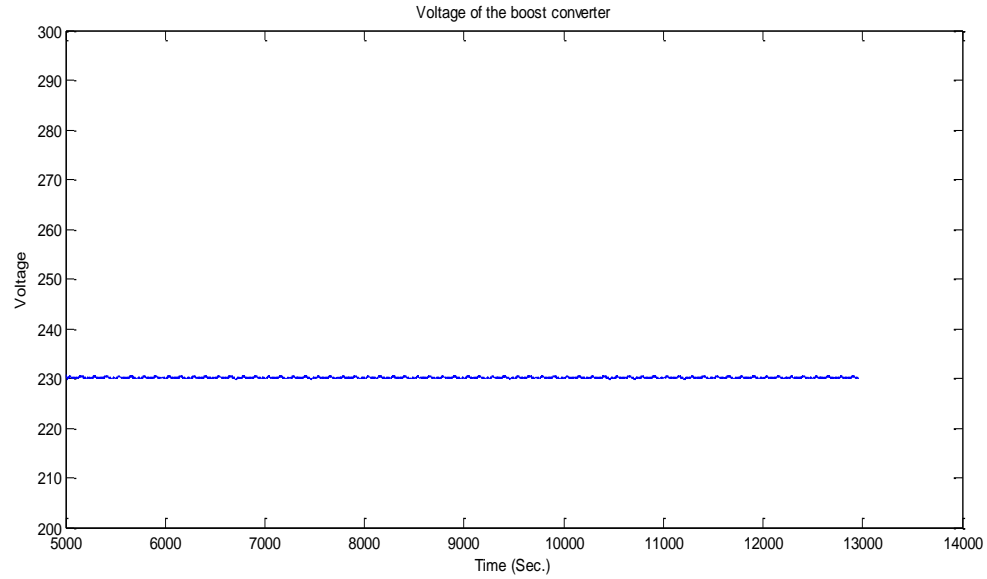


Figure 5.21 Voltage at the boost converter

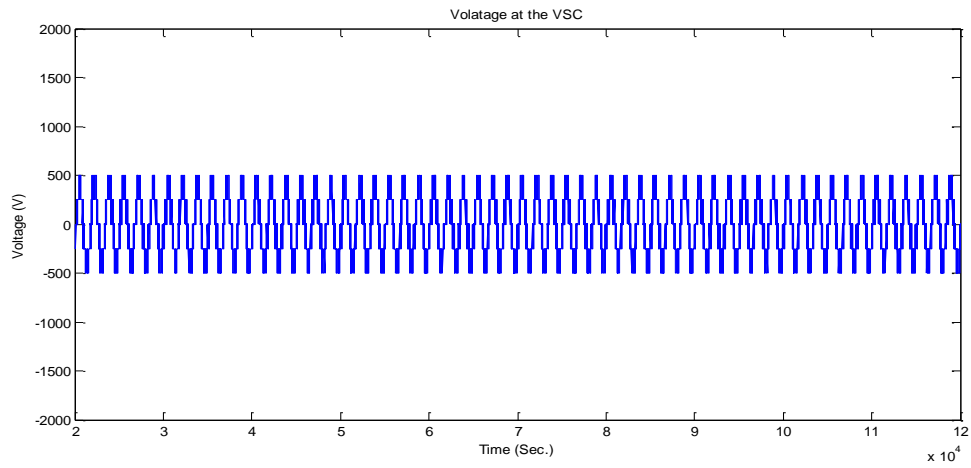


Figure 5.22 Voltage at the VSC

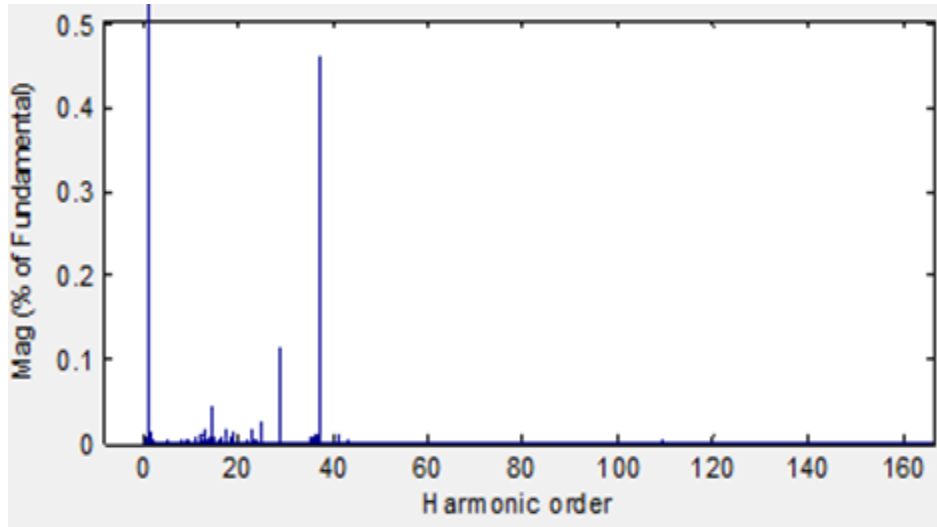


Figure 5.23 Voltage harmonic distortion

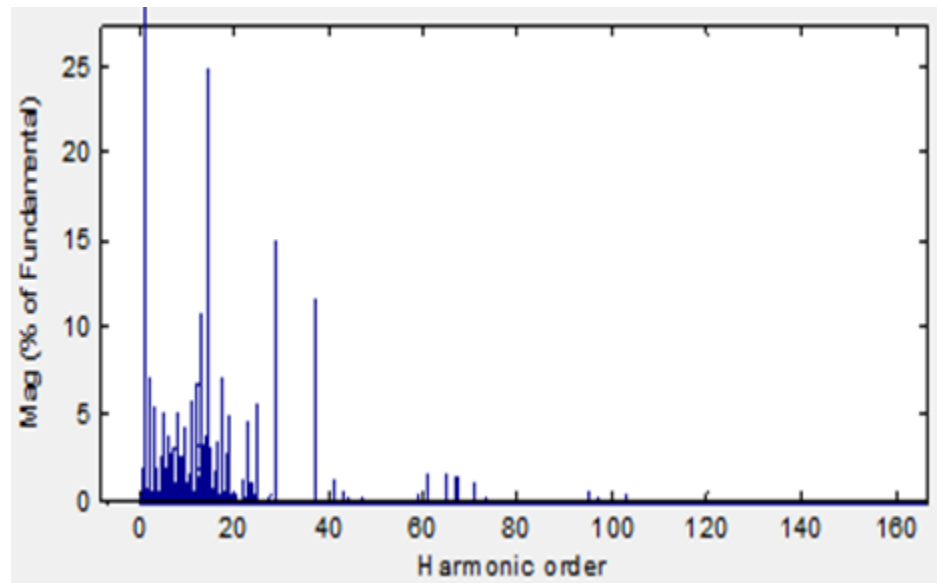


Figure 5.24 Current harmonic distortion at the utility grid

### Case study 3: PV and grid supplying power to load.

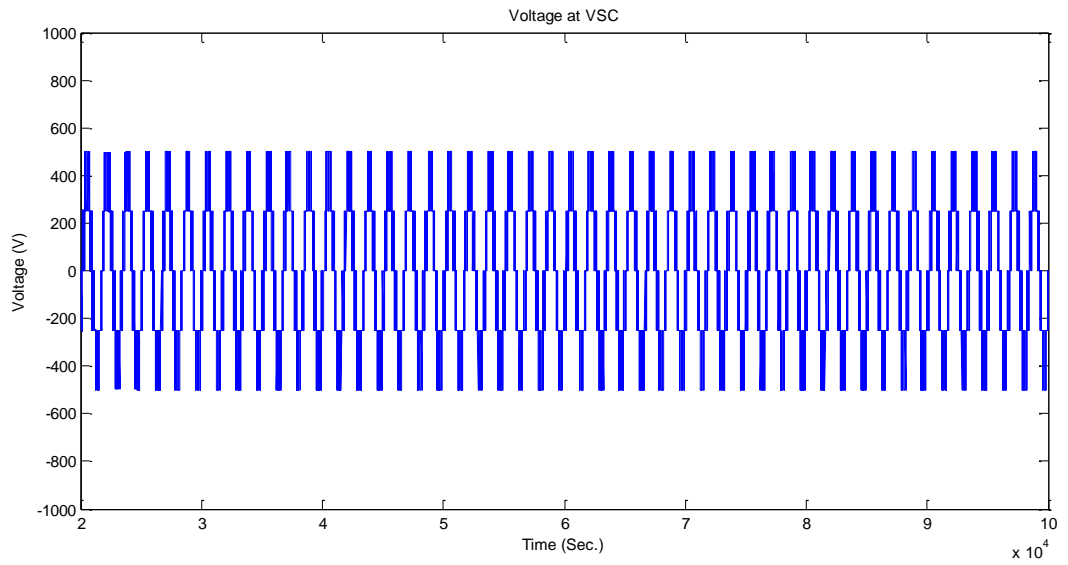


Figure 5.25 Voltage at VSC

### Case study 4 and 5: PV supplying power to load

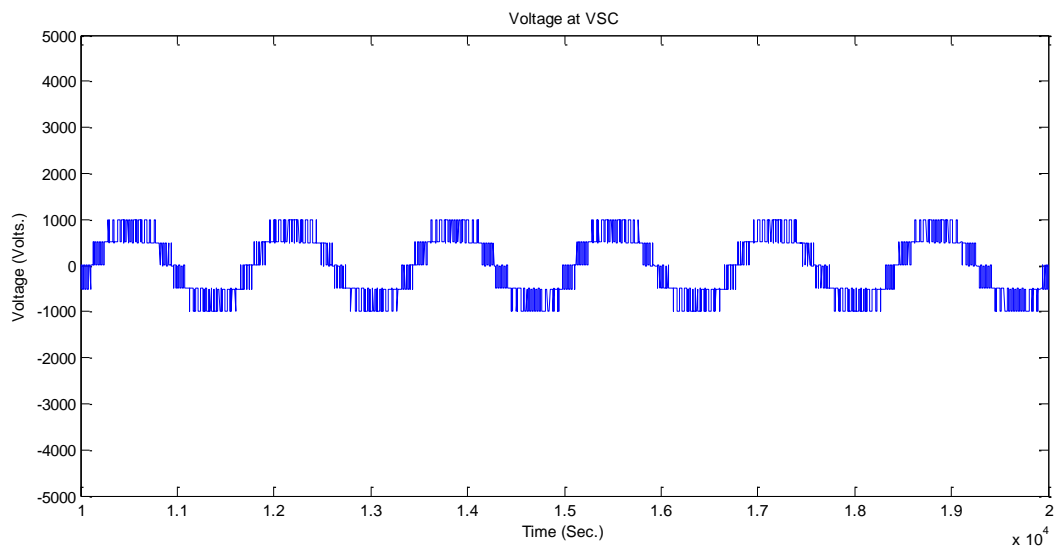


Figure 5.26 Voltage at VSC

The boost converter, voltage source converter, grid and load voltages for different case studies are plotted in Figure 5.21 to 5.26. Voltage and current harmonic distortion for PV inverter connected PHEV with residential load is shown in Figure 5.23 and 5.24. PHEV act as energy storage system. When the grid is off, PHEV can supply the power to the residential load. The harmonic analysis shows that PV and PHEV were injected 0.48 % voltage harmonics and 26.82 % of current harmonics into the grid.

By considering this section, a 12-bus power system network model was developed with PV inverters and PHEV loads to study and analyze the harmonics injected by PV inverters and PHEVs into the grid.

### **5.7 12-bus Power System Network with PHEV load**

The 12-bus power system network with distributed generations and PHEV loads is shown in Figure 5.27. Three distributed generators are connected to the utility grid at bus5, 6 and 9. The input solar irradiance of the PV is considered as constant. Multiple industrial and domestic loads are connected to the utility grid as shown in the Figure 5.21. In total, 15 PHEV loads are connected at bus2, 5 PHEVs are connected at bus3, bus4, and bus10.10 PHEVs are connected at bus 7 and bus 11.

### **5.8 Matlab@Simulink Modeling**

The Matlab Simulink model (Figure 5.21) shows 50 PHEVs connected to the 12-bus power system network at various busses. Positive sequence voltages are considered throughout the simulation.

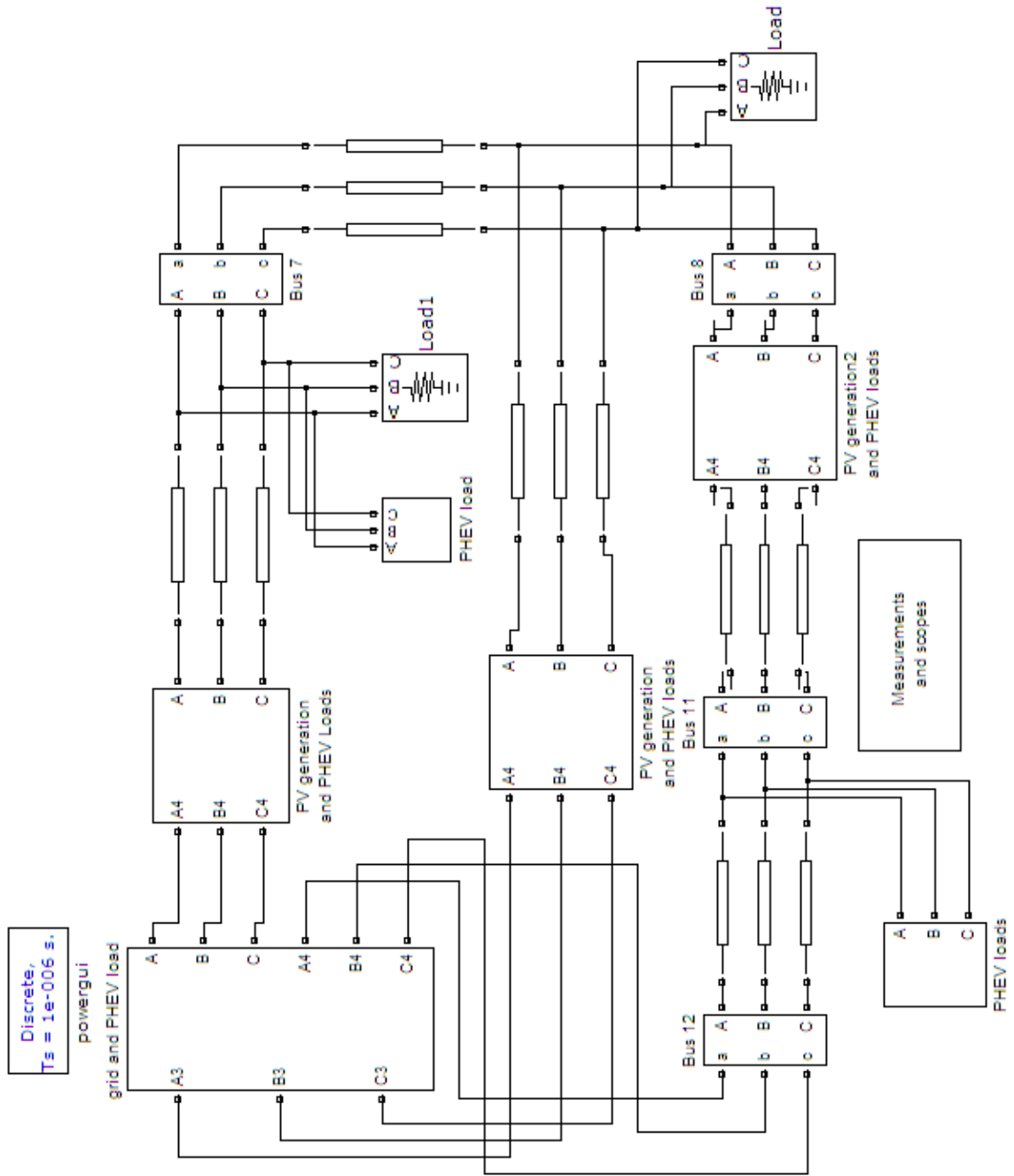


Figure 5.27 Three DGs connected to 12-bus power system network with 50 PHEVs

## 5.9 Simulation Results

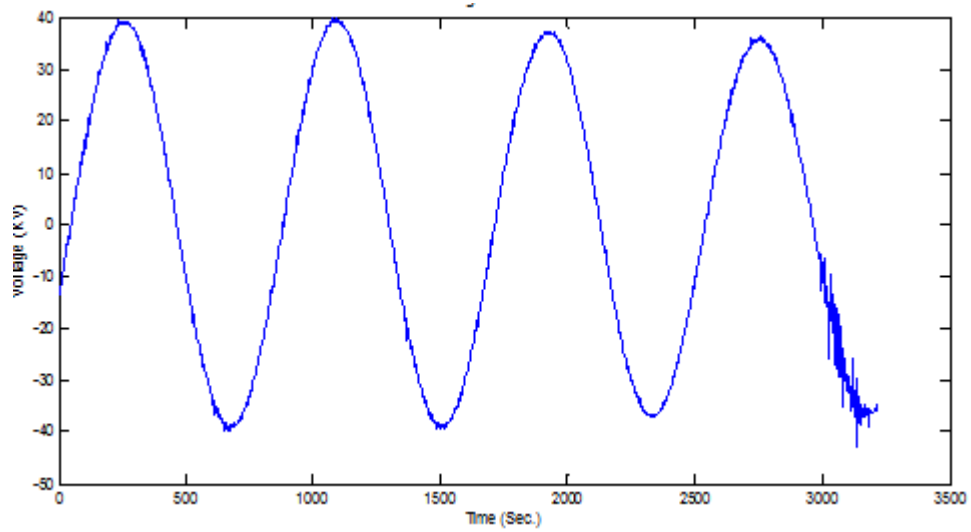


Figure 5.28 Voltage at the PV generator bus

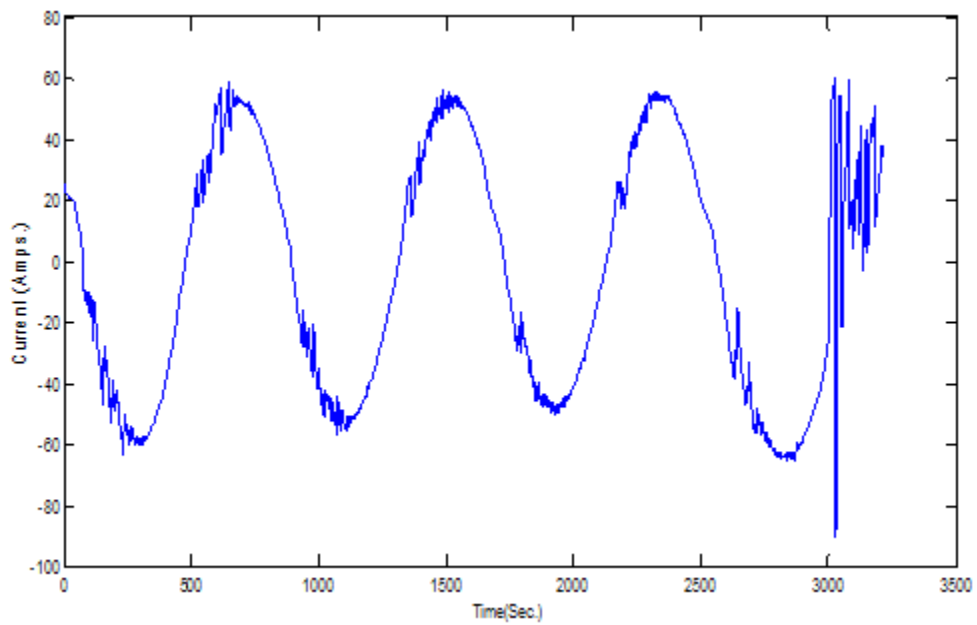


Figure 5.29 Current at the PV generator bus

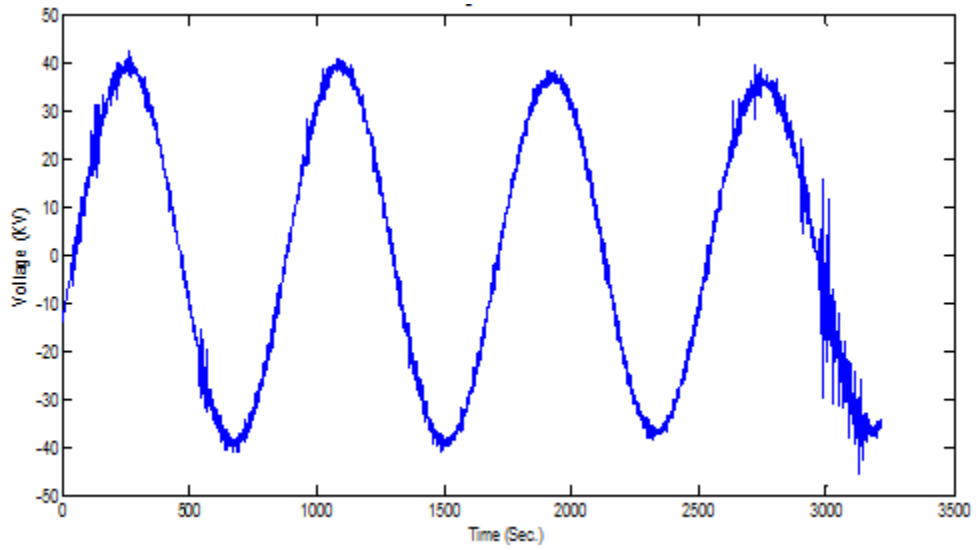


Figure 5.30 Voltage at the PV generator 1 bus

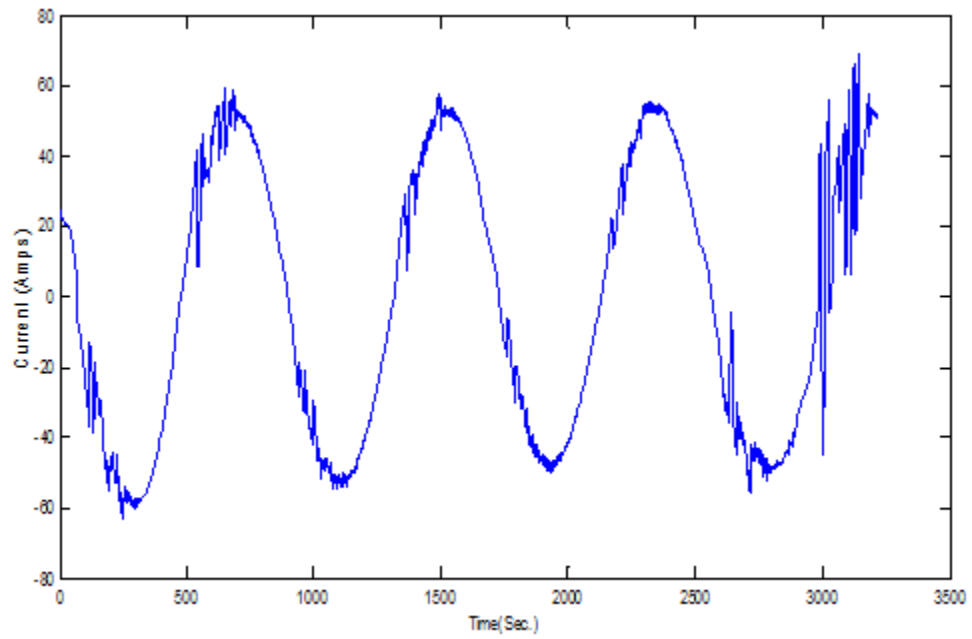


Figure 5.31 Current at the PV generator 1 bus



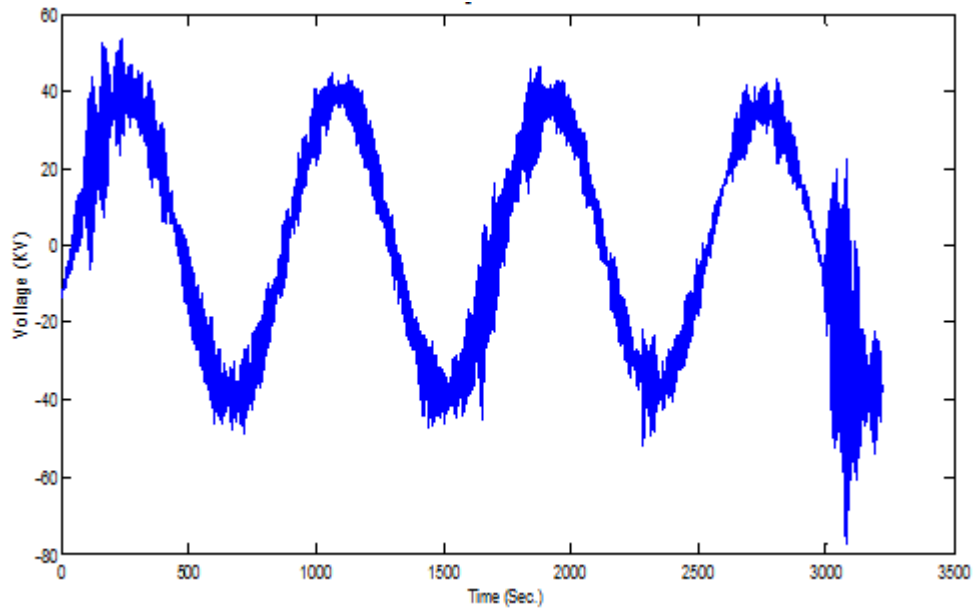


Figure 5.32 Voltage at the PV generator 2 bus

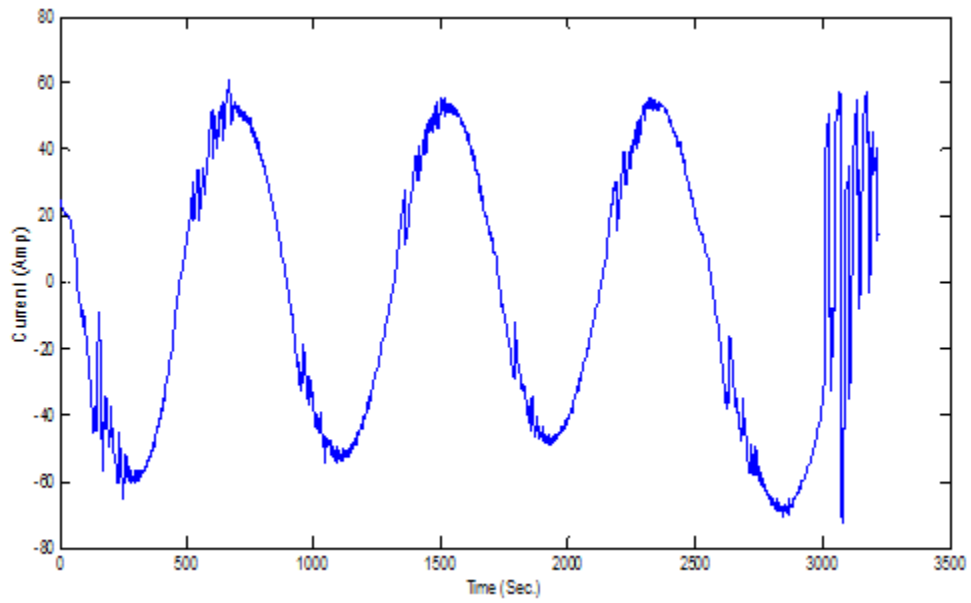


Figure 5.33 Current at the PV generator 2 bus

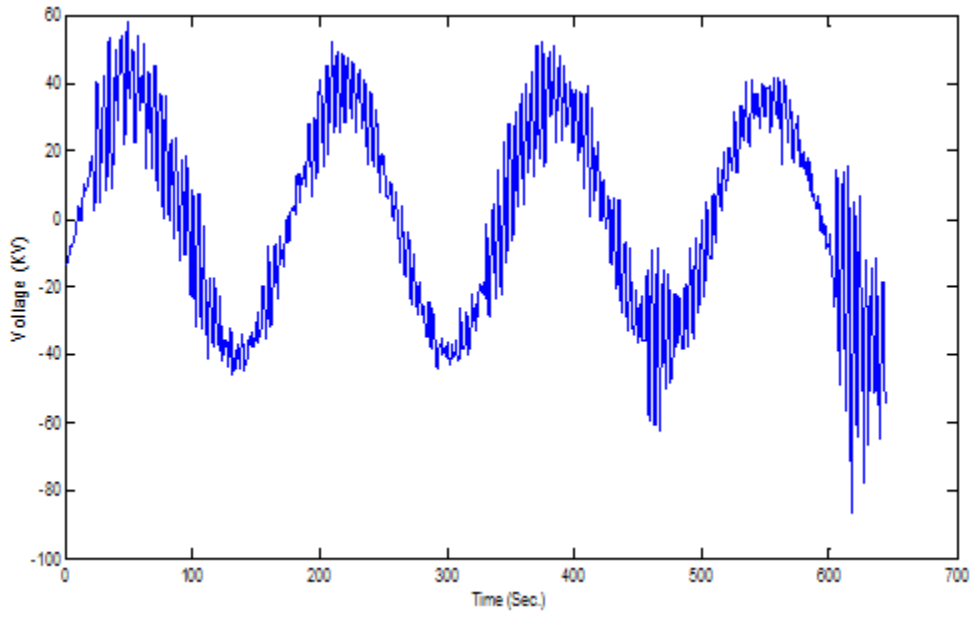


Figure 5.34 Voltage at the bus 7

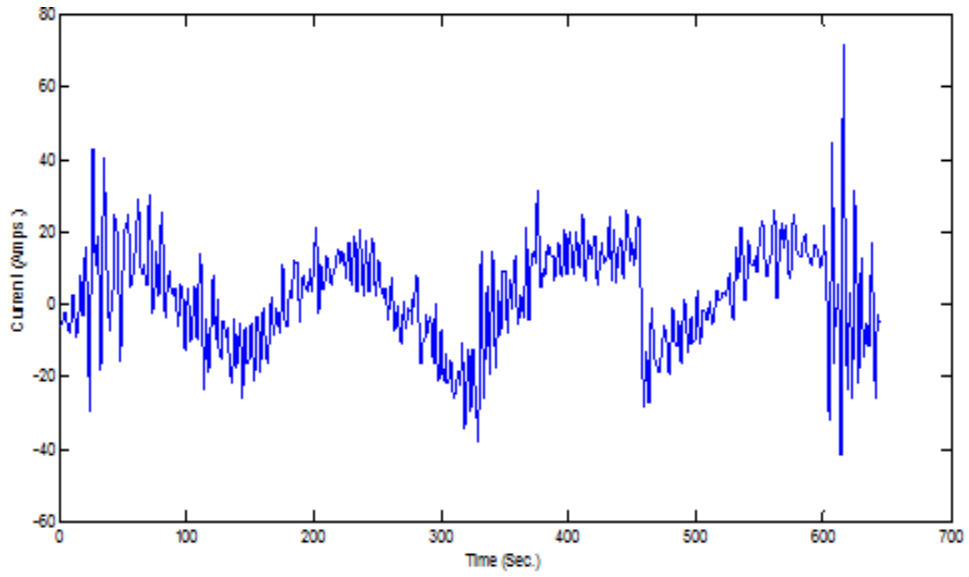


Figure 5.35 Current at the bus 7

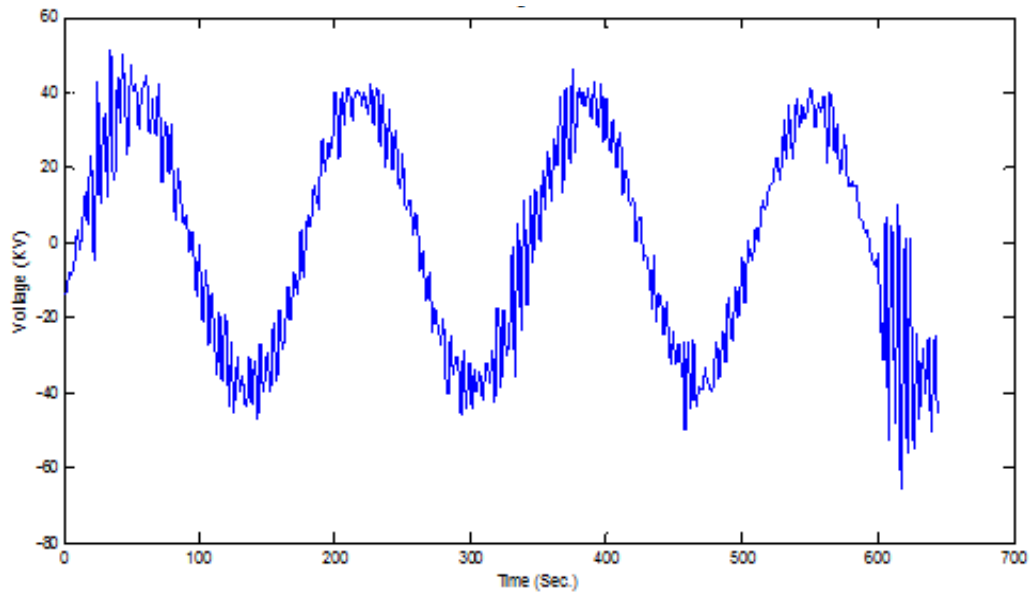


Figure 5.36 Voltage at the bus 8

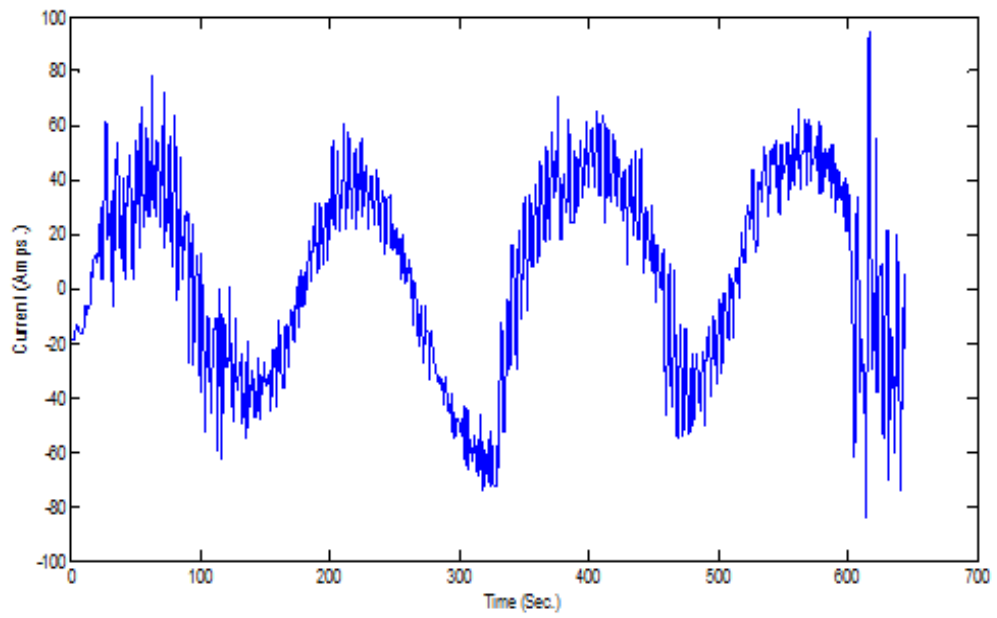


Figure 5.37 Current at the bus 8

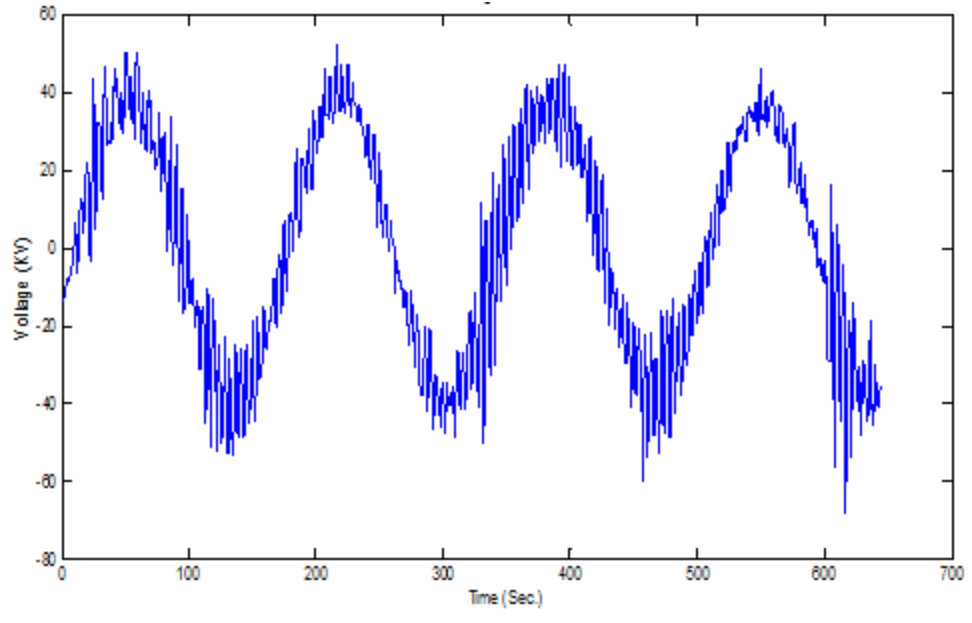


Figure 5.38 Voltage at the bus 11

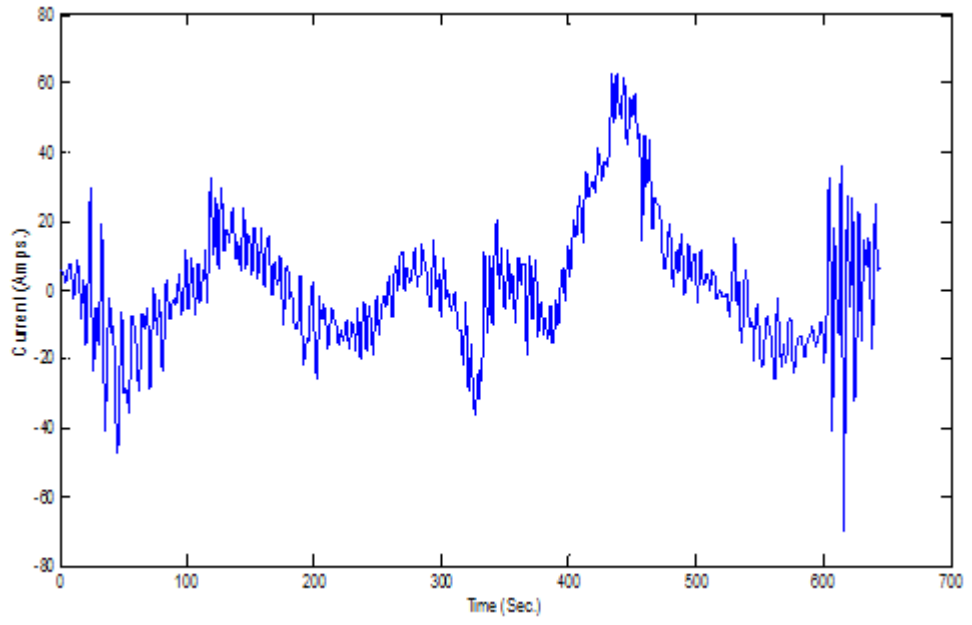


Figure 5.39 Current at the bus 11

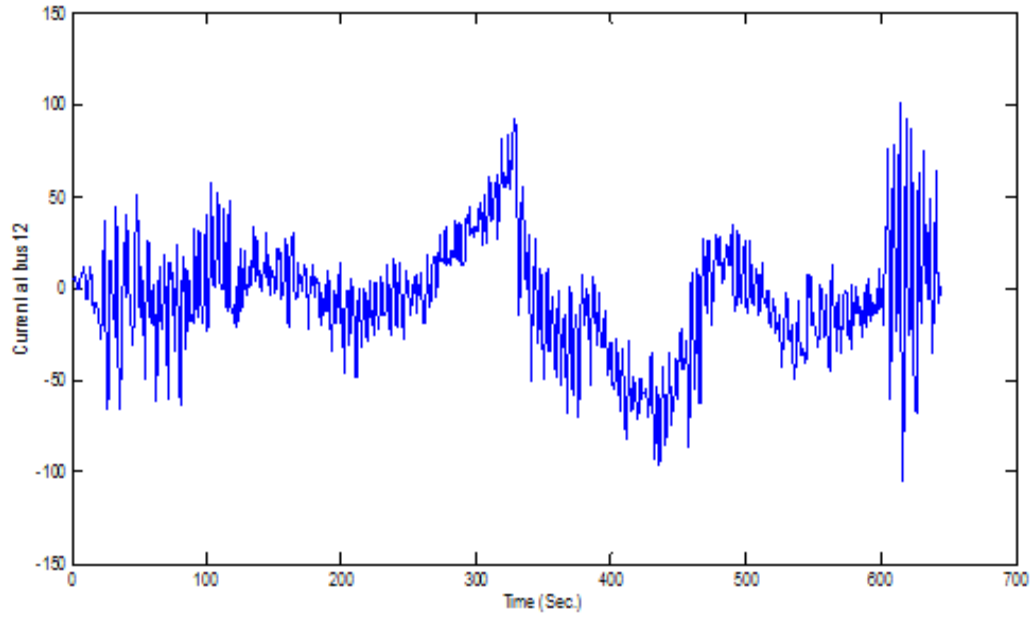


Figure 5.40 Current at the bus 12

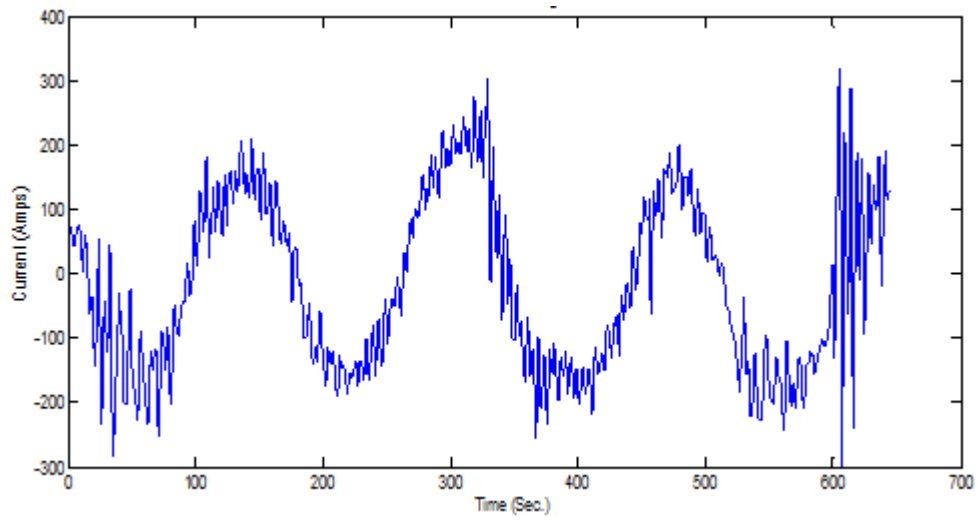


Figure 5.41 Current at the utility grid

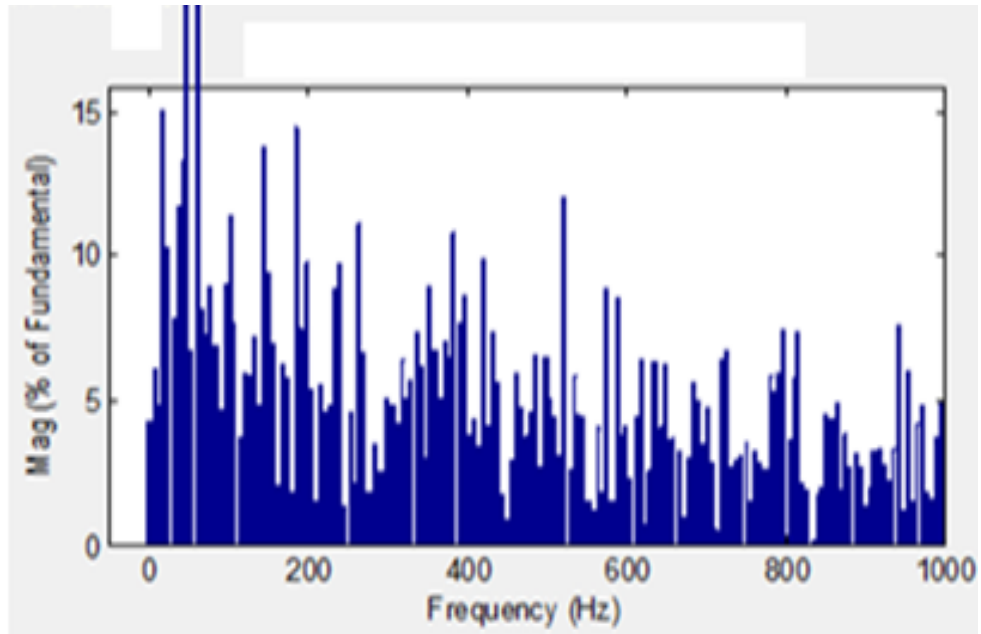


Figure 5.42 Voltage harmonic distortion at the grid

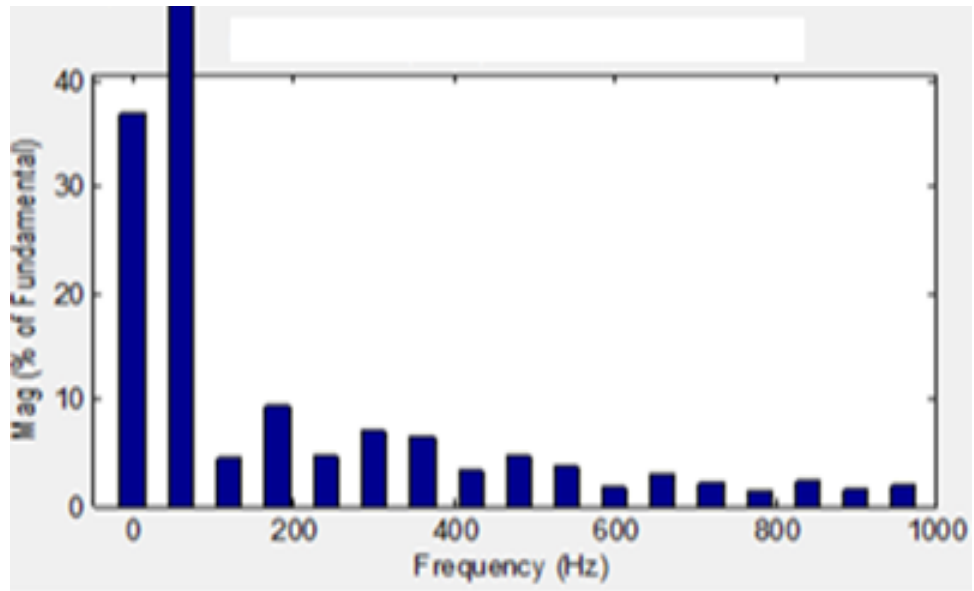


Figure 5.43 Current harmonic distortion at the grid

Voltage and current transients at various buses are shown in Figure 5.28 to 5.41. Impulse response and voltage sags can observe in voltage and current wave forms from the Figures. As discusses earlier, multiple PHEVs are connected at various buses, some of the batteries are charging and other discharging randomly based on the direction of the current and initial state of charge. Because of non-linear behavior of power electronic switches, turn on, turn off of IGBT switches and sudden load variations will affect the power quality of the distribution system. A high switching frequency (8Kz) inverter circuits are used in this study to develop inverter circuit for PHEV. Initially, High voltage and high current harmonics will present at the PHEV buses and high voltage harmonics will present at the other load buses. During sudden load variations, power quality and voltage stability will disturb at the generator and load busses.

Voltage and Current harmonic distortion at the utility grid is shown in Figure 5.42 and 5.43. PHEVs and PV inverters are injected 48.81 % of voltage and 18.97 % of current harmonic distortions into the utility grid. The voltage stability will increase by using the FACTS devices. Installation of suitable FACTS devices will improve the voltage stability, compensate the reactive power and reduce total harmonic distortion injected by the PHEVs into the grid.

### **5.10 Grid Connected PHEV load with Distributed Wind and PV Generation**

An IEEE 12-bus power system model was considered from Chapter 3. PV generation is connected to bus 6 and bus 9. Wind generation is connected to bus 5. Load values are considered from table 3.1 and 3.2. In addition, PHEV loads are connected at bus 2, 3, 4, 7, and 11. Matlab simulation was performed to investigate the voltage transients and harmonics injected by the WTIG, PV, and PHEVs into the grid.

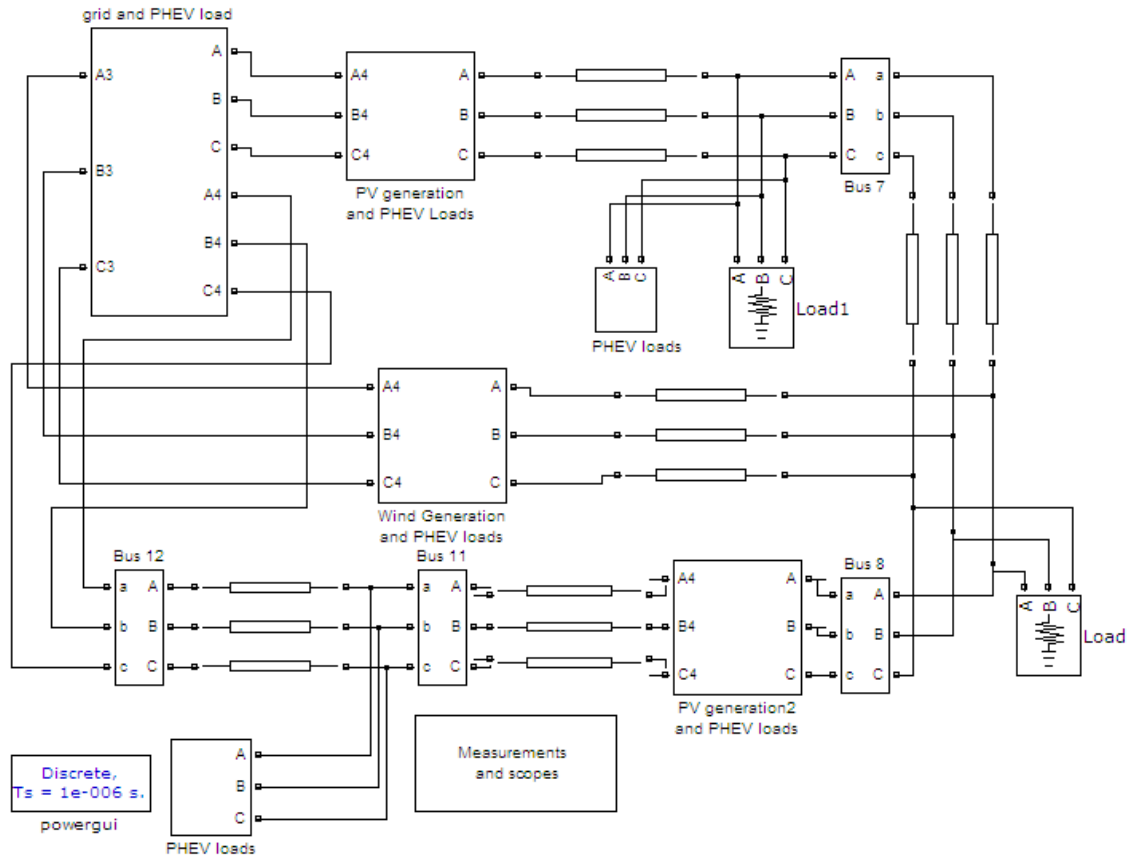


Figure 5.44 Grid connected distributed generations with PHEV loads

### 5.11 Simulation Results

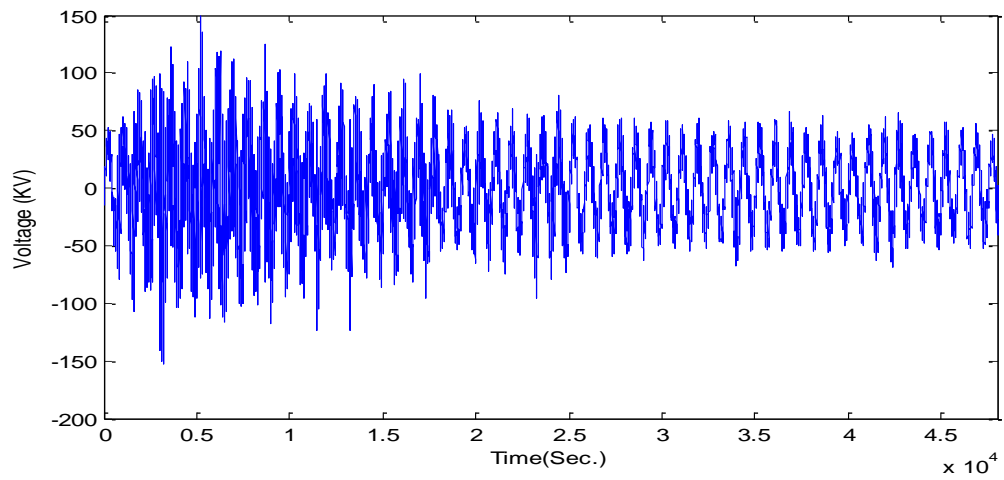


Figure 5.45 Voltage at the PV generator bus



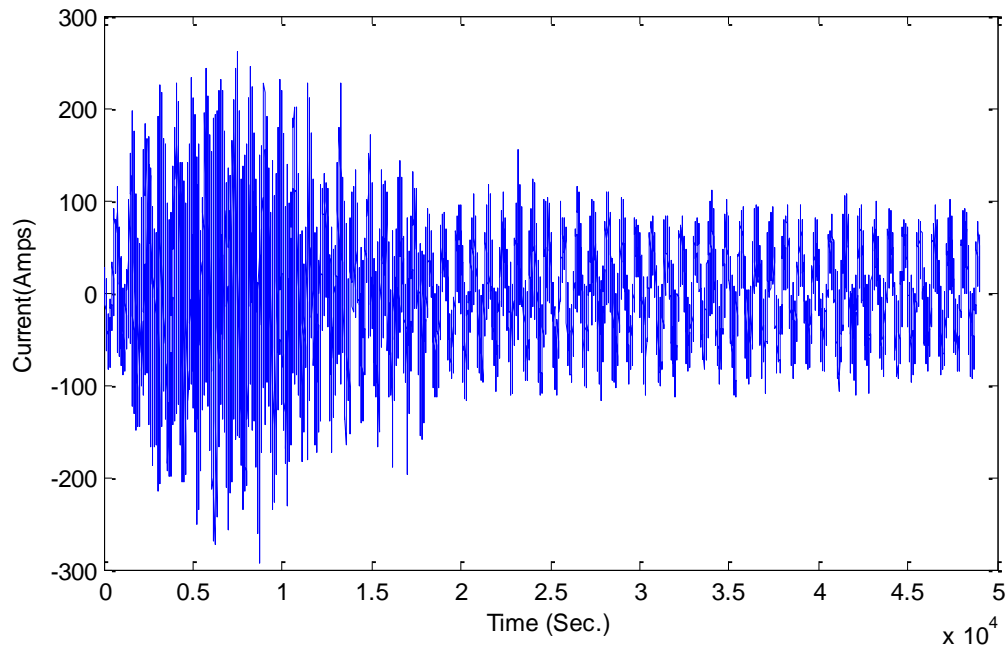


Figure 5.46 Current at the PV generator bus

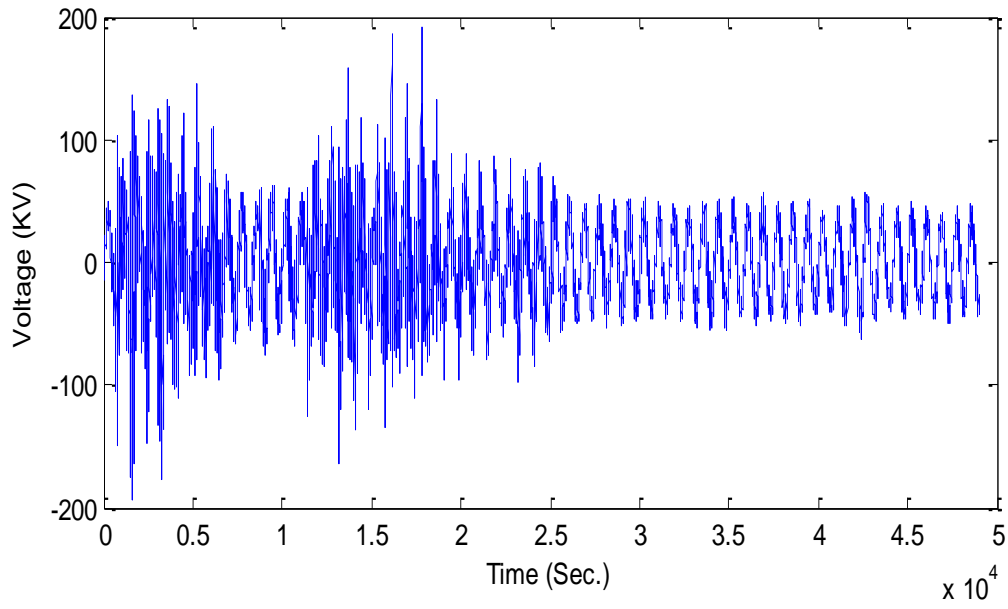


Figure 5.47 Voltage at the WTIG bus

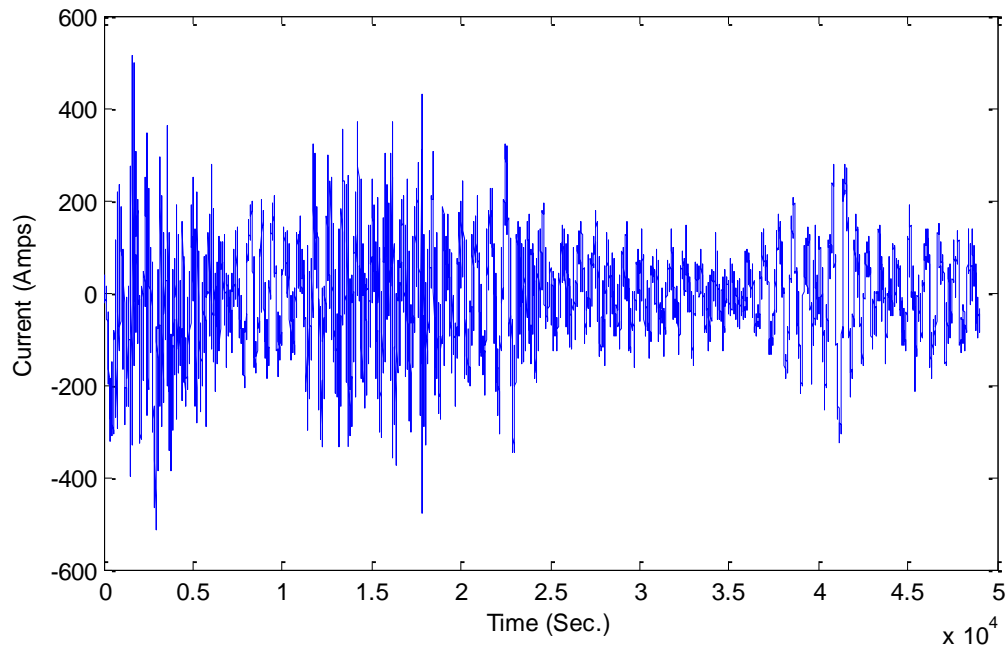


Figure 5.48 Current at the WTIG bus

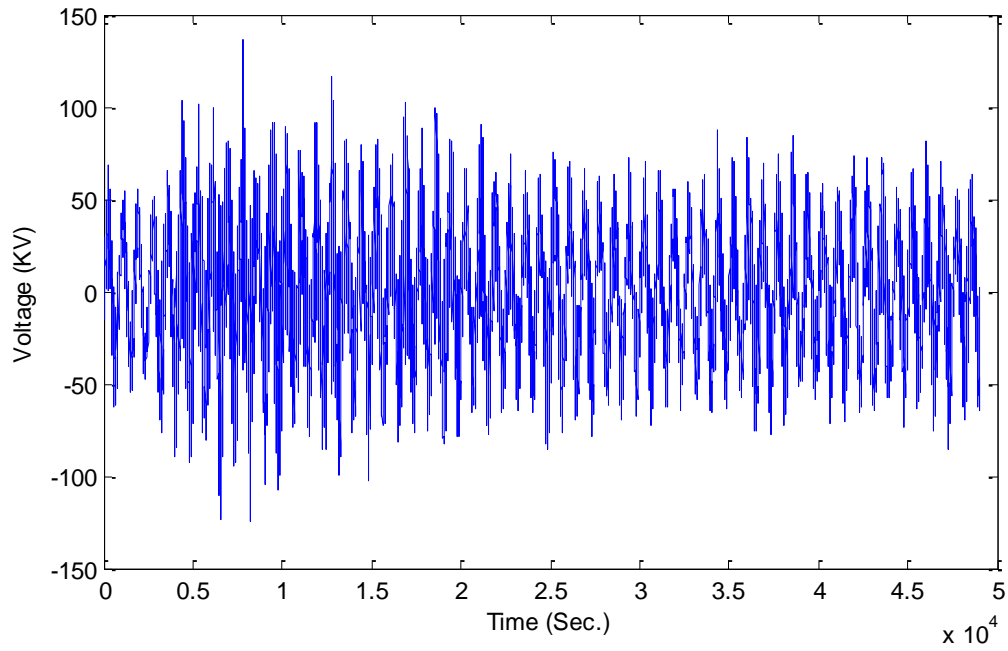


Figure 5.49 Voltage at the PV generator 1 bus

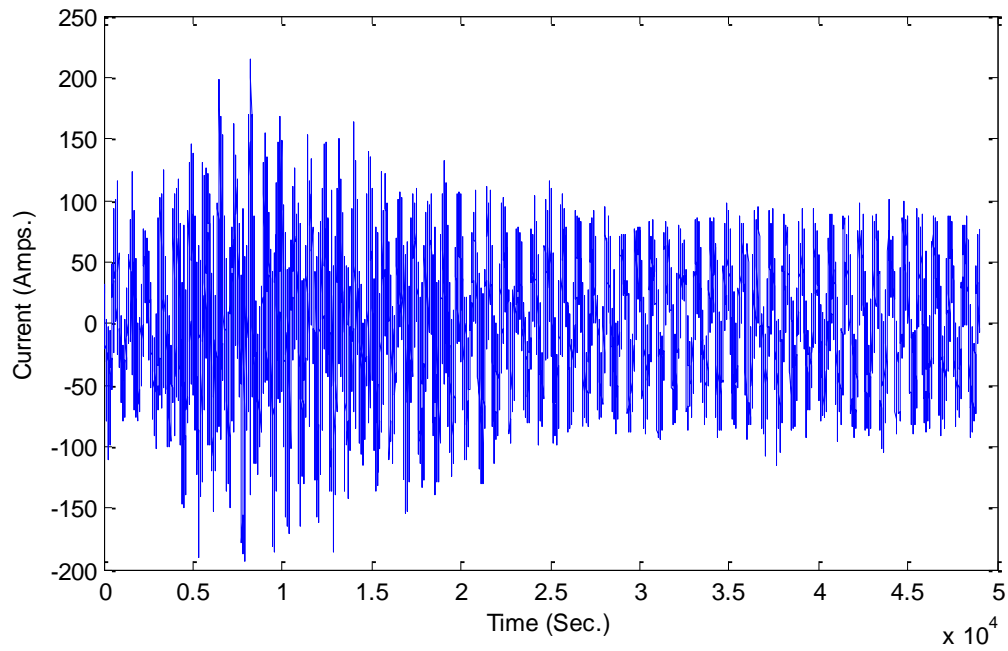


Figure 5.50 Current at the PV generator 1 bus

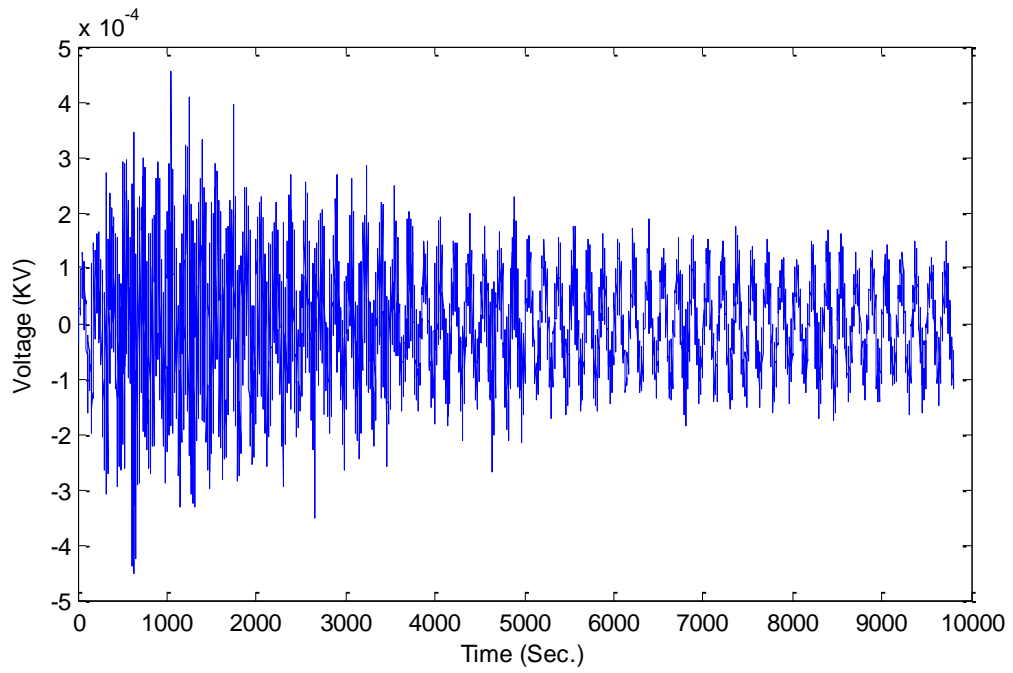


Figure 5.51 Voltage at the bus 4

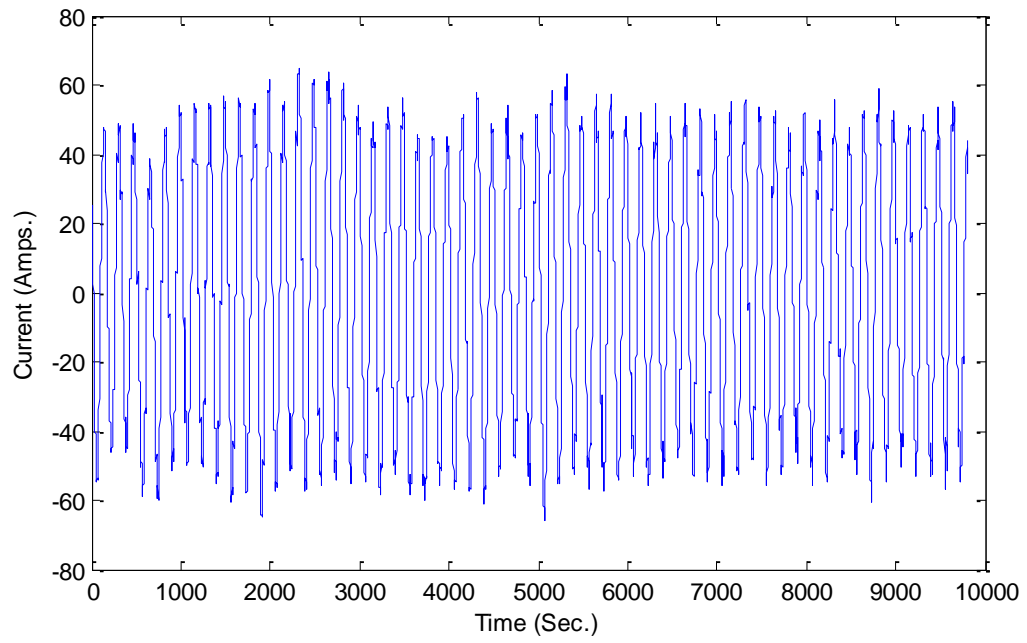


Figure 5.52 Current at the bus 4

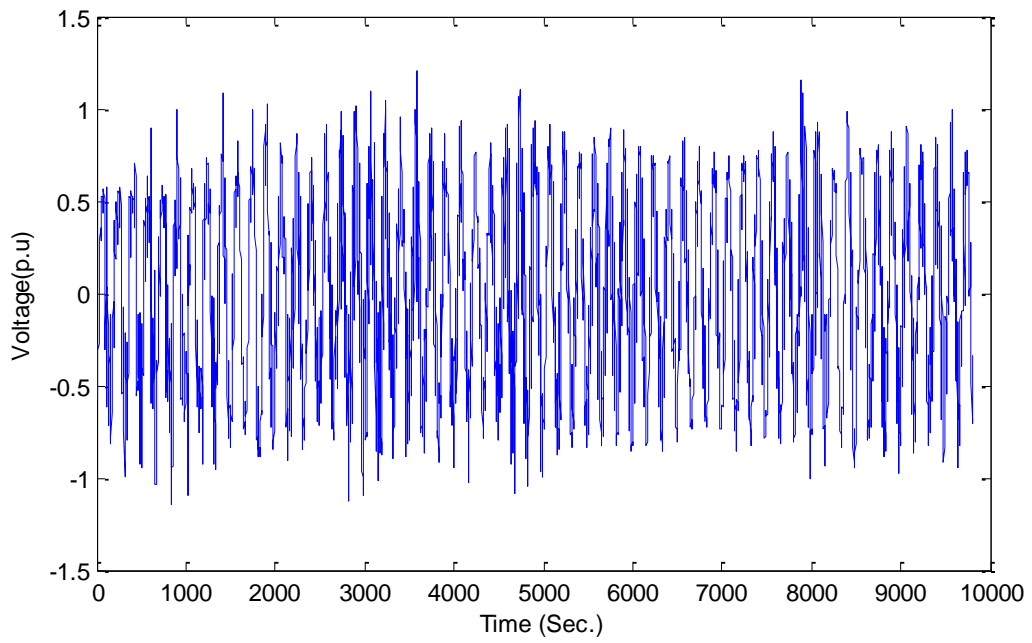


Figure 5.53 Voltage at the PV generator bus 3

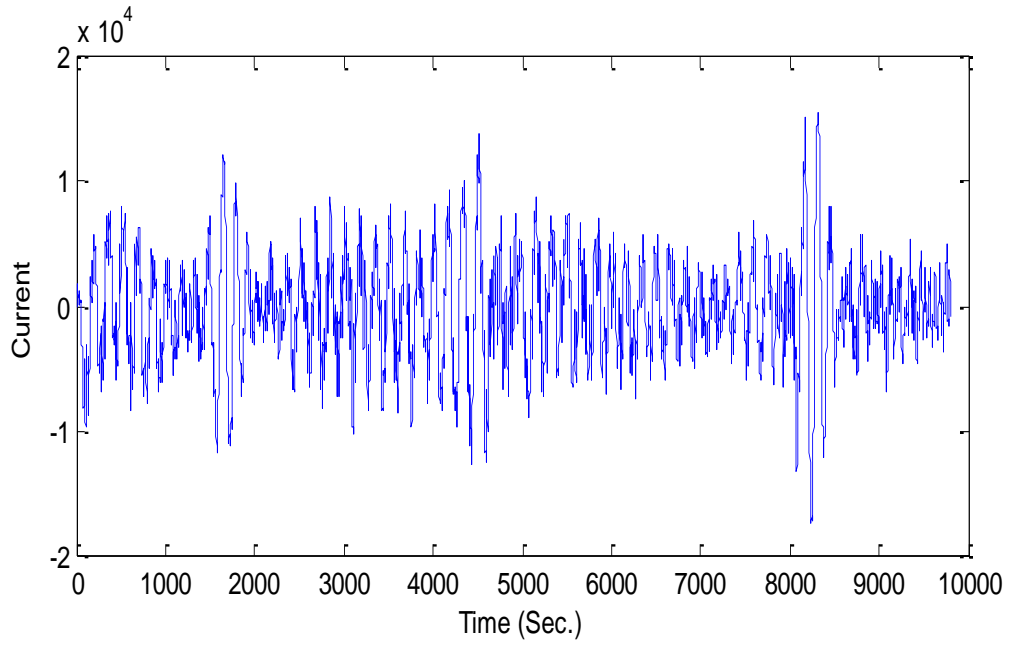


Figure 5.54 Current at the PV generator bus 3

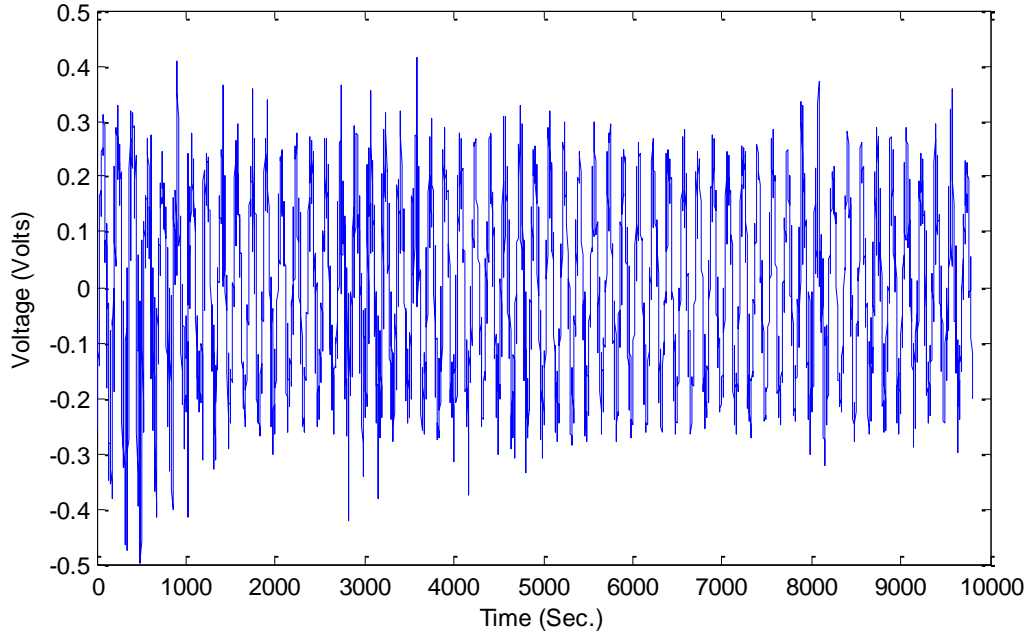


Figure 5.55 Voltage at the PV generator bus 10

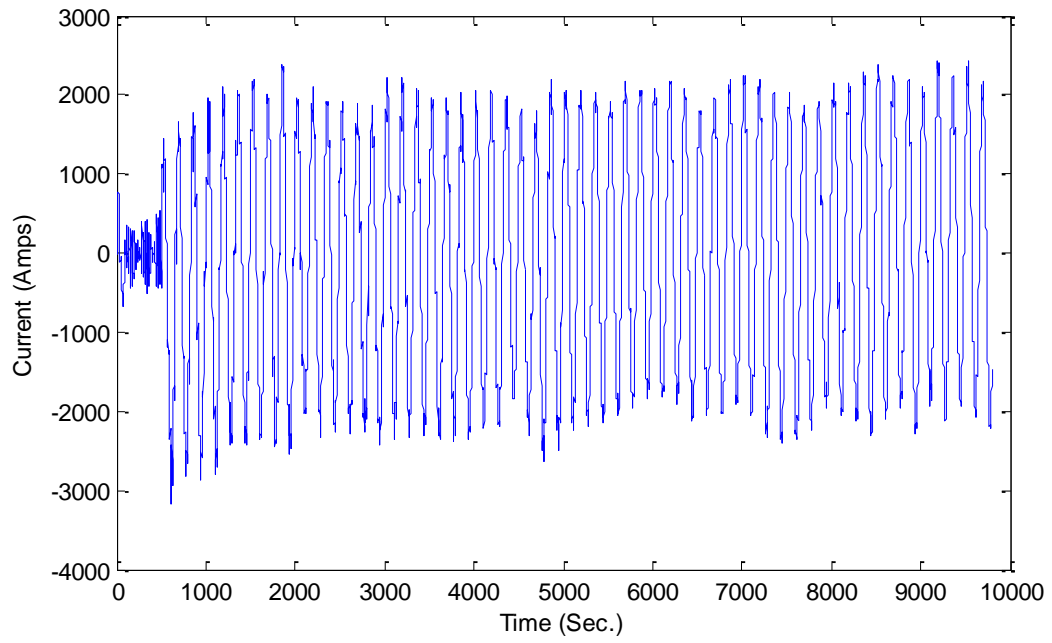


Figure 5.56 Current at the bus 10

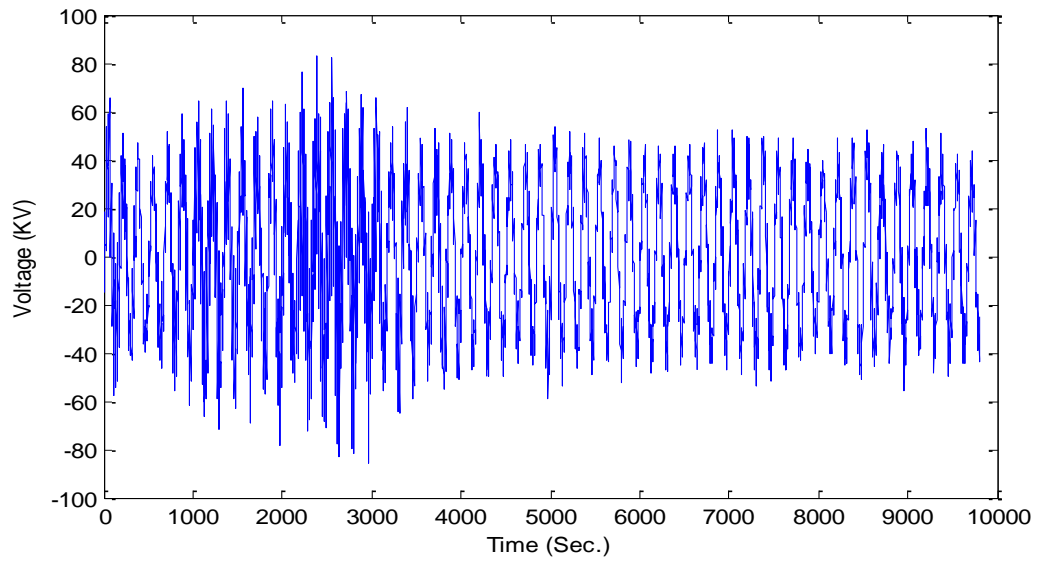


Figure 5.57 Voltage at the PV generator bus 7

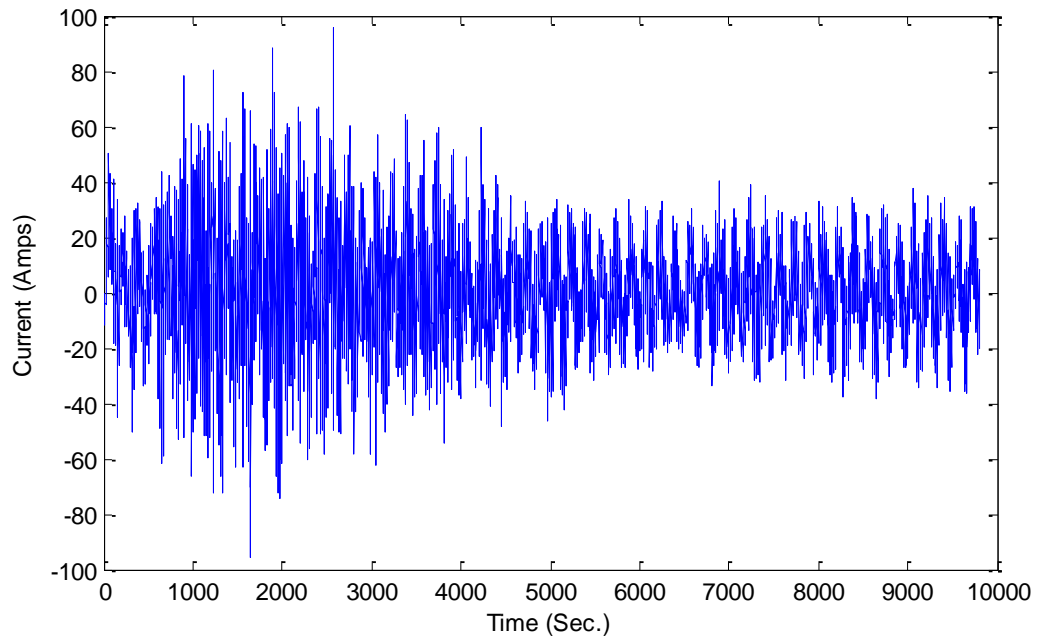


Figure 5.58 Current at the bus 7

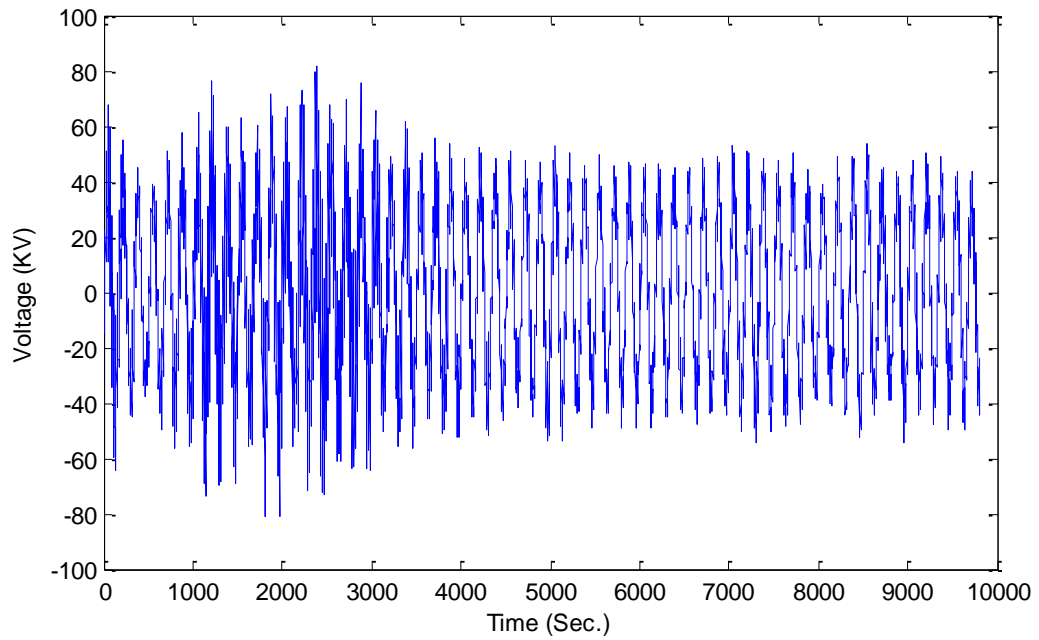


Figure 5.59 Voltage at the PV generator bus 11

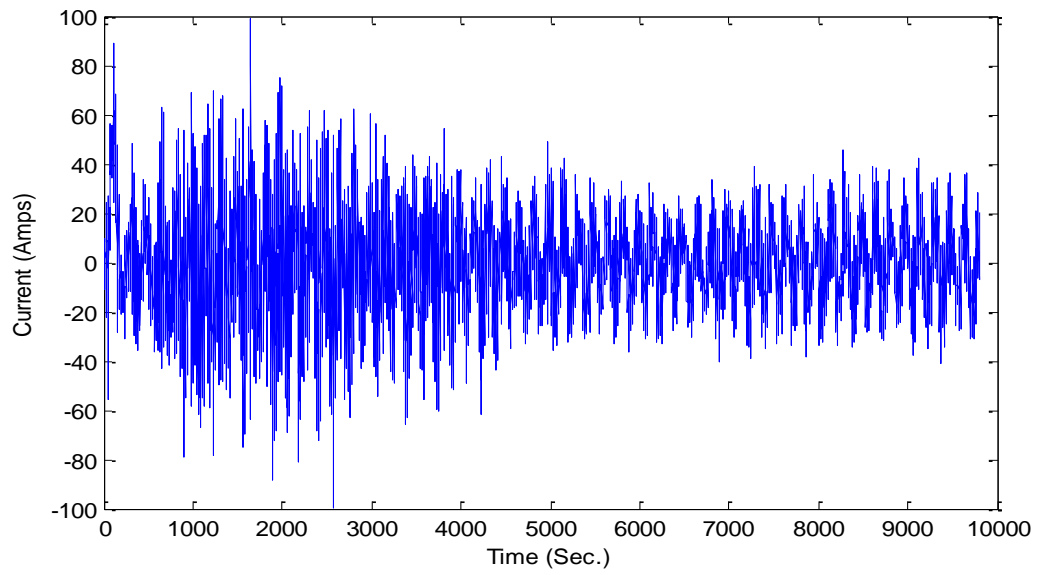


Figure 5.60 Current at the bus 11

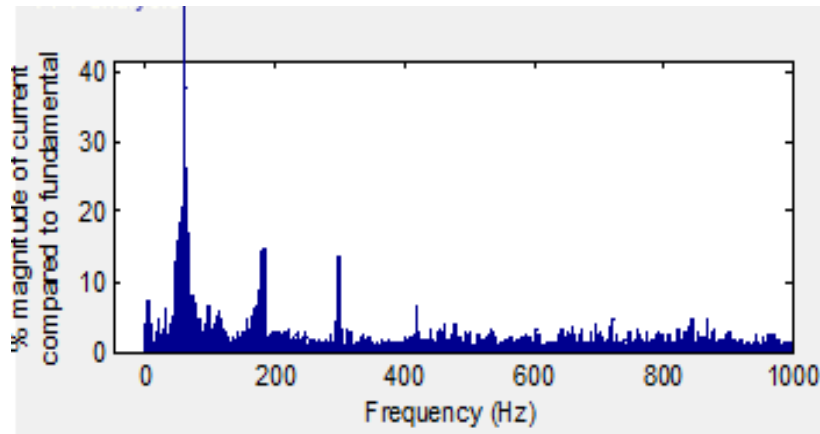


Figure 5.61 Voltage harmonic distortion at the grid

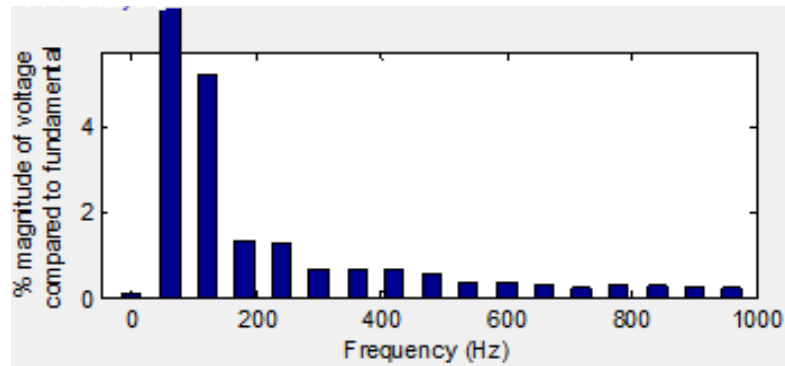


Figure 5.62 Current harmonic distortion at the grid



Each PV generator is generating power of 100KW and WTIG is generating power of 1.5MW at 0.9pf. The respective voltages and currents at the load buses and generator buses are shown in Figure 5.45 to 5.59. PHEV is injecting high current harmonics into the grid. Initially, PV array injected high current harmonics into the grid and WTIG injected high voltage harmonics into the grid. Capacitive banks are provided at the WTIG and PV inverter to maintain the voltage in a limit for stable operation. After few seconds of operation, the system came into the stable state. The total harmonics injected by the wind, PV inverter and PHEV into the grid is 23.95% and 5.50%.

## **Chapter Six**

### **Conclusions and Future Work**

#### **6.1 Conclusions**

Integration of large share of renewable generation into the transmission grid will increase the generation cost. Power quality can be poor because of uncertain weather conditions. Therefore, integration of distributed generation to the utility grid will decrease cost, and greenhouse gas emissions. In addition, power quality will increase because DGs can also work as stand-alone systems.

This thesis described modeling, simulation of stand-alone DG system and grid connected DG system. Simulation results show, that there is significant improvement in the power quality while connecting wind generation and photovoltaic generation to the utility grid.

Bi-directional DC-DC converter was modeled to allow bi-directional power flow from/to the grid. Three level voltage source converters were modeled for PV generation and bi-directional battery charger. Power quality of power system was investigated while connecting PHEV to the utility grid. Chapter five investigated and characterized the power quality of power system while connecting WTIG with PHEV loads, PV with PHEV load, 50 PHEV loads and 3 distributed generations connected to the distribution system and WTIG, PV and PHEVs connected to the IEEE 12-bus power system network.

## **6.2 Future Work**

The extension of this thesis could be modeling and integration of other distributed generation sources for the utility grid. The study and analysis of single phase and three phase topologies for bi-directional converter to reduce the total harmonic distortion injected by the battery charger and the power quality of power distribution network with other distributed energy resources and advanced PHEVs, can also be topics of future work.

## References

- [1] “Annual Energy Review 2011,”  
<http://www.eia.gov/totalenergy/data/annual/pdf/aer.pdf>.
- [2] “Technology for energy efficiency and grid reliability,”  
[http://www02.abb.com/global/abbzh/abbzh250.nsf/0/27c2fdbc96a879a4c12575ee0048777/\\$file/HVDC+-+efficiency+and+reliability.pdf](http://www02.abb.com/global/abbzh/abbzh250.nsf/0/27c2fdbc96a879a4c12575ee0048777/$file/HVDC+-+efficiency+and+reliability.pdf).
- [3] “The World's First Hydroelectric Power Plant Began Operation,”  
[http://www.americaslibrary.gov/jb/gilded/jb\\_gilded\\_hydro\\_1.html](http://www.americaslibrary.gov/jb/gilded/jb_gilded_hydro_1.html).
- [4] “The History of the Transformer,” <http://edisontechcenter.org/Transformers.html>.
- [5] T.G. Wilson, “The Evolution of Power Electronics,” *IEEE Transactions on Power Electronics*, vol. 15, no. 3, pp. 439-446, May 2000.
- [6] G. Pepermans, J. Driesen, D. Haeseldonckx, R. Belmans, W. D’haeseleer,  
“Distributed generation: definition, benefits and issues, *Energy Policy*, vol. 33,  
no. 6, pp. 787-798, April 2005.
- [7] S. Panda, and N. P. Padhy, "Investigating the Impact of Wind Speed on Active and  
Reactive Power Penetration to the Distribution Network," *International Journal  
of Electrical and Electronics Engineering* 1:1 (2008).
- [8] “The photovoltaic cell,” [http://www.enerpoint.net/photovoltaic\\_technology\\_2.php](http://www.enerpoint.net/photovoltaic_technology_2.php).
- [9] B. Alsayid and J. Jallad “Modeling and Simulation of Photovoltaic  
Cells/Modules/Arrays,” *International Journal of Research and Reviews in  
Computer Science (IJRRCS)*, vol. 2, no. 6, ISSN: 2079-2557, December 2011.

- [10] S.B. Kjaer, J.K. Pedersen, F. Blaabjerg, "A Review of Single-Phase Grid-Connected Inverters for Photovoltaic Modules," *IEEE Transactions on Industry Applications*, vol. 41, no.5, pp. 1292- 1306, Sept.-Oct. 2005.
- [11] T. Markel, A. Simpson, "Plug-In Hybrid Electric Vehicle Energy Storage System Design," May 2006.
- [12] O. Tremblay, L.A. Dessaint, A.I. Dekkiche, "A Generic Battery Model for the Dynamic Simulation of Hybrid Electric Vehicles," *Vehicle Power Propulsion Conference*, pp. 284-289, 9-12 September 2007.
- [13] Javier Gallardo-Lozano, M. Isabel Milanés-Montero, Miguel A. Guerrero-Martínez, Enrique Romero-Cadaval, "Electric vehicle battery charger for smart grids," *Electric Power Systems Research*, vol. 90, pp. 18-29, September 2012.
- [14] "EV History", <http://teslarumors.com/EVhistory.html>.
- [15] D.P. Hohmd, M.E. Ropp, "Comparative study of maximum power point tracking algorithms using an experimental, programmable, maximum power point tracking test bed," *Photovoltaic Specialists Conference*, pp. 1699-1702, 2000.
- [16] M. Ferdowsi, "Plug-in Hybrid Vehicles - A Vision for the Future," *IEEE Vehicle Power and Propulsion Conference*, pp. 457-462, 9-12 September 2007.
- [17] R.K. Nema, S. Nema, and G. Agnihotri, "Computer Simulation Based Study of Photovoltaic Cells/Modules and their Experimental Verification," *International Journal of Recent Trends in Engineering*, vol.1, no. 3, May 2009.
- [18] V. Meksarik, S. Masri, S. Taib, C.M. Hadzer, "Development of high efficiency boost converter for photovoltaic application," *National Power and Energy Conference*, pp. 153-157, 29-30 November 2004.
- [19] A. Nagarajan, W. Shireen, "Grid Connected Residential Photovoltaic Energy Systems with Plug-In Hybrid Electric Vehicles (PHEV) as Energy Storage," *Power and Energy General Meeting*, pp. 1-5, 25-29 July 2012.

- [20] S. Arunprasanth, C. Vivekanandan, A. Atputharajah, M.A.R.M. Fernando, “Integrated solution for power system stability improvement: Case studies on IEEE 12 Bus and Sri Lankan transmission networks,” *2011 6<sup>th</sup> IEEE International Conference on Industrial and Information Systems (ICIIS)*, pp. 398-403, 16-19 August 2011.